NKAP Depletion-Mediated Translational Inhibition Increases the Metastatic Behavior in Melanoma

---

Dissertation

zur

Erlangung der naturwissenschaftlichen Doktorwürde
(Dr. sc. nat.)

vorgelegt der

Mathematisch-naturwissenschaftlichen Fakultät

der

Universität Zürich

von

Mario-Emanuel Bonalli

von/aus

Zürich ZH

Promotionskommission

Prof. Dr. Lukas Sommer (Vorsitz/Leitung der Dissertation)

Prof. Dr. Konrad Basler

Prof. Dr. Michael Detmar

Prof. Dr. Reinhard Dummer

Zürich, 2016

This Project was funded by the Swiss Cancer Research in collaboration with the Swiss National Science Foundation in the frame of a fellowship under the MD-PhD program.

KREBSFORSCHUNG SCHWEIZ
RECHERCHE SUISSE CONTRE LE CANCER
RICERCA SVIZZERA CONTRO IL CANCRO

FNSNF
FONDS NATIONAL SUISSE
SCHWEIZERISCHER NATIONALFONDS
FONDO NAZIONALE SVIZZERO
SWISS NATIONAL SCIENCE FOUNDATION

I. Table of contents

II. Index of figures

III. Index of tables

1. Summary

Melanoma is the most deadly form of skin cancer and the incidence rate is continuously increasing worldwide. Interestingly, neural crest cells and melanoma cells share striking similarities and various developmental programs usually active in the neural crest seem to find reuse in melanoma. In the frame of my PhD study I investigated the role of the neural crest-relevant factor NKAP in melanoma.

The goal of my doctoral thesis was to identify a novel neural crest-associated transcriptional regulator involved in melanoma. On the basis of a whole-genome transcriptome analysis, NKAP was identified among a set of 53 genes, which were up regulated in neural crest stem cells when compared to their early-differentiated derivatives. In order to investigate the role of NKAP in melanoma, loss-of-function and gain-of-function studies were performed in human melanoma cell cultures. As a result, NKAP depleted cells showed reduced adhesive potential and presented with a strong G1/G0 cell cycle arrest *in vitro*. Moreover, subcutaneous injections in NSG mice revealed a drastic increase in the metastatic behavior upon NKAP depletion, despite unaffected tumor growth. These results were further substantiated with clinical data retrieved from the TCGA database, highlighting that low NKAP levels in lymph node and distant metastases correlate with poor patient survival. On the other side, exogenous expression of a fluorescently labeled fusion protein confirmed NKAP's exclusive localization to the nuclear speckles. These findings were further corroborated, as NKAP co-immunoprecipitated with numerous nuclear speckle proteins involved in RNA splicing and processing. Furthermore, NKAP depletion induced a drastic reduction in translational activity. Thus, only well-regulated NKAP expression levels guaranteed optimal conditions for protein synthesis, whereas aberrant NKAP expression resulted in reduced translation.

Consequently, the results of my doctoral thesis indicate that NKAP is a tightly regulated nuclear speckle protein involved in co- or post-transcriptional processes. Hence, NKAP depletion results in reduced translational activity and increases the metastatic potential in melanoma. Recently, it has been discovered that translational inhibition leads to the activation of an alternative translational program, which is associated with increased stemness and tumorigenesis. However, whether this is the cause for the increased metastatic proclivity in NKAP depleted melanoma cells has not yet been addressed and requires further investigations.

2. Zusammenfassung

Malignes Melanom beschreibt die tödlichste Form von Hautkrebs mit einer weltweit stetig ansteigenden Inzidenzrate. Interessanterweise teilen sich Neuralleistenstammzellen und Melanomzellen verblüffend viele Eigenschaften, sodass verschiedene entwicklungsbezogene Programme die normalerweise in der Neuralleiste aktiv sind im Melanom Wiederverwendung finden. Während meiner Dissertation habe ich die Rolle des für die Neuralleiste relevanten Faktors NKAP in Melanom untersucht.

Das Ziel meiner Doktorarbeit war es, einen neuen mit der Neuralleiste assoziierten Transkriptionsregulator zu identifizieren, der in Melanom von Bedeutung ist. Anhand einer gesamtgenomischen Transkriptomanalyse wurde NKAP in einer Gruppe von 53 Genen entdeckt, welche in Neuralleistenstammzellen, im Vergleich zu ihren früh-ausdifferenzierten Abkömmlingen, erhöhte Expressionen aufwiesen. Um die Rolle von NKAP in Melanom genauer zu untersuchen, wurden in humanen Melanomzellkulturen verschiedene Experimente durchgeführt, in denen das Gen entweder ausgeschaltet oder überexprimiert wurde. Die Resultate der *in vitro* durchgeführten Untersuchungen zeigten, dass Zellen mit abwesender NKAP Expression eine reduzierte Adhäsion und einen starken G1/G0 Zellzyklusarrest aufwiesen. Zusätzlich konnte an subkutan injizierten NSG Mäusen belegt werden, dass der NKAP Knockout das Metastaseverhalten verstärkte, obwohl das Tumorwachstum unbeeinträchtigt blieb. Klinische Daten aus der TCGA Datenbank untermauerten diese Resultate und zeigten auf, dass tiefe NKAP Levels in Lymphknoten- und Fernmetastasen mit schlechteren Überlebenschancen für den Patienten korrelieren. Auf der anderen Seite konnte anhand eines von außen zugeführten fluoreszierenden Fusionsproteins die exklusive Lage NKAP's in nukleären Speckles demonstriert werden. Dieser Befund wurde mittels einer Ko-Immunopräzipitationsstudie zusätzlich bekräftigt, welche aufgezeigt hat, dass NKAP mit einer Vielzahl von nukleären Speckle Pro-

teinen interagiert, die an der RNA Prozessierung beteiligt sind. Des Weiteren konnte gezeigt werden, dass das Ausschalten von NKAP eine drastische Reduktion der Translationsaktivität auslöste. Zusätzlich konnte verdeutlicht werden, dass eine streng regulierte NKAP Expression notwendig ist, um optimale Bedingungen für die Translation zu schaffen, währendem abweichende NKAP Levels zu verminderter Proteinsynthese führen.

Die Ergebnisse meiner Doktorarbeit deuten darauf hin, dass NKAP ein streng reguliertes nukleäres Speckle Protein ist, welches an ko- oder post-transkriptionellen Prozessen beteiligt ist. Das Ausschalten von NKAP führt zu einer reduzierten Translationsaktivität und zu einem verstärkten Metastasierungspotential. Kürzlich wurde entdeckt, dass die Hemmung der Proteinsynthese ein alternatives Translationsprogramms aktiviert, welches mit einer verstärkten Ausprägung von Stammzell- und Krebseigenschaften verbunden ist. Ob dies der Grund für das verstärkte Metastasierungsverhalten in Melanomzellen ist, konnte bis jetzt noch nicht abschließend behandelt werden und benötigt weitere Untersuchungen.

3. Introduction

3.1. The neural crest

The neural crest is a transient appearing embryonic structure defined by a multipotent migratory stem cell population that emerges from the dorsalmost margin of the neural tube [Le Douarin_2003; Baggiolini_2015] (Figure 1). By definition, neural crest stem cells have the ability to self-renew and to differentiate into various cell derivatives appropriate to their corresponding location in the embryo [Le Douarin_2003]. The fourth germ layer, another name for the neural crest, is a phylogenetic invention of the craniate family and therefore a common feature in all vertebrate embryos including hagfishes and lampreys [Hall_2000].

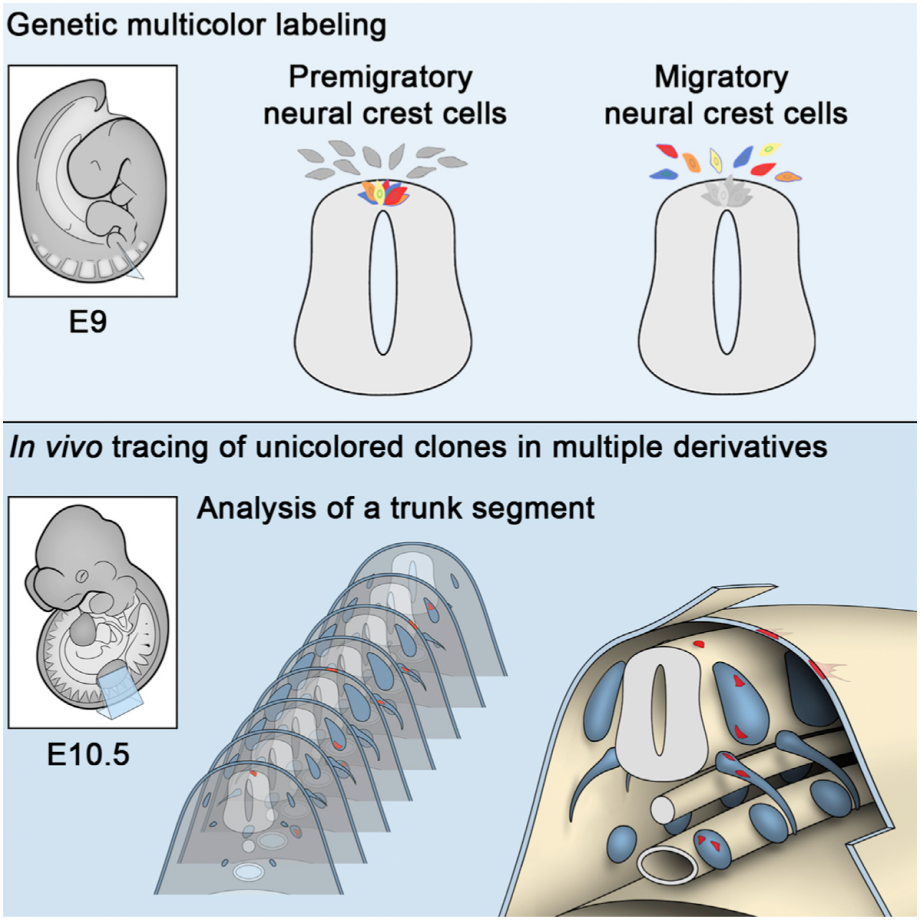

Figure 01. The neural crest is a migratory multipotent stem cell population. *In vivo* lineage tracing using multicolor labeling of premigratory and migratory neural crest cells revealed that the majority of neural crest cells are multipotent [graphical illustration; Mario Bonalli in Baggiolini_2015].

3.1.1. The development of the neural crest

Following the chronology of embryonic development, first neural crest cells appear during gastrulation and remain present until late organogenesis [Monsoro-Burq_2005; Basch_2006]. As mentioned, the induction of the presumptive neural crest region starts at gastrulation and proceeds during neurulation. When the neural plate is specified, the regions flanking the neural plate start to elevate and form the neural folds. With continued elevation, the neural folds converge and build the neural tube. As the folding of the neural tube progresses, neural crest progenitors start to specify at the neural plate border defined as the region between neural and epidermal ectoderm. Upon closure of the neural tube, neural crest progenitors undergo an epithelial-to-mesenchymal transition (EMT) and delaminate from the ectoderm. Finally, neural crest cells start to migrate along predefined pathways and settle in various distant organs where they differentiate into a multitude of derivatives [Betancur_2010] (Figure 2).

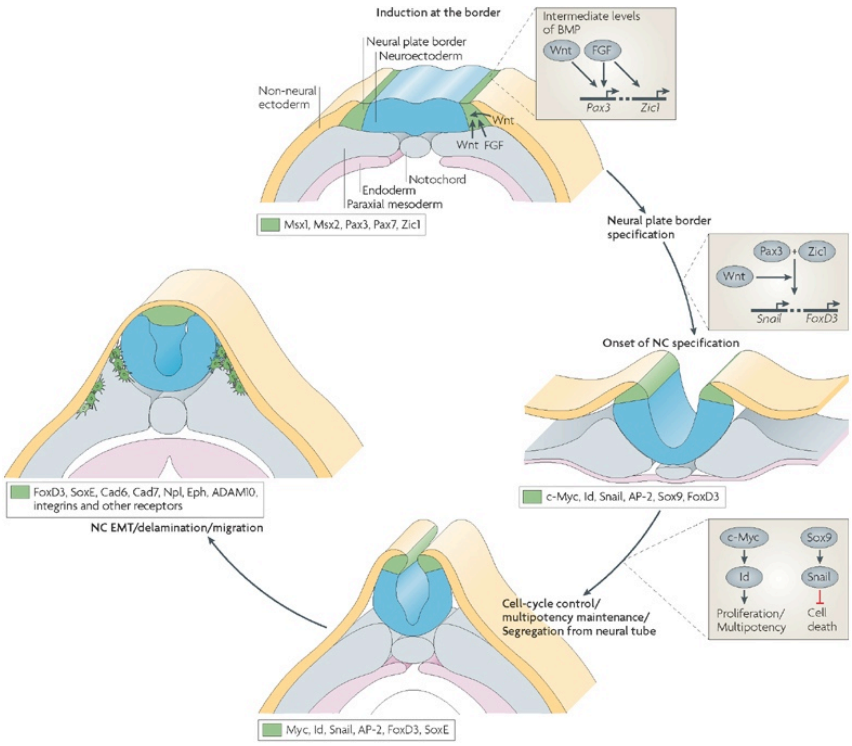

Figure 02. Regulatory mechanisms during neural crest development. From induction to migration, the formation of the neural crest succumbs a tight gene regulatory network. During neural crest induction WNT, FGF and BMP induce the expression of PAX3 and ZIC1. These factors activate the expression of SNAIL1 and FOXD3 to initiate neural crest specification. Subsequently, neural crest cells undergo EMT, delaminate from the neural crest and migrate throughout the embryo to reach their sites of specification [Sauka-Spengler_2008].

3.1.2. Molecular signaling cues during neural crest induction

The induction of the neural crest mainly occurs in response to instructive signaling molecules emanating from adjacent tissues, such as the mesoderm or the neural and epidermal ectoderm. As a consequence of the external influence, a class of transcription factors is activated and initiates the separation of prospective neural crest cells from other neural plate border cells [Basch_2006]. This tightly controlled transcriptional network allows future neural crest cells to control the acquisition of self-renewal, multipotency and the competence to respond to later neural crest-specifying signals. Despite differences between species, neural crest inducing signals appear similar and comprise secreted ligands, such as bone morphogenetic proteins (BMPs), Wingless-type proteins (WNTs), and fibroblast growth factors (FGFs) [Knecht_2002].

While high levels of BMP are necessary for the acquisition of epidermal fate, neural development requires BMP inhibition [LaBonne_1998]. Consequently, the neural plate border is exposed to intermediate levels of BMP signals, as a result of diffusing signaling molecules from the ectoderm. Although BMP signaling is required for neural crest induction, intermediate levels of BMPs alone, are not sufficient to induce neural crest cell markers [Knecht_2002, Nguyen_1998]. Several gain- and loss-of-function experiments in different species have shown the importance of WNT signaling in neural crest development [Garcia-Castro_2002; LaBonne_1998; Lewis_2004]. However, none of the performed experiments addressed the role of WNTs in early neural crest induction during gastrulation. Hence, it remains unknown whether WNT signaling plays an inductive part at early stages. It is difficult to draw a definite conclusion about the role of FGFs in neural crest induction, as the requirement for FGF signaling varies among species. In *Xenopus*, the mesoderm-derived FGF ligands up regulate the expression of early neural crest cell marker, SNAIL2 also known as SLUG [Mayor_1997; Villanueva_2002]. Nevertheless, in mouse or zebrafish, neural crest cells develop normally despite absent FGF signaling [Noden_2005]. Moreover, it is speculated whether local cell-cell signals such as NOTCH/DELTA might be involved during the induction of the neural crest [Endo_2002; Glavic_2004; Williams_1995].

3.1.3. Molecular signaling cues during neural crest specification

Under the influence of external neural crest specifying signals during early neurulation, the area between neural and epidermal ectoderm starts to express so-called neural plate border specifiers. Among those there are homeobox transcription factors such as MSX1/2, DLX5, PAX3/7, GBX2 and the zinc finger-containing ZIC proteins [Monsoro-Burq_2005; Tribulo_2003; Sato_2005; Hong_2007; Luo_2001; Woda_2003]. Upon expression of neural plate border specifiers, presumptive neural crest cells acquire competence to respond to later neural crest specifying signals.

The transcriptional network that controls the process of specification in premigratory and delaminating neural crest progenitor cells is defined by the expression of so-termed neural crest specifier genes. At early neurula stage, neural plate border genes either directly or indirectly regulate the expression of neural crest specifiers such as AP2α, SNAIL1/2, ID, c-MYC and TWIST [Meulemans_2004; Sato_2005; Tribulo_2003; Nikitina_2009; Sauka-Spengler_2008]. It has been proposed, that during the specification process neural crest specifiers play different roles. Thus, SNAIL2 for example has been shown to take over key functions during EMT, while c-MYC and ID maintain neural crest cells in a multipotent state, mediating critical cell cycle and cell fate decisions [LaBonne_2000; Barrio_2002; Bellmeyer_2003; Kee_2005; Light_2005]. Furthermore, c-MYC and AP2α directly regulate ID expression implicating their role in cross-regulating other neural crest specifiers [Nikitina_2008]. At the time of delamination, neural crest fate acquisition is defined by the expression of SNAIL2, FOXD3, SOX9, ETS1, c-MYB and SOX10, while the latter persists in migrating and differentiating neural crest cells. Whereas the winged-helix transcription factor FOXD3 was shown to maintain neural crest multipotency by preventing early differentiation, the functions of ETS1 and c-MYB, though only specific to the cranial crest, are implicated in SOX10 activation [Betancur_2010; Lister_2006; Théveneau_2007].

Summarizing, the specification process is a key event during neural crest development, where external signals mediated by neural plate border specifiers induce a collective interplay of neural crest specifier

genes. These transcription factors in turn orchestrate the expression of downstream effectors that allow neural crest cells to acquire their ultimate migratory and multipotent properties.

3.1.4. Molecular signaling cues during neural crest migration

In order to delaminate from the neuroepithelium and emigrate from the dorsal margin of the neural tube, premigratory neural crest cells lose their compact organization and acquire motility. This so-called EMT process affects changes on a cellular level that include switches in cell junctions and adhesion properties as well as cytoskeletal rearrangements. As a consequence of the cellular conversion, migrating neural crest cells acquire a flat, mesenchymal morphology and start to form filopodia and lamellipodia [Coles_2007].

On a molecular scale, a major characteristic of EMT is defined by the switch in cadherin expression that involves down regulation of type I cadherins such as E- and N-cadherin (CDH1/2) and up regulation of type II cadherins as for example cadherin 7 (CDH7). It has been shown that in response to BMP signaling, SMAD-interacting protein 1 (SIP1), which is expressed in premigratory and migratory neural crest cells, leads to CDH1 repression [Comijn_2001]. Moreover, CDH1 and CDH2 expressions are negatively regulated by SNAIL1 and SOX10, respectively [Cano_2000]. On the other hand, though a direct gene regulatory interaction has not been demonstrated, it is evident that FOXD3 and SOX10 induce the expression of CDH7 and β1 integrin (ITGB1), another factor up regulated upon EMT [Cheung_2005]. Although many of the neural crest specifiers persist during migration, the upstream modulators may vary among the different time points. Hence, it has been shown that during migration SOX10 is directly regulated by FOXD3, AP2α and SOX9 but also receives inputs from the WNT signaling pathway [Werner_2007].

As neural crest cells synchronously leave the dorsal neural tube in S Phase, EMT and migration are tightly linked to cell cycle. It is proposed that this coordinated interplay between delamination and cell cycle progression is regulated by BMP-dependent WNT signaling. It has been demonstrated that

WNT-mediated activation of the transcription factor TCF/LEF is crucial for G1/S transition in neural crest cells most likely through modulation of cyclin D1 [Burstyn-Cohen_2002].

During migration, semaphorins represent important extracellular signaling molecules guiding neural crest cells to the right target site. Semaphorins define the migratory routes as they either attract cells by providing a permissive environment for migration or repel cells and thereby create crest-free zones. Hence, migrating neural crest cells express the corresponding receptors neuropilin 1/2 (NRP1/2) and co-receptors plexin A1 (PLXNA1) [Osborne_2005]. Moreover, ephrins represent a further group of signaling molecules that are involved in directing and maintaining the migratory streams [Mellott_2008].

3.1.5. Molecular signaling cues during neural crest differentiation

After neural crest cells have reached their sites of destination, usually, the expression of early neural crest specifier genes, such as SNAIL1/2, FOXD3, ID and AP2α is down regulated [Meulemans_2004]. However, the SRY-related HMG-box family E (SOXE) transcription factors, SOX9 and SOX10 display remarkable exceptions as they persist in specific subgroups of neural crest derivatives and appear to be master regulators of terminal differentiation [Kelsh_2006]. Although this sustained expression seems paradoxical, it might be explained by the fact that over time transcription factors take over multiple functions, as it has been demonstrated for SOX10. Thus, dependent on the concentration, low SOX10 levels maintain multipotency in migratory neural crest cells, whereas high SOX10 levels inhibit neuronal differentiation and promote melanocytic and glial differentiation [Kim_2003; Paratore_2001]. Alternatively, it is conceivable that SOX9 and SOX10 gain novel instructive roles during fate determination through acquisition of novel interaction partners.

3.1.6. The cranial neural crest

During embryogenesis, the neural crest develops along the neural axis from cranial to caudal in a spatially and temporally deferred manner. Consequently, a neural crest cell turns into the corresponding type of derivative depending on the axial level and the time of emigration. As outlined above, the process of differentiation involves cell intrinsic as well as extrinsic signaling cues. Therefore, it is evident that the surrounding microenvironment has a major impact on the differentiation outcome of an invading neural crest cell (Figure 3).

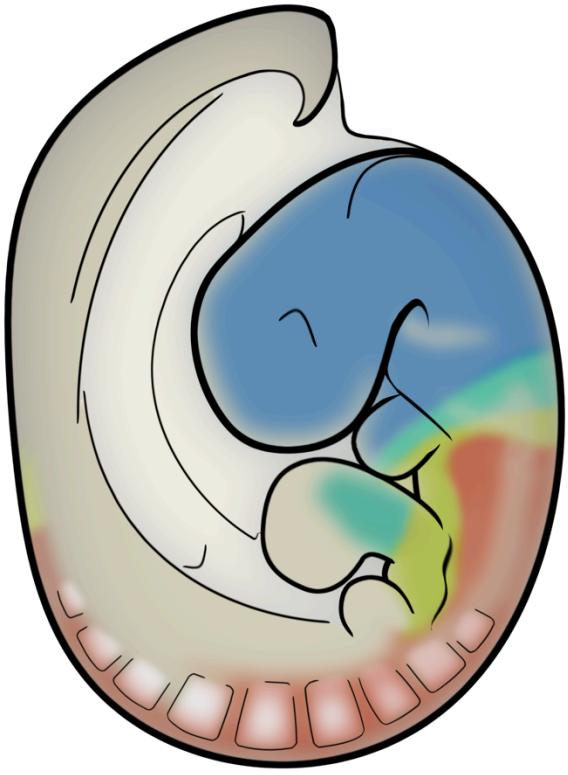

Figure 03. Axial specificity of the neural crest. The neural crest develops from cranial to caudal in a spatially and temporally deferred manner. Cranial neural crest cells (blue) give rise to skeletal structures of the face, cardiac neural crest cells (green) contribute to the proximal outflow tract of the heart, while vagal neural crest cells (yellow) populate the gut and establish the enteric nervous system. Trunk neural crest cells (red) become nerve and glia cells of the peripheral nervous system, form cells of the adrenal medulla and give rise to melanocytes [graphical illustration; Mario Bonalli_2016].

In the cranial region, the formation of the pharyngeal (or branchial) arches represents a prerequisite structure for the developing craniofacial elements, characterized by a complex interplay of all four germ layers including neural crest cells from different cranial levels. Thus, neural crest cells originat-

ing from the midbrain and rhombomeres 1 and 2 (r1 & r2) give rise to neurons and glia of the trigeminal ganglion as well as the skeleton of the upper and lower jaw. Neural crest cells from r4 generate neurons of the proximal facial ganglion and the hyoid bone. Furthermore, postotic crest streams from r6 and r7 become neurons of the proximal and jugular ganglia and skeletal components of the postpharyngeal arches [Graham_2004; Lumsden_1991; Schilling_1994]. In addition to the location, the time of emigration also influences the differentiation process. Hence, early migrating cells populate the pharyngeal arches to generate bone, cartilage and connective tissue (skeletal structures), whereas the later migrating cells generate neurons and glia of the cranial ganglia [Graham_2004]. In a spatially and temporally distinct emigration stream, neural crest cells populate the embryonic epidermis and give rise to melanocytes. As epidermal pigment cells are generated similarly along the entire neural axis, melanocyte differentiation will be discussed in a separate section [3.1.9.].

Dissecting the molecular circuits in the cranial neural crest reveals that during chondrocyte development, SOX9 directly regulates expression of important cartilage markers such as collagen type II α1 (COL2A1), COL11A2, and cartilage-derived retinoic acid-sensitive protein (CD RAP) [Lefebvre_1997; Bridgewater_1998; Xie_1999]. Furthermore, it has been shown that TGF-β-mediated suppression of SOX10 is necessary for neural crest cells to generate mesenchymal progenitors [John_2011]. On the other hand, SOX10 is crucial in neuronal and glial fate specification and might participate in glial end-stage differentiation, as its expression persists within this lineage [Kelsh_2006]. It has been demonstrated that SOX10 directly regulates the expression of major components of the myelination process, such as protein zero (P0), myelin basic protein (MBP), peripheral myelin protein 22, and the gap junction protein connexin 32 (CX32) [Peirano_2000; Bondurand_2001]. In the presumptive trigeminal ganglion, neural crest cells might additionally receive NOTCH input signals that favor neuronal and glial lineage specification. Likewise to SOX10, NOTCH signaling promotes gliogenesis but inhibits neurogenesis [Nakamura_2000; Ohtsuka_1999]. Along this line, glial fibrillary acidic protein (GFAP) might function as direct NOTCH downstream effector gene mediated by HES1 and HES5 [Ijuin_2008; Jarriault_1995]. It is assumed that the regulatory mechanisms during neuronal differentiation are similar in cranial and trunk neural crest cells.

Therefore, neurogenesis will be discussed in the corresponding section [3.1.9.] on trunk neural crest differentiation, as most of the studies on neurogenic differentiation have been performed in trunk neural crest cells.

3.1.7. The cardiac neural crest

Cardiac neural crest cells originate from the posterior region of the otic placode [Kirby_1983]. They migrate through the circumpharyngeal ridge and invade the caudal pharyngeal arches 3, 4 and 6. Subsequently, neural crest cells populate the distal outflow tract cushions and from there a small population migrates to the proximal outflow tract or to the intraventricular septum where they form a sheath around the AV bundle [Kirby_1990]. Under the influence of TGF-β and BMP, crest cells of the distal and proximal outflow tract, undergo a mesenchymal differentiation into smooth muscle cells and form a condensed structure defined as the aorticopulmonary septation complex. Additionally, cardiac crest cells give rise to cardiac ganglia and support the development of the thymus and parathyroid gland [Kirby_1983; Bockman_1984]. However, the molecular mechanisms underlying the generation of these neural crest-derived structures are not yet fully understood.

3.1.8. The vagal and sacral neural crest

Vagal neural crest cells emigrate from the caudal hindbrain region and invade the foregut. In a rostral-to-caudal directed migration, vagal neural crest cells populate the entire gut except for the hindgut and generate the enteric nervous system (ENS). In a first wave, ENS precursors colonize the myenteric (outer) region of the gut, preceding an inward directed radial migration that colonizes the submucosal (inner) layer and an outward directed migration to the pancreas that forms ganglia near the islets of Langerhans [Lake_2013]. Later processes also include the invasion of sacral neural crest cells into the epigastric part of the gut [Avetisyan_2015]. Enteric neural crest-derived cells differentiate into at least 20 neuronal subtypes or enteric glia and control gastrointestinal peristalsis, regulate blood flow, and modulate fluid secretion and absorption [Furness_2006].

On the molecular stage, migrating neural crest cells express the receptor tyrosine kinase RET in response to retinoic acid synthesized by the paraxial mesoderm, which has been shown to support survival, proliferation and migration [Simkin_2013]. This process is likely modulated by glial cell line-derived neurotrophic factor (GDNF) and its receptor GFRA1 through their direct interaction with RET [Enomoto_1998; Manié_2001]. Moreover, it has been shown that endothelin-3 (EDN3), a small (21-aa) vasoactive peptide that binds to a G-protein-coupled heptahelical receptor (EDNRB) is required for proper ENS development especially in the hindgut [Nagy_2006]. However, once neural crest cells have reached the foregut, there are no extrinsic signaling cues known so far that drive the rostrocaudal bowel colonization. Therefore, it is assumed that harmonized distribution throughout the gut is a consequence of competition for space and trophic factors driven by proliferation [Young_2014]. As enteric neural crest derivatives populate the bowel, they prefer to stay in contact with each other, a process called chained migration. It is suggested that this process is mediated by human L1 cell adhesion molecule (L1CAM) [Young_2014; Anderson_2010]. Furthermore, it was shown that matrix metalloproteinase-2 (MMP2) enhances bowel colonization, most probably by creating gaps in the extracellular matrix, thereby facilitating the migration process [Anderson_2010]. After enteric neural crest cells have completed rostrocaudal migration, they start to organize in ganglia, a process that is regulated by the expression of neural cell adhesion molecule 1 (NCAM1) [Faure_2007].

As mentioned previously, enteric neural crest derivatives give rise to over 20 different subtypes of neurons that differ in function, transmitter, neurite patterning, and electrophysiology. Therefore, it is conceivable, that a plethora of neurotrophic factors, morphogens, and transcriptional regulators orchestrate neuronal subtype specification. However, for most neuronal subtype, specific determinants driving their differentiation have not yet been identified [Furness_2006].

3.1.9. The trunk neural crest

In the trunk, neural crest migration is strongly dominated by the physical structures of the somites. The segmental organization of the somites guarantees the metameric formation of the peripheral nerv-

ous system (PNS). Thereby, somite-derived signaling inputs ensure the coordinated development of peripheral ganglia and nerves with skeletal structures of the trunk. Somites gather symmetrically along each side of the neural tube and the notochord. They are defined as an accumulation of cells from the paraxial mesoderm surrounded by an epithelial layer. Subsequently, somites divide into a ventral and a dorsal portion termed sclerotome and dermomyotome, respectively [Gammill_2010].

Comparable to the cranial neural crest, trunk neural crest cells leave the neural tube in a rostral-to-caudal temporally deferred manner and enter a variety of migratory routes. Initially, neural crest cells migrate around the ventral side of the somites or in between somites [Loring_1987; Teillet_1987]. Upon somite dissociation, neural crest cells begin to invade the sclerotome and migrate ventrolaterally. However, neural crest cells only traverse the rostral aspect of each somitic sclerotome [Bronner-Fraser_1986]. Finally, in a third migration wave, neural crest cells follow a dorsolateral pathway between the epidermal ectoderm and dermomyotome [Erickson_1992] (Figure 4).

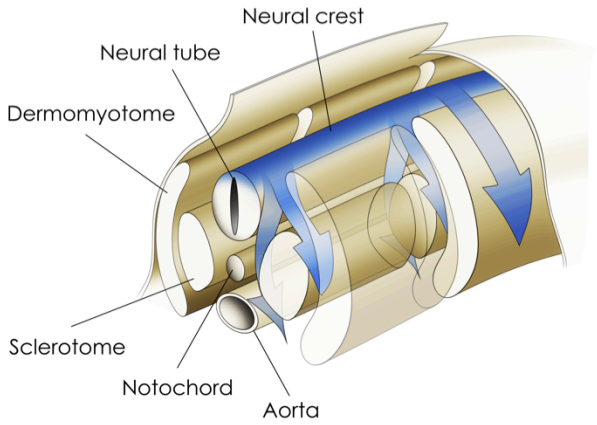

Figure 04. Trunk neural crest cells populate the embryo in different migratory streams. Trunk neural crest cells leave the neural tube from cranial-to-caudal in a temporally deferred manner. Initially, neural crest cells follow a ventral route and later switch to a ventrolateral pathway. Finally, neural crest cells migrate between the epidermal ectoderm and the dermomyotome on a dorsolateral path [graphical illustration; Mario Bonalli_2016].

During migration, environmental signaling cues guide trunk neural crest cells on predefined routes to their target site. Initially, crest cells simply follow blood vessels as they migrate through the intersomitic space, a process possibly mediated by ephrin B2 [Davy_2007]. Upon disconnection from the somite, the sclerotome becomes accessible to invasive neural crest cells. Sclerotome cells create a

permissive and migration-friendly extracellular matrix consistent of fibronectin, laminin and collagen [Duband_1987; Newgreen_1980]. Additionally, with dissociation of the sclerotome, neural crest cells start to express NRP1, thereby receiving repulsive SEMA3A signals from the dermomyotome and the intersomitic space [Schwarz_2009; Roffers-Agarwal_2009]. As a consequence, neural crest cells switch from the ventral to the ventrolateral migration path. Simultaneously, neural crest cells begin to express NRP2, the receptor of the repellent SEMA3F ligand, which is secreted by the caudal aspect of the sclerotome. This leads to the segmental organization of the migratory stream. Finally, it has been shown that ephrin and CXCL12/CXCR4 signaling, as well as other extracellular matrix components such as F-spondin, T-cadherin, and glycoproteins including aggrecan, versican and tenascin-C might influence the migratory behavior of trunk neural crest cells [Krull_1997; Rehimi_2008; Debby-Brafman_1999; Ranscht_1991; Perissinotto_2007; Dutt_2006; Tucker_1991].

It has been shown that the switch to the dorsolateral pathway does not depend on changes in environmental signaling cues but is neural crest cell autonomous and involves alterations in cell surface receptor expression [Erickson_1995]. During early migration, neural crest cell repulsion from the dermomyotome is exerted by the function of the ROBO receptor and its ligand SLIT. However, late migrating neural crest cells down regulate ROBO expression, thereby losing their responsiveness to repulsive signals, which allows them to invade the dermomyotome [Jia_2005]. In addition, the switch from repulsion to attraction seems to be further promoted by differentially expressed ephrin receptors in early and late migratory crest cells [Harris_2008].

There is conflicting data about, whether the path of migration instructs fate restriction or reflects predetermined lineage specification [Erickson_1995; Baggiolini_2015; George_2007]. However, pathway selection and fate acquisition are tightly coupled in neural crest cells. Thus, ventrally migrating neural crest cells are repelled by the notochord and gather at the dorsal aorta to form neurons and glia of the sympathetic ganglia as well as chromaffin cells of the adrenal medulla [Thiery_1982]. Under the influence of BMP2, a factor that is secreted by the dorsal aorta, neural crest cells differentiate into cholinergic neurons mediated by the basic helix-loop-helix transcription factor MASH1 [Guil-

lemot_1993]. However, neuronal differentiation is suppressed by glial growth factor (neuregulin), which directs differentiation towards a glial fate [Shah_1994; Shah_1996]. This mutually exclusive fate acquisition is a time dependent process, as neurogenesis usually occurs prior to gliogenesis. Additionally, it has been shown that NOTCH signaling instructs glial differentiation at the expense of a neuronal fate [Morrison_2000]. In the adrenal medulla, neural crest cells either develop into sympathetic ganglia or into adrenomedullary cells, as they encounter glucocorticoids secreted by cortical cells of the adrenal gland [Anderson_1986].

Neural crest cells taking the ventrolateral pathway invade and remain within the sclerotome, where they form sensory neurons and glia of the dorsal root ganglia and Schwann cells of the ventral roots [Kasemeier-Kulesa_2005]. In order to become sensory neurons, neural crest cells depend on WNT/β-catenin signaling (Hari_2002). The differentiation process is transcriptionally regulated by the basic helix-loop-helix protein neurogenin-2 (NRG2) that promotes expression of tyrosine receptor kinases TRKB and TRKC [Anderson_2001; Ma_1999]. Furthermore, it was shown that the POU-domain transcription factor BRN3A, a lineage specific marker for sensory neurons, is responsible for the maintenance of the sensory fate even in the presence of BMP2 [Greenwood_1999].

Neural crest cells that enter the dorsolateral pathway populate the epidermal ectoderm and give rise to melanocytes [Erickson_1995]. During migration, presumptive melanocyte progenitor cells that arise from the dorsomedial region of the neural tube express the receptor tyrosine kinase KIT. KIT-expressing neural crest cells migrate exclusively in the dorsolateral pathway and appear with a seemingly restricted fate towards a melanocytic fate [Wilson_2004]. Upon epidermal invasion, neural crest cells encounter WNT signaling proteins that inhibit neuronal development and promote melanocyte differentiation [Dorsky_1998]. Additionally, it has been shown that EDN3/EDNRB signaling is important during melanocyte differentiation. However, it is rather necessary for the dispersal and survival of melanocyte progenitors than for the initial specification process [Greenstein_1994; Lahav_1996]

3.1.10. Postmigratory neural crest cells

It has been shown that cells with neural crest stem cell-like properties are present throughout different developmental stages and even persist until late adulthood. Thus, a self-renewing neural crest stem cell-like population with differentiation potential was first identified in E14.5 rat sciatic nerve tissue using the neural crest stem cell marker $p75^{NTR}$ [Morrison_1999]. Succeeding this discovery, multipotent $p75^{NTR}$-positive cells with self-renewal capacity were isolated from the fetal and even more striking from the adult ENS [Bixby_2002; Kruger_2002]. To this day, postmigratory neural crest-like stem cells have been isolated from most if not all neural crest target organs, including sciatic nerve, ENS, DRG, bone marrow, skin, and heart [Morrison_1999; Bixby_2002; Kruger_2002; Hagedorn_1999; Nagoshi_2008; Wong_2006; Tomita_2005; Shakhova_2010] (Figure 5). Despite their differentiation and self-renewing potential, NCSCs display intrinsic differences with variable responses to microenvironmental signals dependent on their location and the developmental stage. While at early stages, WNT and BMP signaling regulates self-renewal of migratory NCSCs, postmigratory NCSCs lose their responsiveness to WNT and BMP and proliferation is regulated by the EGF signaling cascade mediated by small Rho GTPases [Kléber_2005; Fuchs_2009]. Furthermore, it was shown through BrdU incorporation experiments that the self-renewal capacity of neural crest-like stem cells decreases with age. Moreover, the differentiation potential from adult NCSCs differs substantially from the one of fetal NCSCs and gets seemingly restricted towards a distinct cell type [Bixby_2002; Kruger_2002]. Nonetheless, the sustained presence in adult tissue and the easy accessibility as for example in the skin makes postmigratory NCSCs a conceivable target for future therapeutic approaches in regenerative medicine.

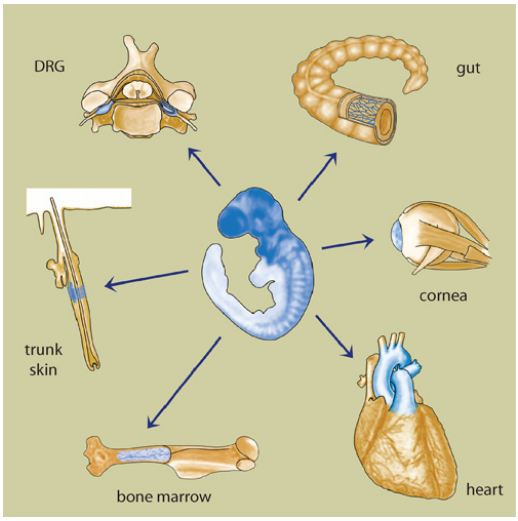

Figure 05. Neural crest stem cells in adult tissue. During adulthood, neural crest cells reside at their post-migratory locations and largely share the self-renewal and differentiation potential of their embryonic counter-parts. In adults, cells with neural crest stem cell-like features have been isolated in the gut, cornea, heart, bone marrow, skin and dorsal root ganglia [Shakhova_2010].

3.2. Melanocyte biology

Melanocytes are the pigment cells in our body and responsible for the production of melanin. Pigment cells arise from melanoblasts and, with exception of those in the retina, are of neural crest origin. Melanocytes are primarily responsible for our skin and hair color as they are located in the basal layer of the epidermis and in hair follicles. However, they can also be found in the uvea, inner ear, meninges, bones, and heart [Barden_1983; Markert_1956; Nichols_1969; Theriault_1970].

3.2.1. Melanocyte development

There are three transcriptional master regulators that dictate melanocyte development consistent of the basic helix-loop-helix leucine-zipper microphthalmia-associated transcription factor (MITF), PAX3, and SOX10. Loss of any of the above mentioned, results in failure of melanocytic development [Thomas_2008]. Furthermore, the forkhead box transcription factor FOXD3 regulates melanocyte differentiation through suppression of the melanocytic lineage at the expense of neurogenesis and gliogenesis. Thereby, FOXD3 acts as a transcriptional repressor that directly down regulates MITF expression [Ignatius_2008].

3.2.2. Microphthalmia-associated transcription factor (MITF)

Soon after emigration from the neural tube and well before entering the dorsolateral pathway, MITF is expressed in prospective melanocyte precursor cells. MITF expression is driven by the transcription factors SOX10 and PAX3 [Bondurand_2000]. In addition, MITF is up regulated by WNT3A in melanocytes [Takeda_2000]. It has been suggested that the WNT down stream effector, LEF1 binds to the MITF promoter in response to nuclear translocation of β-catenin [Dorsky_2000]. MITF and LEF1 then act synergistically to increase dopachrome tautomerase (DCT, also known as TYRP2) transcription [Yasumoto_2002]. Down regulation of FRZB-1, a secreted frizzled-related protein that competes with frizzled receptors for WNT-binding might as well be involved in WNT-mediated up regulation of

MITF [Jin_2001]. It has also been demonstrated that activation of KIT initiates phosphorylation of MITF and concomitant increase in transcriptional activity [Goding_2000]. Moreover, cyclic AMP (cAMP) signaling can up regulate MITF and induce melanogenesis. Nevertheless, this seems to be rather important in adult melanocytes but not for the initial activation of MITF expression [Ji_2005].

MITF expression is crucial for lineage specification and survival of melanoblasts [Kumasaka_2004; Lister; 1999; Nakayama_1998; Opdecamp_1997]. This might partially be explained by the observation that MITF up regulates TBX2, a member of the family of T-box transcription factors known to function in maintenance of cell identity [Carreira_2000]. MITF further controls melanocyte growth and survival by regulating BCL2, $p21^{Cip1}$, DIA1, and INK4A [MCgill_2002; Carreira_2005; Carreira_2006; Loercher_2005]. Additionally, MITF directly regulates many of the genes required for melanogenesis, including tyrosinase, tyrosinase-related protein 1 (TYRP1), and DCT by binding to E-box and M-box elements in their conserved regulatory regions [Aksan_1998]. Finally, MITF regulates the expression of premelanosome protein (PMEL, also called SILVER), protein melan-A (MLANA, also called MART-1), absent in melanoma 1 protein (AIM1), melanocortin 1 receptor (MC1R) and KIT [Baxter_2003; Du_2003; Du_2002; Aoki_2002; Tsujimura_1996].

3.2.3. Melanogenesis

Melanin, the principal product of melanocytes, is an effective absorber of light and dissipates over 99.9% of the UV radiation [Meredith_2004]. Secondly, melanin is a potent scavenger for free radicals, thereby protecting skin cells from high levels of reactive oxygen species that would otherwise damage DNA [Meredith_2006]. Once synthesized, melanin is stored in lysosome-related organelles, termed melanosomes, which are transported along dendrites and delivered to adjacent keratinocytes [Wasmeier_2008]. Generally, melanin is produced by oxidation of the amino acid tyrosine with subsequent polymerization. There are three basic types of melanin. The most common are brown and black eumelanin, which chemically differ from each other in their pattern of polymeric bonds [Meredith_2006]. Pheomelanin, responsible for the red hair phenotype, is distinct from eumelanin as it in-

corporates benzothiazine into its oligomer structure [Greco_2011]. Neuromelanin is a dark polymer pigment and can be found in catecholaminergic neurons in the brain. However, the exact function of neuromelanin has not yet been described [Fedorow_2005].

Melanogenesis is a tightly regulated process including a multitude of intrinsic and extrinsic factors that guarantee a concerted interplay between melanocytes and keratinocytes in response to external stimuli, such as UV radiation. Hence, aberrant melanin synthesis due to deficient melanogenic enzymes causes pigmentation disorders such as albinism or cutaneous hyper- and hypopigmentation [Lin_2007]. Melanogenesis is initiated upon activation of MC1R mediated by melanin stimulating hormone (αMSH) and adrenocorticotropic hormone (ACTH). This leads to the transcriptional activation of tyrosinase and tyrosinase-related proteins, TYRP1 and DCT [Abdel-Malek_1995]. Tyrosinase is responsible for the conversion of L-tyrosine to dopaquinone, which serves as substrate for both, eumelanin and pheomelanin [Cooksey_1997]. Internal cyclization leads to the conversion of dopaquinone to dopachrome and DOPA. Dopachrome is then further rearranged to 5,6-dihydroxyindole (DHI) and to a lesser extent to 5,6-dihydroxyindole-2-carboxylic acid (DHICA). Enzymatic turnover from dopachrome to DHICA is catalyzed by DCT. Finally, DHI and DHICA are further oxidized and polymerized to produce eumelanin. The oxidation of DHICA is enzymatically controlled by TYRP1 or tyrosinase [Edge_2006] (Figure 6).

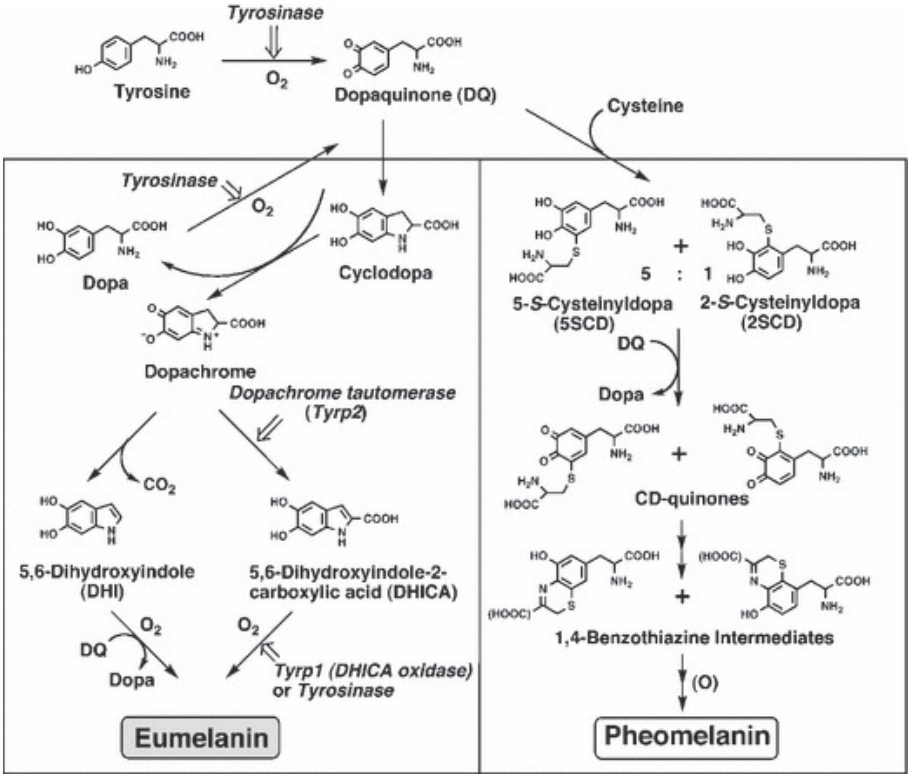

Figure 06. Synthesis of eumelanin is enzymatically controlled by tyrosinase, DCT and TYRP1. At the onset of eumelanin synthesis tyrosinase converts L-tyrosine into dopaquinone, which is internally converted into dopachrome and DOPA. Dopachrome is then rearranged to DHI and with the catalytic support from DCT to DHICA. Finally, DHI and DHICA are oxidized to eumelanin under the enzymatic control of TYRP1 or tyrosinase [D'Ischia_2015].

3.2.4. Melanocyte stem cells

The skin represents one of the most regenerative organs in the body. Every day millions of epidermal skin cells as well as hair are generated and both of which have to be repigmented in an identical manner. In order to overcome this daily challenge, keratinocyte and melanocyte stem cells in concert have to succumb a fine-adjusted regeneration regime that governs self-renewal and differentiation. Although, the coloration process is slightly different between skin and hair, the principles are largely the same- melanin has to be transferred from a melanocyte to a newly produced keratinocyte.

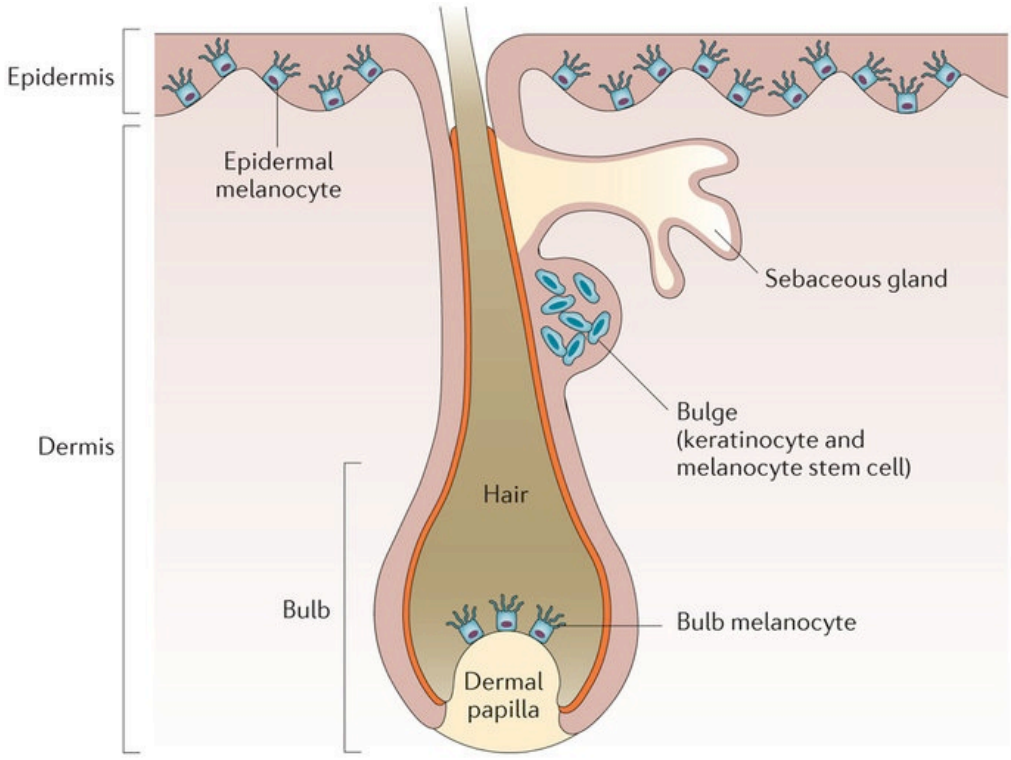

Figure 07. Melanocyte stem cells localize to the hair bulge region. Keratinocyte and melanocyte stem cells have been localized to the hair bulge region, whereas differentiated melanocytes are found in the dermal papilla. While in humans differentiated melanocytes can also be found in the epidermis, the mouse epidermis is free of melanocytes [Picardo_2015].

Previously, keratinocyte and melanocyte stem cells have been localized to the bulge region of the hair follicle [Nishimura_2002; Oshima_2001] (Figure 7). Melanocyte stem cells were identified as DCT positive and slow cycling BrdU-incorporating cell population that features general stem cell characteristics, such as self-renewal and multipotency [Nishimura_2002; Cotsarelis_1990]. In a gene expression profile analysis, differentiated melanocytes from the bulb were compared to bulge melanocyte stem cells. Surprisingly, melanocyte stem cells were only positive for DCT and PAX3 but negative for tyrosinase, PMEL, TYRP1, KIT, MITF, SOX10 and MC1R [Osawa_2005]. These results indicate that despite of their neural crest origin, melanocyte stem cells have a quite distinct expression profile from that of differentiated melanocytes or embryonic melanoblasts.

Investigations on the underlying molecular mechanisms controlling melanocyte stem cell maintenance and differentiation have revealed that MITF and PAX3 bind to the same enhancer element in the DCT promoter, which is located nearby a LEF1-binding site. Even though PAX3 promotes MITF expres-

sion, it is a strong repressor of DCT. Thus, PAX3 and MITF act as competitors on the DCT promoter. This competition is released as in response to WNT activation β-catenin binds to the LEF1-target site. In other words, low WNT signaling activity maintains the stem cell in an undifferentiated state, whereas activated WNT signaling relieves PAX3-mediated repression of the DCT promoter, which induces terminal differentiation [Lang_2005]. In contrast to WNT-induced differentiation, TGF-β signaling retains melanocyte stem cells in a rather quiescent and undifferentiated state [Nishimura_2010]. Furthermore, it was demonstrated that disruption of the canonical NOTCH signaling pathway prevents melanocyte stem cells from self-renewing, which concomitantly leads to hair graying [Wang_2011].

Although the stem cell source responsible for hair shaft pigmentation was recently detected in the hair bulge, the location of the epidermal melanocyte stem cell compartment is still not identified. One option is that the epidermis either shelters its own, so far unidentified stem cell niche or it receives melanocytes from the bulge region likewise to the hair follicle. In contrast to humans, mouse skin is usually unpigmented. In K14-SLF mice however, ectopic expression of KIT ligand in keratinocytes leads to epidermal melanocyte colonization, analogues to human skin. It has been observed that melanocyte stem cells emigrate from the bulge region and populate stem cell niches in the epidermis. Although this does not definitively prove the mutual origin of melanocytes, it is at least an intriguing indication that the bulge region might serve as a common source for melanocytes of the epidermis and the hair follicle [Nishimura_2002].

3.3. Neurocristopathies

Neurocristopathies are defined as a diverse class of pathologies that arise from cells that commonly derive from the neural crest. The expression was coined by the physician Robert P. Bolande in 1974, who tried to denote a group of different diseases having a common origin in the neural crest [Bolande_1974]. Due to the fact that the neural crest originates a plethora of different cell types and tissues, diseases arising from the neural crest are particularly diverse in clinical presentation. They include congenital syndromes as well as acquired neoplastic disorders affecting endocrinological or neurological organs, skin, heart or the digestive tract [Bolande_1997]. The following sections describe only a small selection of neurocristopathies and are by no means exhaustive.

3.3.1. Waardenburg syndrome

Waardenburg syndrome is a rare, usually autosomal dominant hereditary disease that is mainly the result of cranial crest dysgenesis. The disease is characterized by dystopia canthorum, unilateral or bilateral hearing impairment, heterochromia iridis, synophrys, white forelock, and patchy hypopigmentation. Severe forms further comprise microcephaly, mental retardation, and skeletal malformations [Read_1997]. Furthermore, Waardenburg syndrome can be accompanied by other neurocristopathies, such as Hirschsprung's disease or piebaldism [Shah_1981]. Waardenburg's disease has been shown to result from mutations in the PAX3, SOX10, EDN3, EDNRB, MITF, and SLUG genes. These genes primarily affect migration and differentiation of melanoblasts but also glial cells [Pingault_2010]. At present there is no disease-curing treatment available. Therapy is mainly directed towards specific symptoms and involves cosmetic corrections and treatment of deafness, which is in correspondence with the treatment of any other form of irreversible deafness [www.rarediseases.org].

3.3.2. Hirschsprung's disease

Hirschsprung's disease describes a heterogeneous group of disorders characterized by absent or dysfunctional enteric innervation in the hindgut region ultimately leading to a megacolon in the antecedent parts of the bowel. In most cases the defect involves only the myenteric and submucosal plexuses of the most distal colon and does not extend above the rectosigmoid colon [McKeown_2013]. The aganglionic or hypoganglionic colon segment is narrowed and spastic due to the lack of inhibitory signals from the intrinsic nervous system, while external excitatory signals cause constriction and finally constipation [Kubota_2002]. Hirschsprung's disease is usually diagnosed shortly after birth because of the presence of megacolon or because of the delayed departure of the meconium (first stool), which normally passes within the first 24 hours [Kapur_2009]. Pathophysiologically, the most accepted theory suggests a defect in the rostrocaudal migration of neural crest derived cells [Druckenbrod_2009]. It is further debated whether erroneous differentiation or increased apoptotic events might contribute to the onset of the disorder [Uesaka_2010]. The RET gene has been identified as a major susceptibility gene as it was mutated in 80% of all mutations associated with Hirschsprung's disease [Emison_2010]. However, further disease-causing mutations have been found in EDNRB, EDN3, GDNF, and L1CAM genes, or when part of the Waardenburg syndrome, also in the SOX10 gene locus. Nonetheless, the incidence of these mutations is at much lower rate [Amiel_1996; Heanue_2007; Griseri_2009; Bondurand_2007]. At present, the only available treatment involves surgical removal of the dysfunctional bowel. Instead, cell transplantation therapy was proposed as an alternative to surgical resection. However, cellular resubstitution treatments have not yet found their way into clinical application and require further investigations [Metzger_2009].

3.3.3. DiGeorge syndrome

The DiGeorge syndrome, another term for 22q11.2 deletion syndrome, consists of agenesis or hypoplasia of the thymus and parathyroid glands, conotruncal abnormalities of the heart, and craniofacial dysmorphism [Kobrynski_2007]. Affected patients often suffer from chronic recurrent infections, due

to the absent or hypoplastic thymus, which concomitantly leads to an impaired T-cell response [Maggadottir_2013]. Cardiac malformations generally comprise tetralogy of Fallot, interrupted aortic arch, truncus arteriosus, ventricular septal defect, transposition of the great vessels, and right aortic arch [Keyte_2012]. Moreover, the non-functional parathyroid gland causes hypocalcemia due to low levels of parathyroid hormone. This frequently leads to convulsions in newborns and serves, besides present heart defects, as a first indication of the disease. Cranial abnormalities may include a long face, hypertelorism, malar flattening and velopharyngeal incompetence with or without cleft palate [Hacihamdioglu_2015]. Patients might additionally suffer from learning difficulties, psychiatric disorders and bear a significantly elevated risk to develop schizophrenia [Van Amelsvoort_2004]. Although the deletion can be inherited in an autosomal dominant manner, in most cases the mutation is acquired de novo. As a consequence of the incomplete genetic penetrance the syndrome is characterized by a marked variability in clinical expressions [Ryan_1997]. Therefore, early diagnosis of DiGeorge syndrome can be difficult and is commonly suspected in patients with more than one symptom present [Fernandez_2005]. Due to the presence of numerous chromosome-specific low copy number repeats or segmental duplications, the 22q11 region is very unstable and therefore prone to rearrangements during germ cell formation [Edelmann_1999]. The waste majority of the patients have a 3 Mb microdeletion, which affects approximately 40 – 50 genes, many of which have not been well characterized [Kobrynski_2007]. The exact molecular pathomechanism has proven to be of highest complexity and therefore has not yet been entirely understood. It is well conceivable that several of the deleted genes contribute to the entire manifestation of the syndrome. Nevertheless, TBX1 has been supposed as one of the major driver responsible for many, still not for all of the symptoms present in DiGeorge syndrome [Packham_2002]. Furthermore, it has been proposed that TGF-β signaling plays an important role during the onset of the disease. Hence, conditional ablation of TGF-β receptor II (TβRII) in neural crest cells mimics the clinical appearance of DiGeorge syndrome in mice. It was shown that TGF-β signaling controls expression of CRK like proto-oncogene, adaptor protein (CRKL), a gene that is commonly affected by the 22q11.2 deletion. Accordingly, CRKL depletion in mice causes a phenotype reminiscent of the human DiGeorge syndrome [Wurdak_2004]. To this day, there is no cure

known for the 22q11.2 deletion syndrome. Therapy is generally directed towards individual symptoms using standard methods [Hacihamdioglu_2015].

3.3.4. Giant congenital melanocytic nevus

Giant congenital melanocytic nevi (GCMN) are benign hyperplastic melanocytic lesions present at birth or within the first few month of life that reach a diameter >20 cm in adult life. In general, melanocytic nevi describe accumulations of nevus cells clustered as nests in the epidermis, dermis or in other tissues. GCMN usually present as brown lesions with flat or rugose surface, well-demarcated borders and hypertrichosis. Although any localization in the skin can be affected, GCMN are most commonly found in parts of the trunk, head or neck [Lyon_2010; Kincannon_1999]. Apart from the clinical and psychological implications, the most significant feature of GCMN is the associated risk to develop other malignancies such as melanoma, rhabdomyosarcoma, peripheral nerve sheath tumor or in rare cases neurocutaneous melanocytosis [DeDavid_1997; Hoang_2002; DeDavid_1996]. The exact pathomechanism for GCMN has not yet been completely resolved. It is suggested that during embryonic development melanoblasts acquire somatic mutations that induce excessive prenatal proliferation. Consequently, giant congenital nevus cells have been primarily reported with gain-of-function mutations in the neuroblastoma retrovirus-associated DNA sequence (N-RAS) locus, which leads to permanent stimulation of the mitogen-activated kinase (MAPK) pathway [Bauer_2007]. Along this line, ectopic expression of the constitutive active N-RAS^{Q61K} oncogene in the melanocytic lineage of mice results in dermal melanocytic hyperplasia and occasionally in melanoma [Ackermann_2005; Shakhova_2012]. At the moment, surgical intervention represents the only available treatment. However, patients suffering from GCMN might additionally require psychological support [Viana_2013].

3.3.5. Neoplastic neurocristopathies

In contrast to congenital neurocristopathies, acquired neurocristopathies emerge later in life, and among others, include neural crest-derived tumorigenic transformations. Accordingly, neoplastic neu-

rocristopathies comprise malignancies from peripheral and cranial nerves (e.g. peripheral nerve sheath tumor), sympathetic nerves (e.g. neuroblastoma), chromaffin cells of the adrenal medulla (e.g. pheochromocytoma), parafollicular cells of the thyroid gland (e.g. medullary thyroid carcinoma), or cells of the melanocytic lineage (e.g. melanoma), which will be discussed in detail in the following sections [Maguire_2015].

3.4. Melanoma

Melanoma is a neural crest-derived neoplasia that is generally defined as cancer of the melanocytic lineage [Gray-Schopfer_2007]. However, the origin of melanoma is highly controversial. It is assumed that melanoma cells arise from melanocytes or nevus cells, but hypothetically they might also derive from melanocyte stem cells, adult neural crest-like stem cells, or even from glial progenitor cells present in the peripheral nerve sheath. Thus, it is well conceivable that melanoma originates from various different cell types that are not primarily restricted to the melanocytic lineage [Debbache_unpublished data]. Therefore, melanoma might rather be used as an umbrella term that, regardless of its cellular origin, describes a specific clinicopathological disease pattern.

3.4.1. Epidemiology

Melanoma is the most fatal form of skin cancer and advanced-stage cutaneous melanoma has a median survival time of less than 1 year. Unfortunately, the incidence of melanoma is continuously increasing worldwide. Indeed, the incidence rate in the Caucasian population augments annually by 3-7% [Parkin_2001]. The rationales may be found in the better and earlier detection of melanomas and enhanced public awareness. However, it may also be attributed to a change in the sun-seeking behavior, which goes along with increased exposure to natural and artificial UV radiation [Elwood_1997]. Typically, primary melanomas occur in the skin (cutaneous; 91.2%) but they can also be found in the mouth (mucosal; 1.3%), eye (ocular; 5.2%), or without a known primary tumor (2.2%) [Chang_1998; McLaughlin_2005]. Yet another special form of melanoma describes the acral lentiginous subtype that affects non hair-bearing surfaces, such as palms, soles, nail beds, or oral mucosa [Erdei_2010] (Figure 8).

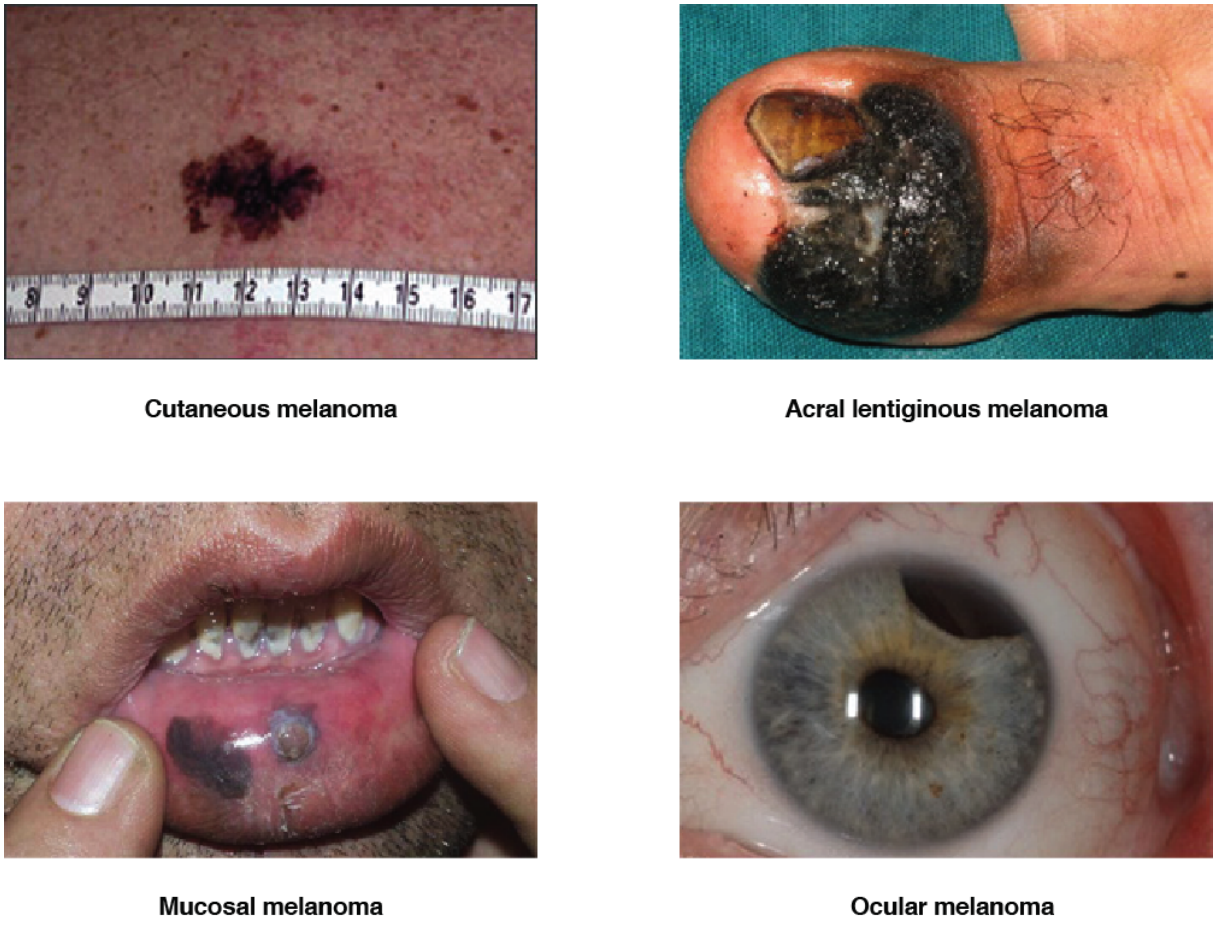

Figure 08. Clinical classification of melanoma. Melanomas are clinically classified according to their localization in the body. Cutaneous melanomas affect the skin and represent the most common form among all subtypes. Acral lentiginous melanomas are less frequent and occur in non hair-bearing regions of the skin. Mucosal and ocular melanomas also represent rare melanoma subtypes and emerge from melanocytes located in the mouth and eye, respectively [adapted from Rager_2005; Disky_2008; Swagata_2011; Mellen_2013]

According to studies from different developed countries, the incidence for cutaneous malignant melanoma in both genders ranks among the seven most common cancers or higher [Jemal_2011; Ferlay_2013; Parkin_2001]. Not surprising, the incidence rate for melanoma is highest in fair-skinned people, yet extremely rare among the black population, which in most cases present with the acral lentiginous subtype [Adegbidi_2007; Asuquo_2009]. The median age of melanoma patients at time of diagnosis is 52 years. In comparison, this is almost a decade before most other solid tumors arise (e.g. breast, colon, lung or prostate) [Hayat_2007; Tas_2011; Erdei_2010; Van der Velden_2009]. While, surgical intervention at early stages seems to prevent progression in most cases, patients with deep primary tumors and regional lymph node infiltration frequently develop distant metastases. Hence, median survival of patients with distant metastases is only 6-9 months, and the 5-year survival rate is

less than 5% [Houghton_2002]. General differences regarding gender singularities mainly concern the anatomical distribution of the lesions. Thus, in women melanoma is more often detected in the lower extremities, whereas in men lesions are more common in the head, neck and trunk region of the body [Bulliard_1997; Naldi_2005; Katalinic_2003]. Furthermore, it was shown that women have a survival advantage over men, as the mortality rate in male patients is twice as high as in female patients [Schmidt_2006].

3.4.2. Melanoma risk factors

Exposure to UV radiation is well accepted to be the major causative factor for melanoma [Elwood_1997]. UV exposure is tightly associated with the geographical location, which determines the distribution of the melanoma incidence. Additionally, the risk strongly underlies the pattern of sun exposure with highest risks for intermittent or cumulative UV exposure. The risk further depends on the frequency of excessive sun exposure and inherited susceptibility to its effects [Solomon_2004; Gandini_2005b]. However, the relationship between UV exposure and genetic factors is not well understood, since a UV footprint (specific UV-induced DNA damage pattern) is not always detected in melanoma tumors [Thomas_2006]. UVA as well as UVB are both considered as putative factors promoting skin carcinogenesis. Hence, independent of the applied UV spectrum, indoor tanning elevates the odds ratio for cutaneous malignant melanoma by 1.74 [Lazovich_2010]. The risk to develop melanoma at different body sites is associated with the amount and pattern of sun exposure. Consequently, recreational sun exposure with intermittent exposition strongly predicts melanoma on less frequently sun-exposed body sites such as the trunk. Occupational sun exposure that implies a continuous pattern increases the risk to develop melanoma on the head and neck. And finally, total sun exposure is associated with a higher risk of melanoma on the limbs [Chang_2009].

There are other risk factors besides UV exposure that influence the melanoma incidence rate, body localization and histopathological characterization of the lesions. These risk factors are associated with fair skin, blonde or red hair color, lifestyle, environmental factors, gender, social class, genetic predis-

position, or might be disease-related (e.g. benign or atypical nevi, xeroderma pigmentosum) [Miller_2006; Erdei_2010]. Moreover, risk factors might diverge among continents and different ethnic groups. Hence immunosuppression, inflammation, and albinism have been identified as specific risk factors in the African population [Asuquo_2009; Seleye-Fubara_2005].

3.4.3 UV-induced pathogenesis

Apart from causing DNA damage, UV radiation is engaged in many diverse cellular processes in the skin including Vitamin D synthesis, local production of growth factors, melanin synthesis, and immunosuppression [Gilchrest_1999]. The ultraviolet spectrum ranges from 200 – 400 nm and is divided into three categories based on the wavelength. While 95% of UVA and 1-10% of UVB reach the earth's surface, almost 100% of UVC is absorbed by the atmosphere and the ozone layer. Generally, UV radiation is absorbed in the skin by light sensitive macromolecules, such as proteins, lipids and nucleic acids. Thereby, UVB often causes direct damage to DNA, while UVA rather generates reactive oxygen species causing indirect oxidative DNA damage [Chen_2015]. As a consequence, UVA and UVB leave a specific mutational signature on the DNA dependent on the mechanism of damage. In particular, UVA-induced reactive oxygen species often generate 7,8-dihydro-8-oxoguanine (8-oxoG) lesions, which are susceptible to miss-repair and lead to G→T or G→A transversions [Garibyan_2010]. In contrast, photochemical reactions induced by UVB cause cyclobutane pyrimidine dimers, which as a result of incorrect repair lead to C→T and CC→TT transitions [Brash_1982]. Although most mutations remain without consequences for the cellular integrity, mutations within a gene that regulates apoptosis, cell cycle progression, DNA damage response, or similar may cause tumorigenic transformation.

3.4.4 Pathohistologic classification and tumor staging of cutaneous melanoma

In 1969, the first classification of primary cutaneous melanoma was established implementing detailed observations and descriptions of clinical and histopathological features. Until present, this scheme

forms the foundation of today's classification system and comprises the following clinical subtypes: superficial spreading melanoma (SSM), lentigo maligna melanoma (LMM), and nodular malignant melanoma (NMM) [Clark_1969]. By the time the classification scheme was expanded with other subtypes, such as acral lentiginous melanoma, mucosal lentiginous melanoma, spindle cell melanoma, desmoplastic melanoma and spitzoid melanoma [McGovern_1983] Weissinger_2014; Lee_2006]. SSM is the most common clinical subtype and accounts for over 70% of cases diagnosed in the Caucasian population. It presents as an irregularly shaped, flat or slightly elevated brown lesion with mottled pigmentation often more than 6 mm in diameter. Lentigo maligna *in situ* (LM) is a slow growing patch of discolored skin with irregular borders and pigmentation. LM often undergoes slow progressive changes and turns into LMM once it has acquired invasive behavior. NMM presents as a rapidly enlarging lump that mostly affects areas of the head and neck. One third of NMM is non-pigmented and might be ulcerated. While certain subtypes such as SSM, LMM and acral lentiginous melanoma follow the common ABCDE (asymmetry, border irregularity, color variation, diameter more than 6 mm, evolving) warning signs, others like NMM might not be detected using the ABCDE rules [McCourt_2014].

This classification system allows for the identification of clinically and histologically distinctive melanoma subtypes. However, this segregation does not allow for the discrimination of subtypes according to their clinical course or overall prognosis. Previously, Breslow's thickness was the most important prognostic factor for melanoma, measuring the depth from the basement membrane of the epidermis to the deepest identified melanoma tumor cell [Breslow_1970]. Nonetheless, Breslow's thickness was not part of the pathohistological classification, therefore a prognostic diagnosis was not possible [Duncan_2009]. For this reason the American Joint Committee on Cancer (AJCC) set up a new classification scheme that in part is based on the TNM staging system. The criteria that form the basis of the AJCC staging scheme include size or thickness of the tumor, mitotic rate and ulceration (T), number of lymph nodes affected (N), serum LDH levels and the presence and location of distant metastases (M). Stages I and II are discriminated by the size of the tumor, presence of ulcerations and mitotic rate, while in both stages regional lymph node and distant metastases are absent. Stage III is

defined by the presence of lymph node but not distant metastases, whereas in stage IV distant metastases are present. The AJCC staging system allows the segregation of patients based on their overall survival and is thereby much more predictive with respect to prognosis. Nevertheless, the AJCC classification system has its limitations, as the scheme does not allow predictions regarding susceptibility or outcome of a specific treatment [Balch_2004].

3.4.5. Melanoma progression model

Classically, melanoma progression is depicted as a linear model, following a strict series of events that ultimately ends in a stage of metastatic disease. This model emphasizes the multistep transition from melanocytes to melanoma based on observations in cutaneous pigmented lesions and was first proposed by Clark et al. in 1984. The first stage (I) in Clark's model of melanoma progression is defined by the formation of a benign precursor lesion (benign nevus or mole) from a melanocyte. This benign lesion then turns into a dysplastic nevus (II) that is larger in size and histopathologically reveals first cellular atypia. The next stage (III) is referred to as the radial growth phase or melanoma *in situ* characterized by a thin, radially growing lesion that expands within or close to the epidermis. The vertical growth phase (IV) is initiated with the breakthrough of the basement membrane and the formation of larger nests of dividing cells in the dermis. Upon dermal invasion melanoma cells get in contact with blood or lymph vessels, which ultimately allows intravasation and formation of metastatic lesions at distant sites (V). Clark's model further suggests that progression through each step is driven by the acquisition and accumulation of genetic or epigenetic changes [Clark_1984; Clark_1991; Miller_2006; Damsky_2013; Bennett_2016].

Nowadays, it is assumed that melanoma progression is much more complex and less linear as initially proposed by Clark et al. [Damsky_2011; Damsky_2013]. Thus, about 65-70% of melanomas develop *de-novo* in normal skin with no visible precursor lesion. In contrast, only 25-30% of melanomas are nevus-associated and less than half of them arise from dysplastic nevi [Bevona_2003; Lin_2015] (Figure 9). This indicates that in most cases melanoma forms *de-novo* and not from senescent nevi, which

is in contrast to the kinetics that were previously proposed by Clark et al. [Clark_1984]. Along this line, the lifetime risk of a particular nevus to undergo malignant transformation is only 1 in 7'000 [Hüsemann_2008]. Although melanocytic nevi are associated with increased risk for melanoma, the presence of multiple nevi might rather represent a symptom of an underlying genetic predisposition or a measure of frequent UV exposure [Gandini_2005a].

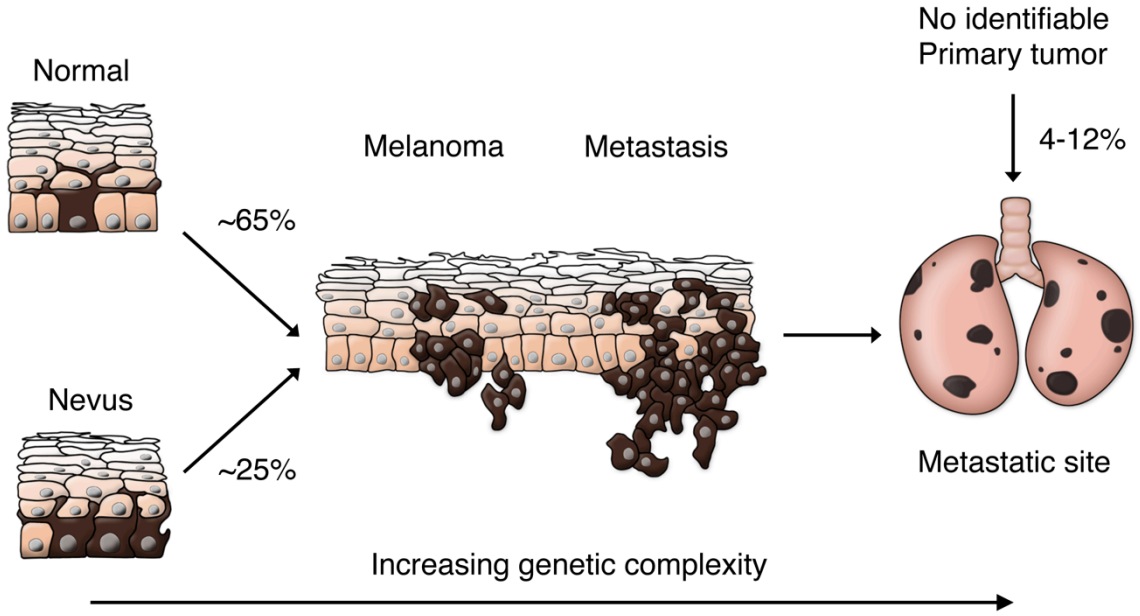

Figure 09. Origins of metastatic melanoma and melanoma progression. Melanoma either arises within a pre-existing melanocytic nevus, which is generally associated with a $BRAF^{V600E}$ mutation or without a visible primary lesion. Hence, up to 12% of the metastases found, have no identifiable cutaneous precursor lesion. Nonetheless, it is assumed that during the course of melanoma progression the genetic complexity increases [adapted from Damsky_2011].

Clark's course of progression predicts that metastasis only occurs after all previous steps have been completed. However, up to 12% of patients with metastatic melanoma do not have a clinically identifiable primary tumor [Clark_1984; Giuliano_1980; Reintgen_1983]. Interestingly, melanocytes can be detected in lymph nodes from normal, non-melanoma patients. These melanocyte clusters are referred to as nodal nevi and resemble benign melanocytic nevi in the skin. Although it is difficult to exclude that these cells are remnants of the embryonic colonization period, it is speculated that nodal nevus cells represent early descendants of benign melanocytic lesions [Bautista_1993; Carson_1996]. This led to the hypothesis that benign nevus cells are able to dissociate from the primary lesion long before

a tumor becomes clinically apparent [Hüsemann_2008; Rhim_2012; Damsky_2013]. After dissemination, melanoma precursor cells remain in a dormant state before progressing to a macrometastatic lesion. Premalignant dissemination might be a possible explanation why melanoma recurs in certain patients after excision of the primary tumor and why it recurs more often at distant sites [Balch_1993].

In conclusion, malignant transformation from a melanocyte to melanoma has traditionally been described using the Clark model. Although, this model best depicts SSM, it helps to understand the course of other melanoma subtypes. However, in most cases melanoma progression is much more complex and does not follow a linear and stepwise process initially proposed by Clark et al.

3.4.6. Molecular pathomechanisms in cutaneous melanoma

The course of neoplastic transformation from a melanocyte to malignant melanoma with metastasizing potential is usually initiated through acquisition of driver mutations in loci of proto-oncogenes. The MAPK pathway is the most prevalently affected signal transduction pathway that drives cell cycle progression and survival in melanoma (Figure 10). Thus, 95% of acquired nevi carry activity-enhancing mutations in members of the MAPK pathway, most (80%) of them in the v-raf murine sarcoma viral oncogene homolog B (BRAF) locus [Pollock_2003; Poynter_2006]. Despite activation of the MAPK pathway, nevi are typically equipped with a remarkably low proliferative potential and progression to melanoma is rare. The absence of progression is associated with a mechanism termed oncogene-induced senescence [Chandeck_2010]. It is suggested that permanent stimulation of the MAPK pathway increases inhibitor of cyclin-dependent kinase 4 ($p16^{INK4A}$) expression and activates acidic β-galactosidase, which finally results in proliferative cessation and senescence [Gray-Schopfer_2006; Michaloglou_2005; Peeper_2011]. Consequently, the acquisition of further mutations in cell cycle regulating genes such as cyclin-dependent kinase inhibitor 2A (CDKN2A), cyclin-dependent kinase 4 (CDK4) or transformation-related protein p53 (TRP53) are necessary to transform a benign nevus into a malignant melanoma [Box_2008; Sharpless_2003].

In general, melanoma has a very high mutational burden relative to other cancers, with a median of >10 mutations/Mb [Alexandrov_2013; Lawrence_2013]. Although the majority of genetic alterations associated with melanoma development are of somatic nature, not all mutations are *de-novo* acquired. Hence, a positive family history and the underlying presence of heritable risk genes is an important component of disease occurrence. Approximately 10% of melanoma cases are associated with a genetic predisposition. Increased familial susceptibility has been reported in conjunction with mutations in so-called high penetrance melanoma predisposition genes such as CDKN2A, CDK4, BRCA1 associated protein-1 (BAP1), protection of telomeres protein 1 (POT1), and telomerase reverse transcriptase (TERT) [Read_2015].

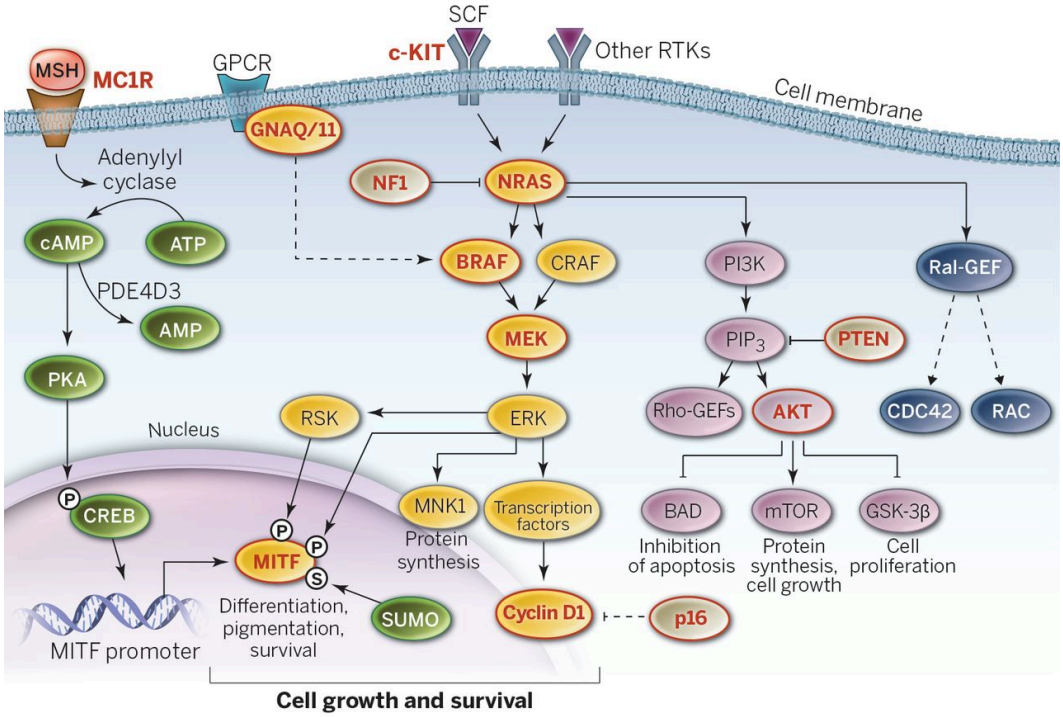

Figure 10. Molecular pathomechanisms in melanoma. In the vast majority of melanomas mutations affect components of the MAPK pathway. In a phosphorylation-dependent cascade growth-promoting signals are transferred from the cell surface to the nucleus. Most mutations in cutaneous melanomas cause constitutive activation of the BRAF or N-RAS kinases. However, in mucosal and acral lentiginous melanoma the receptor tyrosine kinase KIT is most commonly mutated, whereas in uveal melanomas mutations in the GNAQ/11 locus have been most frequently found to activate the MAPK pathway. Other mutations often lead to the activation of the PI3K/AKT pathway, which decreases apoptosis, prolongs cell survival and promotes cell cycle progression. Furthermore, inactivating mutations in cell cycle regulators, such as CDKN2A often confer resistance to oncogene-induced senescence and stimulate cells to re-enter the cell cycle. As the master transcriptional regulator of melanocytes, MITF is often affected in the course of melanoma progression. Hence, while increased MITF levels are associated with increased tumor growth, reduced MITF levels promote invasiveness [Lo_2014].

3.4.7. Mitogen-activated protein kinase signaling pathway in melanoma

Under physiologic conditions, the MAPK pathway, also called extracellular signal-regulated kinase (ERK) pathway stimulates cell growth, survival and migration. In a phosphorylation-dependent manner external signals are transduced from the cell surface to the nucleus [Fecher_2008]. Hence, extracellular ligands bind to receptor tyrosine kinases that subsequently activate RAS, a membrane-associated GTPase. Receptor tyrosine kinases that interact with RAS comprise c-KIT, epidermal growth factor receptor, platelet-derived growth factor receptor, vascular endothelial growth factor receptor, and fibroblast growth factor receptor. Once localized to the membrane, GTP-bound RAS transfers the signal to two main downstream targets, RAF and phosphatidylinositol-3-kinase (PI3K) [Giehl_2005]. RAS signaling activity depends on so-called GTPase-activating proteins (GAPs) such as neurofibromin 1 (NF1) or RAS GTPase-activating protein 2 (RASA2). GAPs strongly increase RAS GTPase activity and promote the conversion of RAS into its inactive GDP-bound form. Following the MAPK pathway, activation of RAS initiates a phosphorylation-dependent cascade that includes RAF, MAPK/ERK kinase (MEK; MAPKK; MAP2K), and ultimately ERK (MAPK). Whereas RAF and MEK have narrow substrate specificity, ERK catalyzes a broad spectrum of cytoplasmic and nuclear factors. The effects of ERK activation include increased proliferation, tumor suppressor inactivation and down regulation of CDK inhibitors [Kortylewski_2001]. Furthermore, ERK activation leads to increased survival through modulation of MITF and protection against FAS-induced apoptosis [Widlund_2003; Wilson_1999]. Lastly, ERK promotes invasion and metastasis due to extracellular matrix remodeling and angiogenesis [Smalley_2003; Giuliani_2004; Cohen_2002].

Although MAPK signaling is usually not present in melanocytes, constitutive activation of the MAPK signaling pathway due to activating point mutations is very common in melanoma. Consequently, melanomas are separated according to their mutations into $BRAF^{mut}$, RAS^{mut}, $NF1^{mut}$, or triple wild type [Krauthammer_2015; TCGA_2015]. The BRAF proto-oncogene, which encodes for a serine/threonine protein kinase is the most prevalently affected member of the MAPK pathway. Thus, about 40-60% of melanomas harbor activating mutations in the BRAF locus, most (90%) of which are

V600E/K substitutions [Kumar_2003; Houben_2004]. While BRAF normally exerts its function as a homo- or heterodimer with another RAF kinase, the mutated form acts as a self-sufficient monomer with permanent signaling activity [Solit_2010]. Interestingly, non-chronically sun-damaged melanomas bear a high frequency of BRAF mutations, while chronically sun-damaged melanomas, acral or mucosal melanomas rarely present with BRAF mutations [Curtin_2005]. These subtypes are usually associated with KIT mutations or cyclin D1 (CCND1) and CDK4 gene amplifications [Curtin_2006; Bastian_2000]. In about 15% of melanomas, mutations occur in the N-RAS GTPase locus, typically characterized by Q61K/L/R transversions that confer increased GTP-binding capacity [Fecher_2008; Liu_2014]. Normally, BRAF and N-RAS mutations occur in a mutually exclusive manner, as they both target the same pathway. Additionally, 12% of melanomas show autosomal dominant mutations in NF1. Mutations in NF1 cause reduced RAS GTPase activity, thereby increasing RAS signaling activity [Ratner_2015). Further mutations have been found in RASA2, which acts likewise to NF1 by activating the RAS GTPase. Consequently, mutations cause increased RAS-GTP binding, followed by activation of the MAPK pathway. RASA2 mutations are likely to act synergistically with NF1, as they mostly occur in NF1-mutant tumors that are wild type for BRAF or N-RAS [Krauthammer_2015].

3.4.8. PI3K/AKT signaling pathway in melanoma

The PI3K/AKT pathway is commonly initiated by the phosphorylation of phosphatidylinositol-4,5-bisphospate (PIP2) to phosphatidylinositol-3,4,5-triphosphate (PIP3) through receptor tyrosine kinases or RAS, which ultimately leads to AKR murine transforming retrovirus protein (AKT; also termed protein kinase B) activation [Cully_2006]. Increased AKT activity prolongs cell survival through inactivation of BCL2 antagonist of cell death (BAD) and promotes cell cycle progression by increasing CCND1 expression. Moreover, AKT affects many other survival and cell-cycle genes through activation of the forkhead (FKHR) transcription factor [Cantley_1999; Wu_2003]. PI3K/AKT signaling activity is well controlled by the phosphatase and tensin homolog (PTEN) tumor suppressor that keeps PIP3 levels low, thereby preventing AKT activation.

In general, mutations in PI3K/AKT pathway components are rare in melanoma. Nonetheless, inactivating mutations of the PTEN tumor suppressor have been reported in up to 25% of melanomas [Wu_2003]. The importance of the PI3K/AKT pathway in melanoma was further substantiated experimentally, as suppression of AKT3 resulted in reduced survival and growth of human melanoma implanted in immunodeficient nude mice [Stahl_2004].

3.4.9. Role of cell cycle regulators in melanoma

Cell cycle regulators represent the guardians of genomic integrity during cell division and guarantee well-controlled conditions to allow cell cycle progression. Consequently, cell cycle regulators function as important tumor suppressors that prevent exuberant cell growth and cancer formation. In melanoma cell cycle regulators play a crucial role as for example 25-40% of familial melanomas are associated with mutations in the CDKN2A gene [Hussussian_1994; Aitken_1999; Goldstein_2000]. CDKN2A encodes for two tumor-suppressor proteins, $p16^{INK4A}$ and alternative reading frame ($p14^{ARF}$). The $p16^{INK4A}$ protein blocks G1-S cell cycle transition through inhibition of CDK4 and CDK6 in response to DNA damage or increased oncogenic activity [Goldstein_2006]. On the other hand, $p14^{ARF}$ is activated upon DNA damage or dysfunctional downstream effectors, such as the retinoblastoma (RB) protein. Consequently, $p14^{ARF}$ either induces cell cycle arrest or apoptosis. The $p14^{ARF}$ protein is part of the core regulatory machinery that controls TRP53 protein levels [Goldstein_2006]. TRP53 represents a tumor suppressor gene that is activated in response to DNA damage as well as oncogenic, genotoxic or oxidative stressors [Box_2008; Vousden_2009]. Normally, the E3 ubiquitin ligase mouse double minute 2 (MDM2) triggers TRP53 ubiquitination, thereby instigating its destruction in the proteasome. Upon activation, $p14^{ARF}$ binds MDM2, which induces its dissociation from TRP53. As a result, TRP53 accumulates and causes a G2-M cell cycle arrest, allowing for the repair of damaged DNA or induction of apoptosis [Pomerantz_1999].

Even though CDKN2A loss of function is not able to initiate melanoma formation alone, it might contribute to the onset of melanoma as a consequence of increased sensitivity towards carcinogens [Serra-

no_1996]. Thus, it has been demonstrated that depletion of CDKN2A in human melanocytes is sufficient to overcome BRAF- or H-RAS-induced senescence, while CDKN2A ablation in melanocytic hyperplasia-harboring mice leads to melanomagenesis [Michaloglou_2005; Serrano_1997; Ackermann_2005]. In comparison to CDKN2A, mutations in the CDK4 locus occur at much lower rate [Hussussian_1994; Aitken_1999; Goldstein_2000]. Mutated CDK4 oncoproteins usually lack responsiveness to $p16^{INK4A}$ inhibition, which results in constant kinase activation [Puntervoll_2013]. Alternatively, increased CDK4 kinase activity has also been reported in association with gene amplifications [Hodis_2012; Krauthammer_2015; Muthusamy_2006]. In about 20% of melanomas deleterious mutations cause TRP53 loss of function. Contrarily, TRP53 inhibitors, like MDM2 are frequently up regulated [Marine_2005; Muthusamy_2006; Polsky_2001]. Hence, TRP53 depletion or MDM2 overexpression have been shown to accelerate melanocyte transformation *in vitro* as well as in melanoma mouse models [Bardeesy_2001; Goel_2009; Serrano_1997].

Summing up, cell cycle regulators represent crucial tumor suppressors and play a central role during melanoma formation. Dysfunctional or aberrantly behaving cell cycle proteins spur cell cycle progression regardless of genomic integrity. Consequently, uncontrolled cell division and genetic instability lead to the acquisition of additional mutations and further fuel the vicious circle of tumorigenic transformation.

3.4.10. Microphthalmia-associated transcription factor in melanoma

MITF, the master regulator of melanocytic differentiation and pigment production, has gained recognition as lineage-specific oncogene through its extended role in melanoma development. MITF is expressed in >80% of melanomas and is present throughout all progression stages [King_2001; Agnarsdóttir_2012; O'Reilly_2001]. Elevated MITF levels are correlated with decreased overall patient survival and have been shown to promote melanoma growth in synergy with activated MAPK signaling [Garraway_2005; Du_2004]. In 20% of melanomas, chromosomal amplifications represent the source of increased MITF activity, whereas activating point mutations, as for example present in

E318K substitutions, are relatively rare and mostly occur in association with familial melanoma [Cronin_2009; Bertolotto_2011; Yokoyama_2012]. MITF is heterogeneously expressed within a tumor, showing cells with high, low or even absent MITF [Konieczkowski_2014; Müller_2014; Sensi_2011]. Interestingly, MITF-negative cells are predominantly regulated by WNT5A and TGF-β [Eichhoff_2011]. In analogy to a rheostat, MITF regulates distinct biological processes dependent on its expression level. Hence, high MITF levels promote differentiation, while moderate MITF levels drive proliferation. On the other side, low MITF levels induce migration and stem cell-like behavior, whereas lack of MITF leads to senescence [Hoek_2008; Goding_2011; Vandamme_2014]. MITF further promotes cell survival by activating the expression of anti-apoptotic genes like BCL2A1, BCL2 and BIRC7 [Hartman_2015; Hartman_2013]. Finally, high MITF levels endow melanoma cells with increased resistance to MAPK pathway inhibitors [Johannessen_2013]. Thus, MITF over expression in $BRAF^{V600E}$ melanoma cells induces resistance towards RAF, MEK, or ERK inhibitors [Roesch_2015].

3.4.11. Readoption of neural crest features in melanoma

The neural crest and melanoma share striking similarities, best exemplified by their exceptional migratory behavior. In order to gain neural crest properties, it is likely that melanoma cells reactivate signaling cues and transcriptional networks from their developmental predecessors. Thus, melanoma cells express a plethora of markers reflecting the entire neural crest differentiation spectrum. Consequently, melanoma presents as a highly heterogeneous tumor, suggesting that within the tumor there is a subpopulation of cells with neural crest stem cell-like features. This subpopulation has the capacity to self-renew and to give rise to other, more differentiated cell types, which eventually have the potential to dissociate from the primary tumor and form distant metastasis.

3.4.12. SOX10 in melanoma

As outlined in previous chapters the transcription factor SOX10 plays a pivotal role in neural crest development [3.1.]. SOX10 is further required for melanocyte differentiation and maintenance of mel-

anocyte stem cells [3.2.1.]. Hence, homozygous depletion of SOX10 in the melanocytic lineage causes hair graying due to deprivation of the melanocytic stem cell pool [Potterf_2001]. However, SOX10 is not only important in neural crest and melanocyte development, it is also expressed in the vast majority of giant congenital nevi and melanoma. Furthermore, it was shown that SOX10 expression levels are increased upon malignant transformation and that N-RAS^{Q61K} is able to activate SOX10 expression [Shakhova_2012]. In an experimental set up using the *Tyr::N-RAS^{Q61K}INK4A$^{-/-}$* melanoma mouse model it was demonstrated that SOX10 haploinsufficiency completely prevents the formation of giant congenital nevi and melanoma. On the other hand, SOX10 haploinsufficiency did not interfere with normal functions of neural crest derivatives [Shakhova_2012]. These results indicate differential SOX10 level requirements in melanocytes, nevus cells and melanoma cells. Therefore, SOX10 represents an interesting target for novel therapy approaches [Shakhova_2014].

3.4.13. WNT signaling in melanoma

Likewise to SOX10, WNT signaling is highly relevant in neural crest development [3.1.], melanoblast specification [3.1.9.] and maintenance of the adult melanocyte stem cell pool [3.2.4.]. Albeit WNT signaling plays a major role in melanomagenesis, its role in melanoma is complex and sometimes appears contradictory. This becomes evident, as there are two major WNT signaling pathways with distinct functional implications. In melanoma, the canonical signaling pathway mediated by β-catenin is activated upon binding of WNT1 and WNT3A ligands to their corresponding receptors, frizzled 1 and 7 (FRZD1 and FRZD7) [Weeraratna_2005; Webster_2015]. Activation of the canonical WNT signaling pathway is critical for melanocyte transformation and helps to overcome cellular senescence. Hence, β-catenin is frequently expressed in human nevi and melanoma [Bachmann_2005; Kageshita_2001; Maelendsmo_2003, Omholt_2001]. Mechanistically, it is suggested that β-catenin activates MITF, thereby promoting cell growth and survival [Damsky_2011; Widlund_2003]. On the other side, canonical WNT signaling circumvents oncogene-induced senescence through repression of CDKN2A [Delmas_2007]. Paradoxically, high β-catenin expression is associated with reduced metastases and correlates with better prognosis for melanoma patients [Bachmann_2005; Chien_2009]. It is suggested

that canonical WNT signaling in conjunction with MITF expression promotes a more differentiated state that allows proliferation. However, β-catenin-dependent signaling seems to suppress the acquisition of invasive properties thereby preventing metastasis formation. It is assumed that the switch from a proliferative state, to a more motile, invasive state is associated with the activation of the non-canonical pathway and down regulation of the canonical pathway. Thus, it was demonstrated that WNT5A initiates ubiquitination and proteasomal degradation of β-catenin, thereby down regulating the canonical pathway. This leads to the suppression of LEF1 and concomitantly to the switch to a more invasive phenotype [Topol_2003]. To conclude, WNT signaling plays a central role in malignant melanocyte transformation and confers high plasticity to melanoma cells allowing them to switch between proliferative and invasive phenotypes.

3.4.14. TGF-β signaling in melanoma

It is well accepted that in epithelial cells TGF-β acts as a growth inhibitor and tumor suppressor during early-stage carcinogenesis [Oshimori_2015; Tian_2011]. Functionally, TGF-β exerts its suppressive function through up regulation of cyclin-dependent kinase inhibitors (p21, p15, p27Kip1 and p57Kip2), while repressing proliferation drivers such as c-MYC [Perrot_2013]. Apart from the cytostatic effect, TGF-β signaling regulates the expression of several pro-apoptotic genes [Pardali_2006]. In contrast to its role as a tumor suppressor in early cancerogenesis, TGF-β promotes proliferation and dissemination in advanced tumors. Additionally, TGF-β signaling favors peri-tumoral angiogenesis, EMT and immune evasion, thus acting as a tumor driver [Perrot_2013].

Similar to epithelial cells, TGF-β causes a growth arrest in melanocytes, whereas melanoma cells are no longer responsive to the anti-proliferative effect of TGF-β [Rodeck_1994; Kragasakis_1999]. However, the exact underlying mechanisms inducing this switch are not well understood but might be due to differential activation of transcriptional programs [Oshimori_2015; Tian_2011]. Melanoma cells secrete TGF-β in an autocrine and paracrine manner, while TGF-β ligands further induce their own expression in a positive feedback loop [Lasfar_2010]. This is of clinical relevance, as enhanced

TGF-β secretion correlates with increased tumor thickness and disease progression [Reed_1994]. As outlined previously [3.4.10.], TGF-β suppresses MITF expression, which is associated with acquisition of neural crest stem cell-like features such as the invasive behavior [Hoek_2006; Javelaud_2011; Pierrat_2012]. Along this line, it was shown that ectopically applied TGF-β ligands activate EMT transcription factors such as SNAIL1, TWIST, and GLI family zinc finger 2 (GLI2) and induces invasiveness of melanoma cells under *in vitro* conditions [Alexaki_2010; Javelaud_2011; Menon_2013]. Unpublished data from our lab further demonstrate that depletion of the TGF-β downstream target, SMAD4 efficiently counteracts melanomagenesis in the *Tyr::N-RAS^{Q61K}INK4A$^{-/-}$* melanoma mouse model. On the other side, interference with the TGF-β pathway inhibitor, SMAD7, activates the TGF-β signaling cascade, thereby accelerating melanoma cell dissemination and metastasis formation [Tuncer_unpublished]. Although TGF-β-induced EMT in melanoma appears reminiscent of the delamination process in the neural crest, it needs to be further investigated to which extent they share a common mechanistic background.

3.4.15. NOTCH signaling in melanoma

There are four evolutionarily conserved NOTCH receptors that play an essential role during neural crest and melanocyte development [Gordon_2009]. The NOTCH signaling cascade is initiated through direct interactions of the NOTCH receptor with DELTA-like and JAGGED ligand proteins on neighboring cells. This interaction induces a two-step cleavage process, in which the extracellular portion is first cleaved by ADAM10 and ADAM17 proteases preceding the second cleavage by the presenilin γ-secretase complex ultimately leading to the release of the active NOTCH intracellular domain (NICD) [Brou_2000; Mumm_2000; Sotillos_1997]. The liberated NICD translocates to the nucleus, where it binds to the transcriptional repressor complex CBF1/RBP-jk, Suppressor of Hairless, LAG-1 (CSL) [Kopan_2009]. The NICD replaces the repressor complex, which consequently leads to the transcriptional activation of CSL target genes, such as Hairy/Enhancer of Split (HES) and Hairy/E (spl)-related with YRPW (HEY) [Kopan_2009; Bedogni_2014].

Even though NOTCH signaling plays a pivotal role during development, NOTCH expression is low or undetectable in mature melanocytes and nevi [Bedogni_2008; Pinnix_2009; Zhang_2012]. Nonetheless, NOTCH1 NICD expressing melanocytes significantly accelerate cell growth *in vitro* and show better survival under growth limiting conditions [Pinnix_2009]. Albeit NOTCH1 NICD expression alone is not able to induce melanoma tumors in mice, NOTCH signaling promotes malignant transformation of primary human melanocytes [Pinnix_2009]. NOTCH1 expression is elevated in 50-60% of melanomas and 65% of melanoma cell lines [Bedogni_2008; Zhang_2012]. Melanoma cells often depend on NOTCH1 expression for their growth and survival, while NOTCH1 signaling has also been shown to promote aggressiveness in primary melanoma [Liu_2006]. Hence, blockade of NOTCH1 activity in melanoma cells results in cell death, whereas melanocytes are not affected [Qin_2004]. In this context, NOTCH1 expression is elevated upon activation of the AKT/PI3K pathway, mediated through the nuclear factor kappa-light-chain-enhancer of activated B cells (NF-KB) transcription factor [Bedogni_2008]. On the other side, it is likely that in a positive feedback loop NOTCH1 activates the AKT/PI3K pathway [Bedogni_2014]. Although most studies in melanoma focus on the NOTCH1 receptor, other NOTCH receptors also play a role in melanomagenesis. Thus, NOTCH4 for example promotes vasculogenic mimicry in aggressive melanoma, while NOTCH3 is specifically up regulated in melanoma upon co-culturing with endothelial cells [Hardy_2010; Howard_2013]. Moreover, NOTCH3 activity is associated with enhanced melanoma cell migration [Howard_2013].

First clinical trials using a γ-secretase inhibitor revealed melanoma among the most frequently observed tumors in patients with prolonged stable disease. This suggests that melanoma may indeed be more sensitive to γ-secretase inhibitor therapies [Tolcher_2012]. Considering the importance of the NOTCH signaling cascade in melanoma growth and progression, targeting the NOTCH pathway indeed represents a valuable alternative for future therapy approaches.

3.4.16. Role of enhancer of zeste homologue 2 in melanoma

Besides genetic modulations, aberrant epigenetic activity often leads to developmental disorders and is associated with oncogenic transformation [Reik_2007; Sharma_2009]. Enhancer of zeste homologue 2 (EZH2), a subunit of the polycomb repressive complex 2 represents a major epigenetic modifier. EZH2 catalyzes trimethylation of lysine 27 in histone 3 (H3K27me3), which leads to chromatin condensation and subsequent transcriptional repression of target genes [Margueron_2011; Ciferri_2012]. During embryonic development and in tissue-specific stem cells, EZH2 prevents early lineage restriction through transcriptional repression of differentiation genes. However, in neural crest stem cells EZH2 does not interfere with differentiation or proliferation, but rather induces the acquisition of a mesenchymal fate [Schwarz_2014].

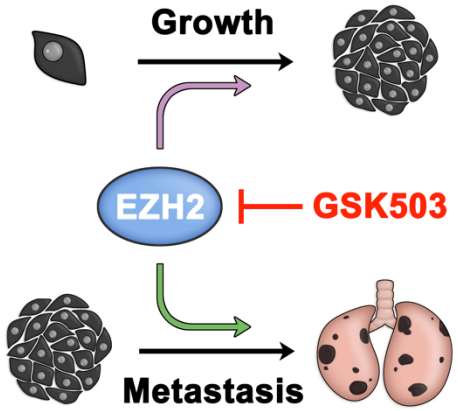

Figure 11. Role of EZH2 in melanoma. The epigenetic modifier EZH2 is a methyltransferase that represses gene expression through trimethylation of lysine 27 in histone 3. While EZH2 plays a crucial role during neural crest development, melanoma is often associated with aberrant EZH2 expression. Thus, EZH2 promotes tumor initiation as well as metastasis formation in melanoma. Blocking EZH2 function in melanoma using a preclinical EZH2 inhibitor completely abolished metastases formation and therefore represents a powerful strategy for novel therapy approaches [graphical illustration; Mario Bonalli in Zingg_2015].

In many cancer types including melanoma, EZH2 is highly expressed and associated with poor prognosis [Sauvageau_2010; Bachmann_2006; McHugh_2007]. Likewise to its function in embryonic tissue and adult stem cells, EZH2 promotes proliferation and growth in tumors [Sauvageau_2010]. Thus, loss of EZH2 in human melanoma cells partially interferes with proliferation and the invasive

capacity [Fan_2011; Luo_2013a; Luo_2013b]. In addition, conditional deletion of EZH2 in the melanocytic lineage using the murine *Tyr::N-RAS^{Q61K}INK4A$^{-/-}$* melanoma model drastically reduces the number of melanoma tumors and prolongs survival of the animals. Furthermore, EZH2 ablation in already established melanoma tumors efficiently blocks disease progression, indicating that EZH2 is crucial for the initiation and progression of metastatic melanoma [Zingg_2015]. Therefore, blocking EZH2 activity might represent a powerful strategy for novel therapy approaches (Figure 11).

3.4.17. Melanoma stem cells and tumor heterogeneity

Melanoma often presents with remarkable intratumoral heterogeneity, histopathologically as well as genetically [Berger_2012; Hodis_2012; Anaka_2013]. Hence, apart from melanocytic markers, melanoma cells express neuronal, glial, and mesenchymal markers, reflecting the entire neural crest library [Banerjee_2008; Civenni_2011; Cruz_2003; Laga_2010; Mete_2010; Parente_2013]. Although melanoma is assumed to be a clonal event, tumors subsequently evolve and acquire heterogeneity in response to genomic instability and selective pressure [Bennett_2008; Grichnik_2006]. These findings are of particular clinical relevance, since increased clonal diversity contributes to the metastatic potential and promotes therapy resistance. As a consequence, tumor heterogeneity is linked with poor prognosis in melanoma patients [Civenni_2011].

Besides more specified cell populations within the melanoma tumor, there is a particular cell type that strongly resembles undifferentiated neural crest stem cells. This multipotent cell type is characterized by the expression of the neural crest stem cell markers CD271(p75^{NTR}) and SOX10 [Civenni_2011]. Upon transplantation into recipient mice, isolated CD271(p75^{NTR})-positive but not CD271(p75^{NTR})-negative melanoma cells are able to form tumors [Boiko_2010; Civenni_2011]. These CD271(p75^{NTR})-positive cells faithfully mimic the heterogenic cellular composition of the parental tumor after transplantation. Moreover, CD271(p75^{NTR})/SOX10 cells correlate with higher metastatic potential and worse prognosis [Civenni_2011].

In analogy to the neural crest, CD271($p75^{NTR}$) marks a cell population with self-renewal and multipotent differentiation capacity in melanoma, suggesting the presence of so-called cancer stem cells. Melanoma stem cells are crucially involved in the establishment of tumor heterogeneity, which is associated with increased metastatic potential, therapy resistance and poor prognosis. Hence, the surface marker CD271($p75^{NTR}$) might be a valuable target in future diagnostics and prognostics, while eliminating melanoma stem cells represents a potential approach in prospective treatment strategies [Ward_2007; Civenni_2011].

3.4.18. EMT in melanoma

EMT describes an embryonic program that defines a reversible transversion from an epithelial cell with tight intercellular adhesion and apical-basal polarity to a more mesenchymal cell type with stemness features and increased cellular motility [3.1.4.]. EMT is driven by a network of embryonic EMT-inducing transcription factors, including members of the SNAIL1, TWIST, or ZEB families [Kalluri_2009]. Besides its essential role in developmental processes as for example during neural crest delamination, EMT is also observed in wound healing or cancer progression [Yan_2010; Kalluri_2009]. Hence, aberrant expression of EMT transcription factors is a common event in various cancer types and has originally been found in carcinoma, a tumor of the epithelial lineage. In cancer, EMT transcription factors trigger neoplastic transformation, stemness, and metastatic dissemination [Peinado_2007; Vega_2004; Mejlvang_2007; Mani_2008; Morel_2008]. Consequently, expression of EMT transcription factors in cancer patients is associated with poor prognosis and high risk of metastasis formation [Caramel_2013].

Functionally, EMT is thought to be regulated analogously in embryogenesis and cancerogenesis, characterized through down-regulation of adhesion molecules like E-cadherin and up regulation of developmentally important transcription factors such as SNAIL1, SNAIL2, TWIST and ZEB1/2 [Kalluri_2009]. However, in melanocytes SNAIL2 and ZEB2 function as tumor suppressors by activating an MITF-dependent differentiation program [Gupta_2005]. On the other side, ZEB1 and TWIST1 are

up regulated in response to MAPK pathway activation and induce oncogenic transformation [Caramel_2013]. This indicates that melanoma cells do not undergo a classical EMT, which might be explained by their non-epithelial origin. Nonetheless, melanocytes express E-cadherin in order to form contacts with neighboring keratinocytes in the basal layer of the epidermis. These cell-cell communications maintain melanocyte homeostasis by suppressing proliferation and promoting differentiation. Hence, down regulation of E-cadherin, which represents a hallmark of EMT, is associated with increased proliferation in melanoma [Hsu_2000]. Furthermore, melanoma cells increase the expression of N-cadherin, which is assumed to support the acquisition of stem cell-like features and dermal invasion, thereby facilitating the interaction with dermal fibroblasts and vascular endothelial cells that express the same cadherins [Li_2001].

It has been estimated that approximately one million cells per gram of tumor mass dissociate from the primary tumor per day [Butler_1975]. However, the presence of tumor cells in the blood cannot be used as a prediction criterion for a metastatic event to occur [Fidler_1970]. Therefore, the EMT concept is controversially discussed in cancer, as it neglects the terminal components of the metastatic cascade such as adhesion, extravasation, survival, and growth at a distant site [Tarin_2005; Talmadge_2010]. Hence, apart from acquiring invasive properties, the capacity to survive and propagate growth in a foreign microenvironment has proven equally important for the establishment of distant metastases. In contrast to EMT, this process is assumed to be associated with loss of mesenchymal and reactivation of epithelial characteristics and is therefore termed mesenchymal-epithelial-transition (MET) [Polyak_2009; Yao_2011].

To sum up, the EMT model serves well to describe the initial but not the entire metastatic process in melanoma. This emphasizes the critical role of the terminal phase in tumor progression, which most likely represents a reversal of the EMT process and allows adhesion, extravasation, survival and growth at distant sites. In melanoma, cells only partly undergo classical EMT, which might be due to their non-epithelial origin. Moreover, it is still nebulous to which extent melanoma cells undergo MET

at distant sites in order to establish macrometastases. Thus, further investigations are required to prove the applicability of the EMT/MET paradigm in melanoma.

3.4.19. Melanoma therapy

Although melanoma is not among the most prevalent types of skin cancer, it has a considerably higher propensity to metastasize, therefore leading to a disproportionate high number of skin cancer-related deaths. Therefore, early detection prior to metastasis formation followed by surgical resection correlates with a high survival rate. However, once metastasis has occurred, surgical excision only yields about 10% five-year survival rate [Bhatia_2009]. Apart from surgery, radiotherapy is mostly applied locally in unresectable lesions but has proven little effect on metastatic melanomas [Bhatia_2009]. In metastatic melanoma, dacarbazine was considered the best treatment option for a long time, although the response rate was only about 15-20% [Bajetta_2002]. Dacarbazine or dimethyltriazeno-imidazol carboxamide (DTIC) represents a DNA-alkylating chemotherapeutic agent [Eggermont_2004]. Other single agent chemotherapies comprise cisplatin, nitrosoureas, vindesine and the microtubule-disrupting agent taxane. However, their response rate is less efficient in comparison to dacarbazine [Gogas_2004; Bajetta_2002; Bhatia_2009].

The lack of satisfying treatment options in metastatic melanoma highlights the exigence for novel therapy approaches. As the majority of melanoma patients harbor activating mutations in members of the MAPK pathway, the identification of these mutations has offered novel opportunities to develop oncogene-specific drugs that target the MAPK pathway. In the past few years the US food and drug administration (FDA) approved two inhibitors, vemurafenib and dabrafenib that specifically target mutated BRAF. Both BRAF inhibitors present with better overall responses in comparison to dacarbazine. Vemurafenib achieves a 48-53% response rate with 6% showing a complete response, while dabrafenib receives a 59% response rate in melanoma patients with $BRAF^{V600E/K}$ mutations [Chapman_2011; Ascierto_2013; Hauschild_2012]. However, in most patients, treatment efficacy has only short duration, as the median progression free survival ranges from 5.1 to 6.8 months [Sosman_2012;

Hauschild_2012]. Vemurafenib and dabrafenib are contraindicated in melanomas without BRAF mutation. Moreover, the MEK inhibitors, trametinib and cobimetinib have been approved for $BRAF^{V600E/K}$ mutated melanomas and achieve response rates similar to BRAF inhibitors [Flaherty_2012a; Eroglu_2016]. MEK inhibitors are not allowed in wild type BRAF or in patients that were previously treated with BRAF inhibitors. Although BRAF and MEK monotherapies have shown promise, the responses are not long lasting due to acquired resistances. In order to overcome limitations in single drug treatments, the combination of BRAF and MEK inhibitors has markedly improved the response rate and progression free survival. Hence, simultaneous application of BRAF and MEK inhibitors has become the standard care for patients with BRAF mutated advanced melanoma [Flaherty_2012b].

Melanomas heterogeneously express a multitude of different tumor antigens and are frequently infiltrated with cytotoxic T-lymphocytes (CTLs). CTLs are primed in the lymph node by dendritic cells to recognize a particular antigen. Once CTLs reencounter their cognate antigen upon tumor infiltration, they get activated and exert cytotoxicity towards antigen-expressing tumor cells [Schatton_2014]. Consequently, increased numbers of tumor-infiltrating T-cells correlate with better prognosis for melanoma patients [Azimi_2012, Erdag_2012]. However, with advanced progression, melanoma cells evolve under selective pressure and undergo immunosuppressive adaptations rendering the T-cell response ineffective [Schatton_2014].

In a first approach to manipulate the patient's own immune system, high-dose interleukin 2 (IL-2) was intravenously infused in order to activate and prompt natural killer cells to attack cells without major histocompatibility complex class 1 (MHC1) expression [Mule_1984; Bajetta_2002]. Furthermore, IL-2 has been shown to stimulate proliferation and maturation of T cells [Boyman_2012]. Although IL-2 treatment has a response rate of 16-17%, it is associated with serious side effects resulting in increased morbidity [Schwartz_2002]. Combinational treatment of IL-2, interferon alpha (IFN-α), and dacarbazine improved the response rate to 31% [Bajetta_2006].

Recently, fundamental discoveries have been achieved regarding the molecular mechanism how melanoma cells abscond from the immune system, paving the way for novel approaches in immunotherapy. Cytotoxic T-lymphocyte-associated antigen 4 (CTLA-4) typically acts in the lymph node as a negative immune checkpoint regulator by blocking potentially autoreactive T-cells [Rudd_2009; Alegre_2001; Rudd_2003]. CTLA-4 and CD28 compete as coreceptors for CD80/86 ligand binding on antigen presenting cells. While CD28 mediates T-cell proliferation, differentiation and cytokine production, CTLA-4 inhibits T-cell activation, thereby limiting the immune response [Krummel_1995].
In contrast to CTLA-4, PD-1 inhibits T-cell proliferation in peripheral tissues in a later phase of the immune response [Fife_2008]. PD-1 binds PD ligand 1 and 2 (PD-L1/2), which are more widely expressed as for example on leukocytes, non-hematopoietic cells, and on parenchymal cells upon induction by inflammatory cytokines (IFN-γ) [Chen_2004; Parry_2005; Chen_2012; Latchman_2004].

Melanoma and many other tumors have found ways to evade the immune system by expressing immunosuppressive receptors such as CTLA-4 or PD-1. Hence, blockage of the immune checkpoint pathways using inhibitory antibodies represents a novel form of immunotherapy in melanoma. Ipilimumab belongs to the group of humanized monoclonal antibodies that stimulate T-cell activity by blocking CTLA-4 receptor interaction with CD80/86 [O'Day_2010; Melero_2007; O'Day_2007; Peggs_2006]. It has been reported that CTLA-4 blockade with ipilimumab significantly augments T-cell diversity in the peripheral blood [Robert_2014]. The response rate in stage III and IV melanoma patients is 11.1%, while side effects are observed in 15% of patients [Wolchok_2010; Farolfi_2012]. Pembrolizumab and nivolumab represent humanized monoclonal antibodies that target the PD-1 receptor. In a phase III trial, pembrolizumab reached a response rate of 33-34% with a 1-year survival rate of 68-74% [Farolfi_2012]. Preliminary data suggest combinatorial inhibition of CTLA-4 and PD-1 increases the efficacy over single drug application [Buchbinder_2016]. Further trials will follow to confirm the benefits of the double treatment.

While first trials have revealed response rates of up to 70% for combinatorial BRAF and MEK inhibition, tumor relapse occurs within a fairly short period of time. This stands in contrast to immune

checkpoint inhibitors that offer significant durability, even though their response rates are rather low [Schadendorf_2015; Robert_2015b; Ribas_2013; Hodi_2010]. Consequently, there are interests in combining these two treatments, as it has been shown that MAPK inhibitors increase the number of tumor-infiltrating CD8+ T cells. Furthermore, experiments using murine melanoma models have demonstrated prolonged survival in mice treated with BRAF/MEK and PD-1 inhibitors [Hu-Lieskovan_2015]. However, further follow up studies and clinical trials will determine whether combination therapy effectively leads to a high response rate with a long lasting effect.

3.5. NKAP

Human NKAP is located on the X chromosome and encodes for a 415 amino acid long highly charged and basic protein with a p*I* of 10 [Chen_2003; Burgute_2014; Worlitzer_2014]. NKAP is present ubiquitously in various tissues but is particularly expressed in spleen, skin, testes, kidney and lung [Burgute_2014]. Furthermore, NKAP is highly expressed in adult mouse subventricular zone neural progenitor cells [Worlitzer_2014]. From flies to humans, NKAP is well conserved throughout the evolution, while the human and mouse protein share 86% sequence homology [Burgute_2014]. Eponymously, NF-KB activating protein (NKAP) was initially identified to stimulate the NF-KB pathway. In a NF-KB-luciferase reporter assay using 293 cells, NKAP overexpression induced NF-KB activation in a dose-dependent manner [Chen_2003]. More recent studies reported that NKAP modulates the NOTCH signaling pathway through interaction with HDAC3 and CBF1 interacting co-repressor (CIR), both components of the NOTCH co-repressor complex. This interaction seems to be pivotal in different phases of T-cell and natural killer T (NKT) cell development [Pajerowski_2009; Hsu_2011; Thapa_2013]. Thus, conditional ablation of NKAP in early T-cell development using LCK-cre transgenic mice revealed that NKAP is necessary at the double negative 3 (DN3) to double positive (DP) transition, as well as for post-positive selection maturation of single-positive thymocytes [Pajerowski_2009; Hsu_2011]. Specific NKAP depletion in stage 0 invariant NKT (iNKT) cells using the PLZF-cre mouse line prevented proliferation of iNKT cells and blocked differentiation into ROR-γt-expressing NKT17 cells. However, despite dramatically reduced cell number, differentiation into NKT1 and NKT2 cells was still possible [Thapa_2016]. Moreover, NKAP is required for the maintenance and survival of hematopoietic stem cells (HSCs). Inducible ablation of NKAP using the Mx1-cre mouse line leads to hematopoietic failure and loss of the HSC pool within days [Pajerowski_2010].

In an extensive yeast two-hybrid screening approach, NKAP has been found as a core component of the splicing complex and interaction partner of RNA binding proteins. Functionally, NKAP has thus been implicated in RNA metabolism and splicing [Giot_2003; Hegele_2012]. RNA processing factors

and elements of the splicing machinery tend to accumulate in so-called nuclear speckles [Lamond_2003; Hall_2006; Raska_1995]. Proteins that localize to nuclear speckles are often associated with an arginine/serine-rich domain (RS domain) of variable length and therefore referred to as SR proteins. The RS domain has been shown to be important for nuclear speckle localization but also functions as a protein interaction domain [Caseres_1997; Hedley_1995, Li_1991]. In addition to the RS domain, SR proteins principally contain one or two RNA recognition motifs (RRM) that provide RNA binding specificity [Graveley_2000]. Proteins that lack the RRM are defined as SR-related (or SR-like) proteins. Despite absent RRM, SR-related proteins might be involved in RNA processing [Long_2009]. In general, SR and SR-related proteins represent crucial regulators of constitutive and alternative splicing of precursor messenger RNA (pre-mRNA) [Lin_2009; Long_2009]. Hence, *in vivo* depletion of the SR proteins SRSF1 and SRSF2 dramatically reduces the synthesis of nascent RNA [Lin_2009].

NKAP has been characterized as a SR-related protein that contains a N-terminal RS domain, a central basic domain and a C-terminal domain of unknown function termed DUF926. In correspondence with other SR-related proteins, NKAP localizes to nuclear speckles but lacks the RRM [Burgute_2014]. However, it has been shown that unlike to other SR proteins, NKAP's nuclear speckle localization depends on the basic domain, whereas the RS domain has no impact on the subnuclear distribution. Although, NKAP is not required for the organization of nuclear speckles, NKAP overexpression dramatically increases the size and number of nuclear speckles [Burgute_2014]. Previously, the mRNA-bound proteome has been described in human embryonic kidney (HEK) cells and NKAP has been identified as a novel RNA binding protein [Baltz_2012]. Subsequently, NKAP was shown to interact with various RNA binding factors such as heterogeneous nuclear ribonucleoproteins (hnRNPs), splicing factors and RNA helicases. Although NKAP has no RRM, it has the ability to interact with pre-mRNA as well as with spliced mRNA and has no preferential binding motif such as the 5'-cap or other particular regions of the mRNA [Burgute_2014]. Crosslinking and immunoprecipitation followed by RNA sequencing (CLIP-Seq) revealed that NKAP mostly associates with exonic regions of pre-mRNA. NKAP further binds to various non-coding RNAs (ncRNAs), most abundantly to small

nuclear RNAs (snRNAs) and ribosomal RNAs (rRNAs). More specifically, NKAP interacts with U1 and U4 snRNAs, which contribute to the formation of complex B during splicing. Furthermore, NKAP has been found associated with specific spliceosomal complexes such as the B* complex, C complex and P complex [Burgute_2014] (Figure 12). Along this line, it was shown that the ratio between GAPDH pre-mRNA and spliced GAPDH mRNA was significantly increased upon NKAP knockdown [Burgute_2014]. Consequently, NKAP's regulatory function might be mediated through its role in snRNA biogenesis and the assembly of the spliceosome. However, NKAP's specific function in RNA processing remains obscure and requires further investigations.

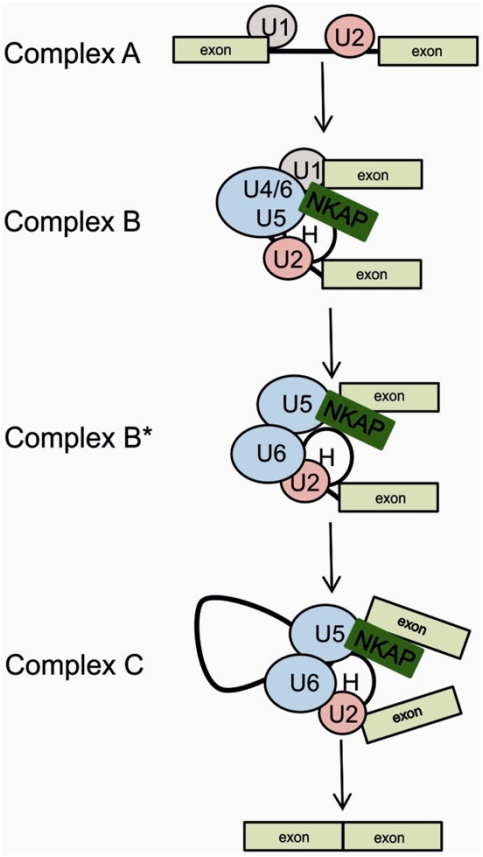

Figure 12. NKAP is a RS-related speckle protein involved in RNA processing and splicing. NKAP is a 415 amino acid long, highly basic protein that has been shown to exclusively localize to nuclear speckles. It directly binds to RNA and interacts with various RNA processing factors. Hence, NKAP knockdown leads to the accumulation of unprocessed RNA, whereas mature mRNA levels decrease. However, NKAP's exact molecular function during RNA splicing is not yet completely resolved [Burgute_2014].

Apart from its role in RNA splicing, NKAP functions as a transcriptional repressor and interacts with components of the NOTCH co-repressor complex. Thereby, the basic domain is important for the in-

teraction with CIR, whereas the DUF926 domain is required for the binding to HDAC3 [Pajerowski_2009]. In this context, it was shown that the DUF926 domain is necessary for transcriptional repression, whereas the other domains have no influence on transcription. Therefore, it is suggested that NKAP's repressive function is mediated by HDAC3 [Pajerowski_2009]. As a transcriptional regulator of the NOTCH signaling pathway, NKAP directly interacts with chromatin in order to repress NOTCH target genes. Experiments using ChIP followed by real-time quantitative PCR for the NOTCH target site in the SKP2 promoter revealed that NKAP associates with a NOTCH-regulated promoter [Pajerowski_2009]. Another study using ChIP-sequencing in NKAP over expressing HeLa cells confirmed that NKAP precipitates with chromatin but mostly interacts with centromere and other heterochromatic sequences [Burgute_2014].

So far, NKAP has not been associated with melanoma nor with any other kind of cancer. Nevertheless, NKAP plays a pivotal role in diverse cellular processes and has been implemented in mRNA splicing and transcriptional repression. However, NKAP's molecular mode of action is hypothetical and the link between mRNA splicing and transcriptional repression is still missing. Interestingly, the NICD and many NOTCH regulators including CIR, CSL, SKIP, SMRT and MAML are also distributed in a punctate nuclear pattern [Hsieh_1999]. This indicates that the NOTCH co-repressor complex at least partially operates in nuclear speckles. Therefore it is tempting to speculate that NKAP serves as a mediator between mRNA splicing and transcriptional repression of NOTCH target genes.

3.6. Nuclear speckles

Nuclear speckles represent compartments that form within the nucleoplasm in regions containing little or no DNA and are therefore also referred to as interchromatin granule clusters [Thiry_1995]. Generally, nuclear speckles appear as 20-50 irregularly shaped structures that vary in size [Spector_2011]. Nuclear speckles are highly dynamic and there is a continuous exchange of individual speckle components with the surrounding nucleoplasm [Misteli_1997; Kruhlak_2000; Phair_1995]. Along this line, nuclear speckles are supposed to act as storage, assembly, and modification compartments that supply splicing factors to active transcription sites [Lamond_2003]. Hence, it has been shown that nascent pre-mRNA preferentially localizes outside of nuclear speckles as fibrillary structures, termed perichromatin fibrils [Cmarko_1999]. Therefore, it is assumed that mRNA transcription, co-transcriptional splicing and exon junction complex (EJC) assembly does not occur within nuclear speckles but in the perispeckle region [Daguenet_2012]. In addition to pre-mRNA splicing factors, including small nuclear ribonucleoproteins (snRNPs) and SR proteins, several kinases and phosphatases have been localized to nuclear speckles [Fu_1995; Brede_2002; Colwill_1996; Ko_2001; Sacco-Bubulya_2002; Trinkle-Mulcahy_1999; Trinkle-Mulcahy_2001]. Phosphorylation and dephosphorylation has thus been assumed as an important regulatory mechanism that controls the shuttling of nuclear speckle components [Misteli_1998; Mermoud_1994]. Upon transcriptional inhibition, splicing factors accumulate predominantly in enlarged, rounded speckles, while diffuse speckles disappear [Melcak_2000; Spector_1991; O'Keefe_1994]. Furthermore, nuclear speckles do not contain factors primarily involved in ribosome subunit biogenesis or tRNA production [Spector_2011]. To conclude, nuclear speckles represent highly dynamic compartments within the nucleoplasm that are involved in storage, assembly, and modification of splicing factors. Hence, nuclear speckles provide splicing factors to active transcription sites, which are located in the perispeckle region.

3.7. RNA splicing and spliceosome assembly

Following transcription, primary RNA transcripts are processed into mature messenger RNA. This process includes 5'-capping, 3'-polyadenylation and RNA splicing. Unprocessed primary RNA transcripts, so-called pre-mRNAs, usually contain several protein-coding exons, which are intercepted by non-coding introns. During RNA splicing, the non-coding introns are cleaved out and exons are religated [Berget_1977; Chow_1977]. The splicing reaction is catalyzed by five U snRNPs (U1, U2, U4, U5, and U6) that together form the large spliceosome complex [Lerner_1980; Jurica_2003] (Figure 13). Each snRNP consists of one stable snRNA bound by several proteins, plus additional less stably associated splicing factors. These snRNAs recognize conserved consensus sequences within the intron [Mount_1982]. Most commonly, intron splice sites start with a GU dinucleotide and end with AG. These consensus sequences are known to be critical, as nucleotide substitution results in inhibition of splicing. The branch point represents a second conserved sequence within introns and is located between 18-40 nucleotides upstream of the 3' end [Burge_1999]. Spliceosome assembly follows a precise sequence of short-lived intermediate stages termed E, A, B, B*, and C complexes. In brief, intron excision from a nascent pre-mRNA transcript occurs in two steps, both requiring two distinct transesterification reactions. Initially the 5' splice site is cleaved and the cut end of the intron folds back in order to bind to an adenosine residue at the branch point thereby forming a lariat. Subsequently, a new phosphodiester bond ligates the two adjoining exons, while the intercalated intron is released as a product of the reaction [Burge_1999; Will_2011; Matera_2014]. Recently another type of spliceosome has been identified that processes a minor category of introns, therefore referred to as the minor spliceosome complex. This complex consists of the snRNPs U11, U12, U4atac, and U6atac, which represent functional analogs of the U1, U2, U4 and U6 snRNPs, respectively. The snRNP U5 remains unaltered in the minor spliceosome complex. Consequently, introns bound by the minor spliceosome complex are defined as U12-type introns, while the major spliceosome complex binds to U2-type introns [Tarn 1997; Patel_2003].

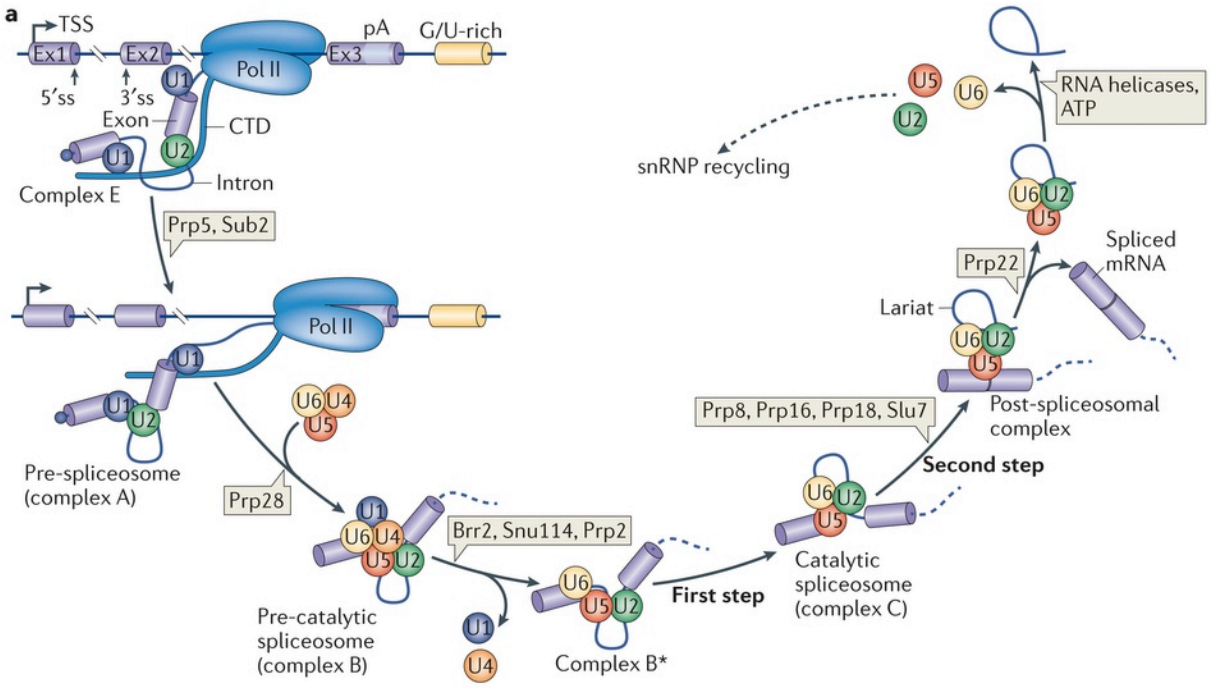

Figure 13. RNA splicing requires the assembly of the large spliceosome complex. In general, unprocessed primary mRNA transcripts consist of several protein-coding exons that are interspersed with non-coding introns. During the mRNA maturation process introns are cleaved out and the exons are religated. This process requires the formation of a spliceosome complex, which follows a strict sequence of short-lived intermediate stages termed E, A, B, B*, and C. The spliceosome complex consists of 5 U snRNPs, while each snRNP contains 1 snRNA bound by several proteins [Matera_2014].

Alternative splicing describes the process that is responsible for the generation of multiple isoforms from a single gene, thereby creating high protein diversity despite a low number of genes [Wang_2008; Nilsen_2010]. In this process, particular exons of a gene may or may not be included in the final transcript [Black_2003]. The expression of a particular transcript might vary substantially among different tissues or distinct developmental stages [Wang_2008; Matera_2014]. Thus, alternative splicing is tightly regulated through trans-regulatory proteins that bind to cis-regulatory elements on the primary transcript. However, the splicing code containing all cis-regulatory sequences has not yet been fully deciphered [Barash_2010]. Moreover, signaling factors that regulate alternative splicing are poorly understood [Lynch_2007]. Hence, prediction tools for alternatively spliced transcripts are so far not available [Barash_2010]. While alternative splicing helps explaining how new genes are created during evolution, a large proportion of human genetic disorders results from abnormal variations in splicing [Matlin_2005]. Additionally, abnormal splicing variants are implicated in cancer de-

velopment, whereas splicing factor genes are frequently mutated in various cancer types [Skotheim_2007; He_2009; Fackenthal_2008; Sveen_2015].

4. Goals of the thesis

As outlined in the introduction, there is compelling evidence that distinct genetic programs, usually active during the development of the neural crest are reactivated in melanoma [Civenni_2011; Eichhoff_2011; Shakhova_2012; Zingg_2015; Cheng_2015]. Therefore, in the initial phase of my doctorate, I planned to identify novel transcriptional regulators that are involved in neural crest stem cell maintenance, to subsequently determine their roles in melanoma. On the basis of the obtained results I aimed to focus on one particular factor to further dissect its functional contributions to the formation and metastatic progression of melanoma.

5. Preliminary investigations

The experiments described in this section were performed by Dr. Sandra Varum and served as the basis for my PhD thesis project.

In order to identify putative transcriptional regulators that are relevant in neural crest stem cell maintenance, a preliminary experiment was performed using *in vitro* cultured neural crest cells [Sommer_2001; Sommer_2002] In brief, neural tubes of E8.75 mouse embryos were isolated and plated under hypoxic conditions in fibronectin-coated dishes, in the presence of a permissive medium. These conditions allow the dissociation of migratory neural crest cells from the neural tube. Following the emigration, neural crest cells were primed for differentiation into specific cell fates, namely autonomic neurons, glia and mesenchymal progenitors. Therefore, previously identified instructive growth factors were subjected to neural crest cells for 6 hours in order to prime for a specific cell fate at the expense of other lineages. BMP2 was applied to generate autonomic neurons, TGF-β induced mesenchymal progenitors, and heregulin and forskolin promoted gliogenesis. The obtained populations were characterized based on canonical markers, such as SOX10 and GFAP for glia, MASH1 and neurofilament for autonomic neurons and smooth muscle actin for mesenchymal progenitors to confirm the high grade of homogeneity.

A whole-genome transcriptome analysis was performed, comparing multipotent neural crest stem cells to their corresponding early-stage derivatives. Genes that were down regulated upon differentiation were considered as putative stemness gatekeepers. Thus, the obtained results revealed four transcriptional regulators among a set of 53 genes that were at least 2.8-fold down regulated in early-differentiated derivatives compared to neural crest stem cells ($P>0.05$). These transcriptional regulators include lin-9 homolog (LIN9), lin-28 homolog A (LIN28A), single stranded DNA binding protein 2 (SSBP2), and NKAP (Figure 14).

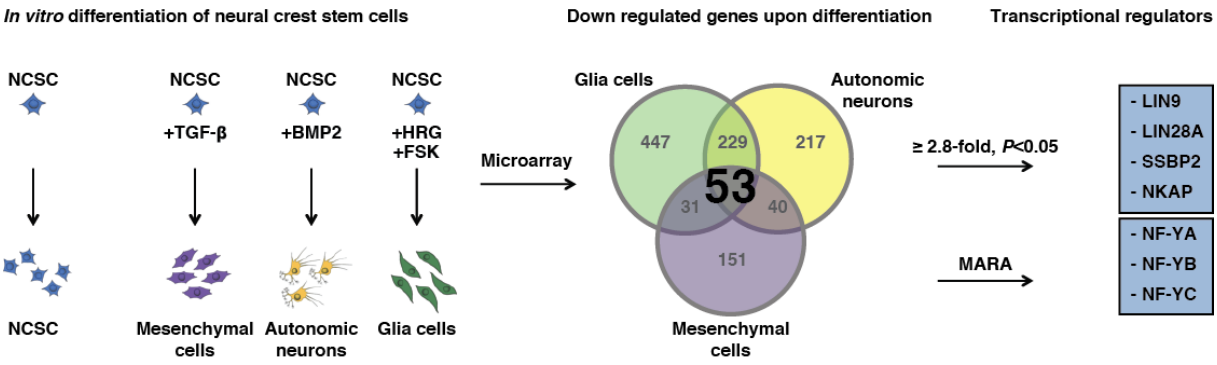

Figure 14. A genome-wide transcriptome analysis reveals 7 transcriptional regulators. To identify potential transcriptional regulators involved in the maintenance of neural crest stemness, a whole genome transcriptome analysis was performed comparing neural crest stem cells to early-specified neural crest derivatives. Neural crest stem cells were primed for 6 h with respective instructive growth factors in order to obtain early-differentiated neural crest cells. Genes that were 2.8-fold down regulated (P>0.05) upon differentiation were considered as putative stem cell genes. The analysis revealed 4 transcriptional regulators consistent of LIN9, LIN28A, SSBP2, and NKAP, among a set of 53 differentially expressed genes. Additionally, the gene expression dataset was evaluated using the online available algorithm MARA. This extended data analysis further suggested members of the NF-Y family as potential target factors.

To broaden the spectrum of potential neural crest stem cell factors, the gene expression dataset was evaluated using an online available algorithm termed motif activity response analysis (MARA) provided by the Biozentrum Basel. Comparative transcriptomic signatures of two or more cell populations serve as the basis for MARA to identify key transcription factors that drive the observed expression state changes. MARA reconstructs transcription regulatory dynamics using computational methods by incorporating comparative genomic information and positional preferences of transcription factors relative to the transcription start site in the prediction of regulatory sites [The FANTOM consortium_2009]. Among others, the extended data evaluation using MARA identified the nuclear transcription factor Y family (NF-YA, NF-YB, NF-YC) with differential activities in neural crest stem cells and their early-differentiated counterparts.

I would like to remark that the evaluation of the whole genome transcriptome array including MARA further revealed the transcription factors SALL4 and YY1. It is the current objective of two other members in the Sommer group to unravel their roles in melanoma.

6. Results

6.1.1. The neural crest-relevant transcriptional regulator NKAP plays a role in melanoma

On the basis of the whole-genome transcriptome analysis comparing neural crest stem cells to early-differentiated derivatives, seven transcriptional regulators were identified including LIN9, LIN28A, SSBP2, NKAP, NF-YA, NF-YB, and NF-YC [5.]. Since numerous developmental signaling cues and transcription factors of the neural crest find reuse in melanoma, I planned to screen the newly discovered neural crest-associated transcriptional regulators in melanoma. Therefore, I utilized the previously characterized human melanoma cell culture M010817, which is well established in the Sommer group [Hoek_2006; Zipser_2011]. The cells were obtained from a 37 years old female patient and contain an N-RAS^{Q61R} mutation. M010817 represents a fast proliferating melanoma cell culture with low invasive capacity under *in vitro* conditions. Nonetheless, their metastatic potential after subcutaneous injection in NSG mice is considerably high. M010817 cells were provided by the URPP biobank, UZH and *in vitro* manipulations using these cells have been successfully performed in earlier experiments [Civenni_2011; Shakhova_2012; Zingg_2015].

Cell cycle analysis using propidium iodide is a simple and robust method to examine the proliferation status of *in vitro*-cultured melanoma cells. Uncontrolled cell growth represents a major hallmark in melanoma and generally in tumor biology. Hereby, cancer cells often activate cell intrinsic growth stimulating factors and signaling pathways to continuously spur cell division. However, this illustrates their dependence on the growth promoting machinery and concomitantly highlights their vulnerability. Hence, genetic modulations that affect the functional integrity of one of these components, consequently interferes with proliferation. Therefore, I subjected a selected assortment of small interfering RNAs (siRNAs) to M010817 cells targeting the previously identified neural crest-associated factors and assessed their impact on the cell cycle.

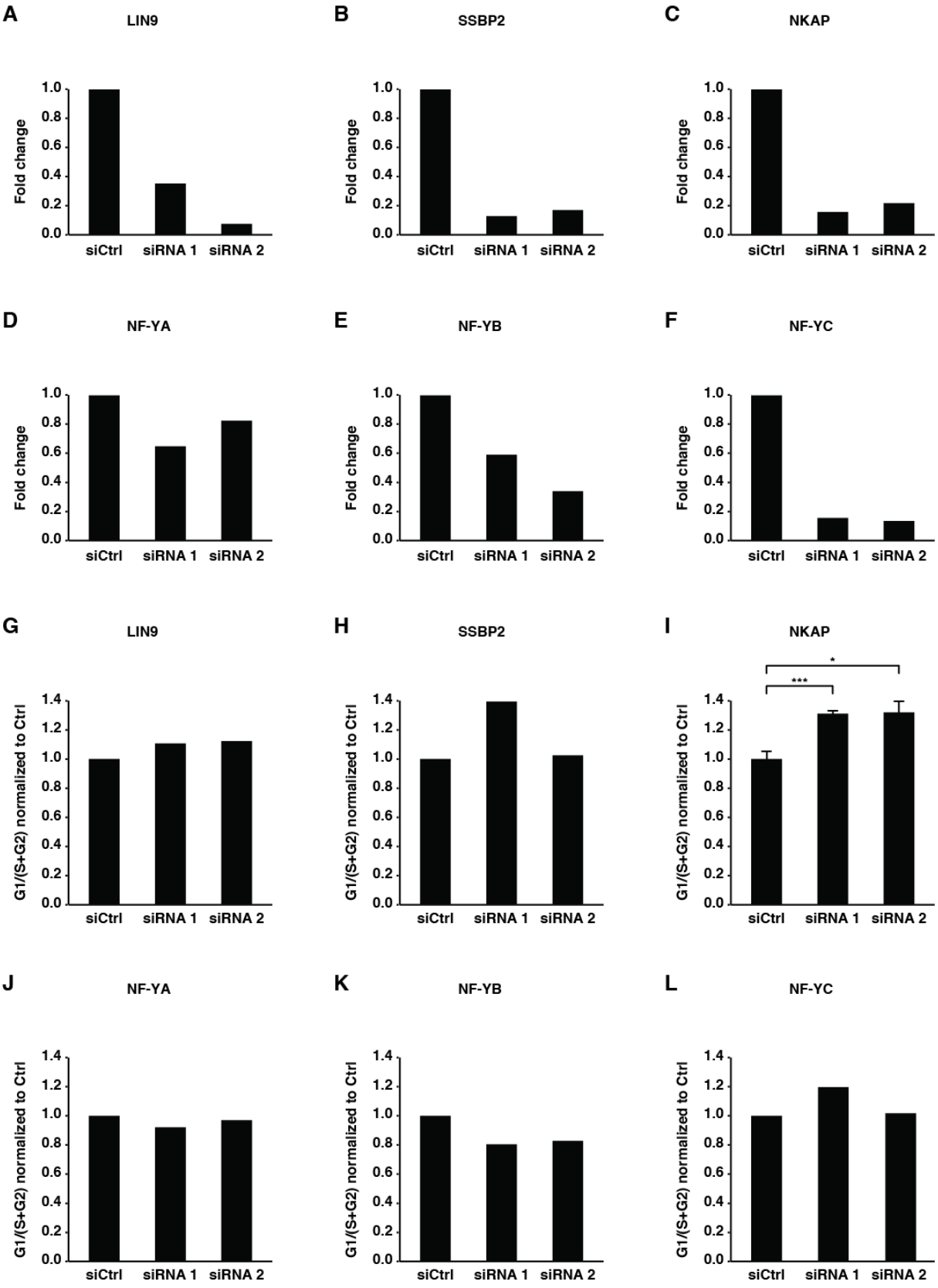

Figure 15. The RNAi screening approach reveals NKAP to play a role in melanoma. To test the role of the newly discovered target genes in melanoma, the cell cycle profile was assessed after subjecting a set of siRNAs (55 nM) to the human melanoma cell culture M010817. **(A-F)** The knockdown efficiencies were confirmed using RT-qPCR. **(G-L)** Cells were stained with propidium iodide and subsequently the cell cycle profile was analyzed using flow cytometry. Computational evaluation was performed on the FlowJo 7.6 software using the

Dean-Jett-Fox algorithm. In case a statistical analysis was performed, the unpaired student's t-test was applied and data are represented as mean ± s.e.m. of n=3.

To evaluate the efficiency of the knockdowns, the expression of the corresponding genes was determined using RT-qPCR. The obtained knockdown efficiencies were sufficient (70-90%) for LIN9, SSBP2, NKAP, NF-YC, moderate (40-65%) for NF-YB, and low (65-85%) for NF-YA (Figures 15A-F). The RT-qPCR results further revealed that LIN28A is not expressed in M010817, which was later confirmed by RNA sequencing (data not shown). Thus, LIN28A was excluded from further investigations.

The results from the cell cycle analysis revealed that, both siRNAs targeting NKAP induced a significant G1/G0 cell cycle arrest. Transient depletion of the residual genes either resulted in minor cell cycle alterations or the applied siRNAs had no consistent effect on the cell cycle. Therefore, it is likely that these factors do not affect proliferation or it might be that the achieved knockdown was not sufficient to induce a significant change in the cell cycle profile. Furthermore, the observed inconsistencies might be a consequence of siRNA off target effects (Figures 15G-L). According to the results of this preliminary screening approach, I decided to further study the role of NKAP in melanoma.

6.1.2. NKAP is expressed in primary human melanoma cell cultures

Previously, NKAP has been reported to be required for T cell development and for the maintenance and survival of hematopoietic stem cells. However, NKAP has not yet been described in the context of melanoma or other kinds of cancer. To expand the field of view on NKAP's role in melanoma, I tested NKAP protein expression in different primary human melanoma cell cultures by immunoblot analysis. In accordance with previous findings that NKAP is ubiquitously expressed, all tested melanoma cell cultures expressed NKAP protein at detectable levels [Burgute_2014]. Although NKAP theoretically weighs 47 kDa, it effectively runs with a molecular weight of approximately 60 kDa when separated by SDS-PAGE. This observation is in analogy with earlier reports and is suggested to be a cause of the exceptionally high content of basic and charged residues, or yet unknown posttranslational modifica-

tions [Burgute_2014; Worlitzer_2014]. As shown in a former study, melanoma cell cultures can be classified into a proliferative or an invasive state, according to their phenotype-specific gene expression profile [Widmer_2012]. The URPP biobank, UZH has previously characterized the provided primary human melanoma cell cultures as follows; M000921, M130427, M980514, M130429, and M010817 are proliferative, whereas M121224 and M130219 are invasive. Interestingly, NKAP expression is markedly reduced in invasive cells as compared to proliferative cells. This indicates that NKAP is either required for proliferation or NKAP down regulation might be necessary to promote invasiveness (Figure 16A).

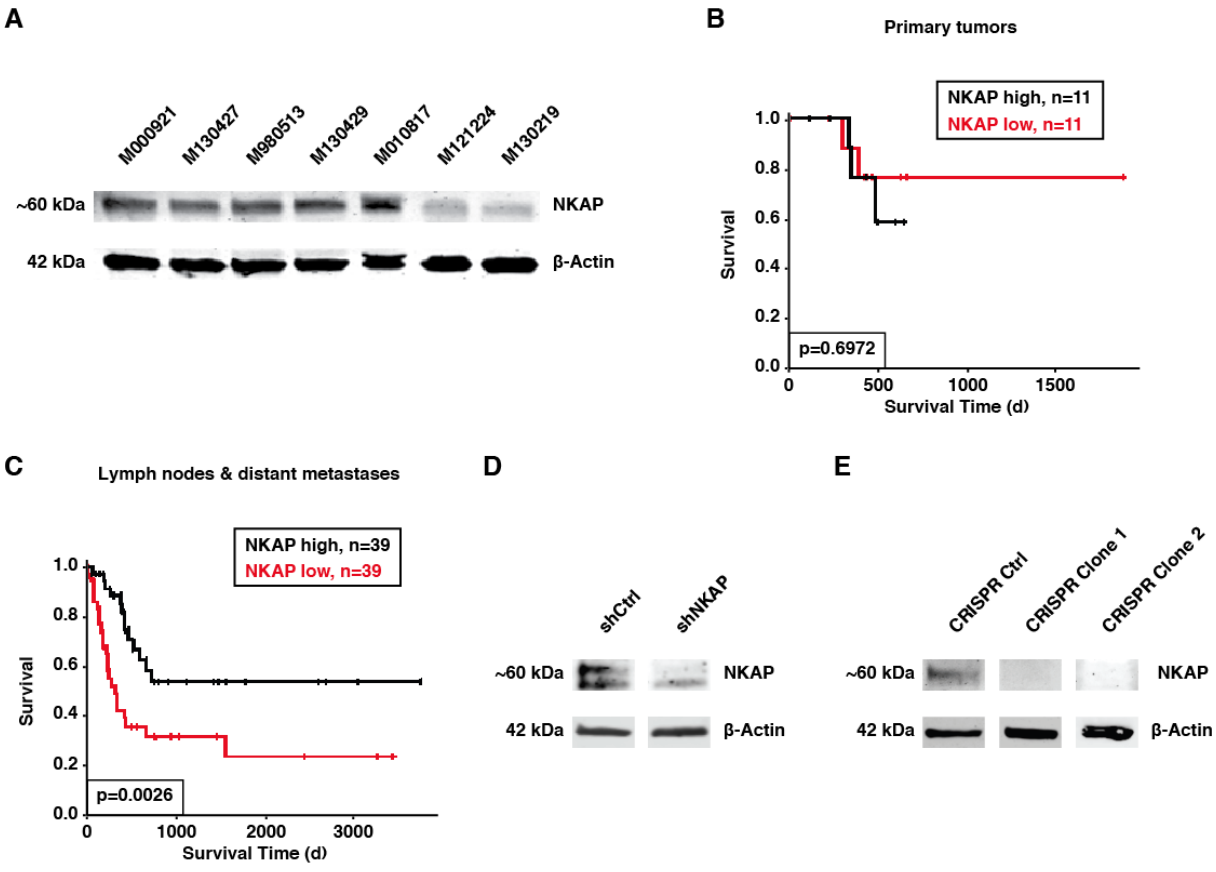

Figure 16. Low NKAP levels correlate with poor patient survival. (A) Immunoblot analysis of NKAP expression in different human melanoma cell cultures. M000921, M130427, M980513, M130429, and M010817 were previously characterized as proliferative, whereas M121224 and M130219 are annotated as invasive cell cultures. **(B-C)** Clinical data were retrieved from the TCGA database in order to assess the correlation between NKAP expression and patient survival. Therefore, a comparative analysis was performed assessing the survival of patients that provided samples with highest (top 15%) and lowest (bottom 15%) NKAP expression. *P*-values were calculated using the Log-rank (Mantel-Cox) test. **(D-E)** To address the role of NKAP in melanoma, stable NKAP loss-of-function M010817 cells were generated using shRNA and CRISPR-CAS9. The absence of the protein was confirmed by immunoblot.

6.1.3. Decreased NKAP expression is linked to poor patient survival

In order to interrogate whether NKAP plays a clinical role in melanoma patients, I assessed the overall patient survival based on NKAP expression using the The Cancer Genome Atlas (TCGA) database. TCGA represents a publicly available data collection that catalogues about 33 different cancer types, including melanoma. The database comprises patient information and data from collected patient material, which was analyzed by gene expression profiling, copy number variation profiling, single nucleotide polymorphism (SNP) genotyping, genome wide DNA methylation profiling, microRNA profiling, and exon sequencing. For data analysis and statistical evaluations I used the TCGA browser v0.9, an online available program developed by Dr. Phil Cheng. To address whether NKAP expression correlates with melanoma patient outcome, I compared the survival data of patients that provided highest (top 15%) and lowest (bottom 15%) NKAP-expressing samples. To better distinguish the effect of NKAP on different phases of melanomagenesis, primary tumors and lymph node/distant metastases were analyzed separately. Differential NKAP expression in primary tumors had no significant influence [*P*=0.6972] on patient survival (Figure 16B). However, patients with low NKAP expression in lymph node and distant metastases had a significantly (P=0.0026) shorter survival. NKAP low patients had a median survival of 0.9 years, whereas the NKAP high patients had a median survival of >10 years (Figure 16C). Consequently, these data demonstrate that NKAP has a beneficial impact on the outcome of melanoma patients. Furthermore, these data suggest that NKAP only interferes with patient survival once melanoma has metastasized.

6.1.4. CRISPR-CAS9 and shRNA efficiently ablate NKAP expression

To keep a closer eye on NKAP's function in melanoma I planned to generate a stable knockdown using RNA interference. Therefore, I used the primary human melanoma cell culture M010817, which presents among the strongest NKAP expressing cell cultures, as shown in (Figure 16A). I applied a lentiviral construct to deliver shRNA plus GFP marker. In order to increase the knockdown efficiency I sorted for cells with high GFP expression using fluorescence-activated cell sorting (FACS). The

knockdown efficiently reduced NKAP expression in M010817, which was confirmed by RT-qPCR (data not shown) and immunoblotting (Figure 16D).

Additionally, to exclude the effect of remaining NKAP activity and shRNA off-target effects, I generated a complete NKAP knockout in M010817 cells using the clustered regularly interspaced short palindromic repeats (CRISPR)-CAS9 technique. The RNA-guided CRISPR-CAS9 method defines a powerful genome-editing tool that allows fast generation of knockout cell cultures. Originally, CRISPR-CAS9 has been found as a prokaryotic adapted immune defense mechanism that confers resistance to foreign genetic elements. Thereby, the CAS nuclease recognizes and cuts exogenous genetic material that is bound by a CRISPR spacer [Barrangou_2007; Marraffini_2008; Redman_2016]. In genome engineering, the single guide RNA (sgRNA) recognizes and binds to its complementary sequence on the genome. Generally, sgRNAs contain a target specific CRISPR RNA sequence (crRNA) and a trans-activation RNA (tracrRNA) that recruits the CAS9 nuclease to the target site. In order to exert nuclease activity, CAS9 requires a protospacer adjacent motif (PAM) consistent of the three base pairs 5'-NGG-3', which are located directly after the sgRNA recognition sequence. Upon binding to the sgRNA, CAS9 introduces a double strand break into the DNA, which is usually repaired by non-homologues end-joining (NHEJ). Errors during the repair process lead to random integration of so-called indel mutations at the target site. This often causes the formation of a frame shift and consequently to the introduction of a premature stop-codon, which results in the abrogation of the gene product [Jinek_2013; Ran_2013].

Although the NKAP gene locus encodes four alternatively processed transcripts, only one is translated into a protein. Hence, to completely abolish protein expression I decided to target the NKAP gene at exon 1 of the protein-coding transcript. Using the online available Optimized CRISPR Design tool I generated an sgRNA (TGATGAACATACACCAGTGG) with a quality score of 69 out of 100, predicting a low chance for off-target binding. Subsequently, M010817 cells were simultaneously transfected with an sgRNA expressing vector and a construct that encodes the CAS9 nuclease and a GFP reporter. Ultimately, GFP positive cells were seeded as single colonies and screened for NKAP protein

expression by Western blot analysis. The complete disappearance of the presumed bands in two selected clones, clearly demonstrates the loss of NKAP expression (Figure 16E). The knockout was further confirmed by Sanger sequencing, revealing the presence of a premature stop-codon in all samples tested (data not shown).

6.1.5. Loss of NKAP affects cell adhesion *in vitro*

As a first observation, NKAP deficient M010817 cells display an evident adhesion phenotype in culture. After trypsinization, NKAP depleted cells remain in suspension as clumps and adhere to the cell culture dish in a temporally deferred manner (Figure 17A). To confirm this observation, I conducted an adhesion assay followed by a crystal violet staining to quantitatively assess the adhesive potential of NKAP deficient M010817 cells. Therefore, I seeded 500'000 cells in normal 6-well cell culture plates and determined the area covered by cells and the number of cells in suspension after a 12 hours incubation period. As expected, the area covered by NKAP deficient M010817 cells was dramatically reduced, whereas the number of cells in suspension was significantly elevated as compared to control cells (Figure 17B-C). Additionally, to exclude enhanced cellular detachment due to increased apoptotic events, I stained floating cells with trypan blue and examined the live-dead cell ratio (Figure 17C). However, the live-dead cell ratio was not significantly altered between control and knockout cells, indicating that the increased number of cells in suspension is not a consequence of a higher apoptotic rate. Hence, these results suggest that NKAP effectively interferes with the adhesive capacity of M010817 cells.

6.1.6. NKAP deficiency increases invasiveness *in vitro*

To test whether NKAP deficiency also affects invasiveness *in vitro*, I performed a Boyden chamber invasion assay. Previous experiments have shown that regardless of the treatment, M010817 cells become hardly invasive under *in vitro* conditions and cannot be used in Boyden chamber assays. Consequently, I generated a stable NKAP knockdown in the primary human melanoma cell culture

M050829 using two different shRNAs. M050829 cells possess proliferative as well as invasive properties and have been used previously in invasion assays. The results of the invasion assay revealed that either of the two applied shRNAs significantly (P>0.05) enhanced the invasive capacity of M050829 cells (Figure 17D-E). Summing-up, these findings demonstrate that NKAP depletion leads to enhanced invasiveness, suggesting that NKAP acts suppressively on invasion *in vitro*.

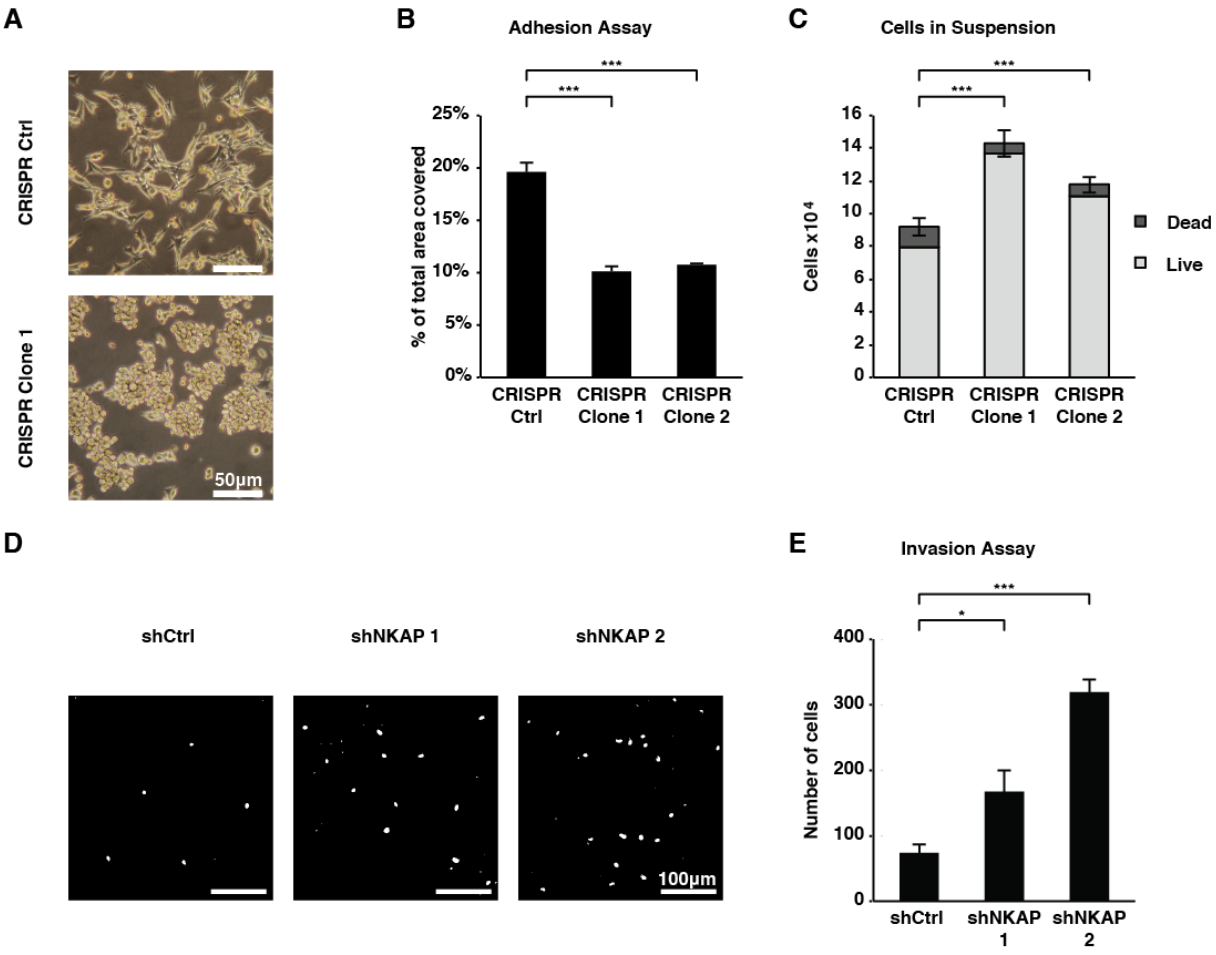

Figure 17. NKAP depletion affects adhesion *in vitro*. (A) Bright-field image of M010817 NKAP knockout and control cells. Scale bars, 50 µm. **(B-C)** To assess the adhesion capacity of M010817 knockout and control cells, 500'000 cells were seeded in a 6-well-plate and incubated for 12 h. To determine the relative area (%) covered by cells, 5 random regions were analyzed using the CellProfiler 2.0 software. **(D)** To determine the invasive capacity of M050829 NKAP knockdown and control cells, a Boyden chamber invasion assay was performed. Microscopic image of invading cells fluorescently labeled with Hoechst 33342. Scale bars, 100 µm. **(E)** The exact number of invading cells was quantified with the CellProfiler 2.0. software. **(B, C, E)** For statistical analysis the unpaired student's t-test was applied and the data are depicted as mean ± s.e.m. of n=3.

6.1.7. Stable NKAP depletion induces a G1/G0 cell cycle arrest *in vitro*

As mentioned previously, transient NKAP depletion in M010817 cells induced a G1/G0 cell cycle arrest *in vitro* [6.1.1]. To confirm these results, I analyzed the cell cycle profile of stably transfected NKAP knockdown and NKAP knockout M010817 cells. Furthermore, I conducted a growth curve analysis to assess the proliferative potential of these cells. Analogous to transiently transfected cells, stable NKAP knockdown as well as complete NKAP ablation induced a drastic G1/G0 cell cycle arrest (Figure 18A). Along this line, the growth curve analysis revealed that NKAP deficiency significantly reduced proliferation, circumstantiating the previously obtained results (Figure 18B).

6.1.8. Forced adhesion does not rescue the G1/G0 cell cycle arrest

Generally, adhesion to the extracellular matrix is a precondition in normal cells to allow cell cycle progression. If cellular attachment to solid substrate is disrupted, normal cells are not able to complete cell division and arrest in the G1 phase of the cell cycle [Otsuka_1975; Matsuhisa_1981; Benaud_2001]. This prompted me to investigate whether the G1/G0 cell cycle arrest in NKAP depleted cells is mediated through reduced cellular adhesion. Therefore, I seeded cells in fibronectin-coated cell culture dishes to force their attachment to the plate surface. Subsequently, I determined their cell cycle profile and performed a growth curve analysis to assess their proliferative behavior. Expectedly, fibronectin treatment rescued the adhesion phenotype, as the attachment rate for NKAP depleted and control cells was equal (data not shown). However, although NKAP deficient cells were forced to adhere, their cell cycle profile remained unaltered (Figure 18C). The results of the growth curve analysis further substantiated that despite adhesion, NKAP depleted M010817 cells present with impaired proliferation (Figure 18D). This indicates that NKAP deficiency effectively interferes with proliferation *in vitro* and that decreased cellular adhesion is most likely not the cause of the induced G1/G0 cell cycle arrest.

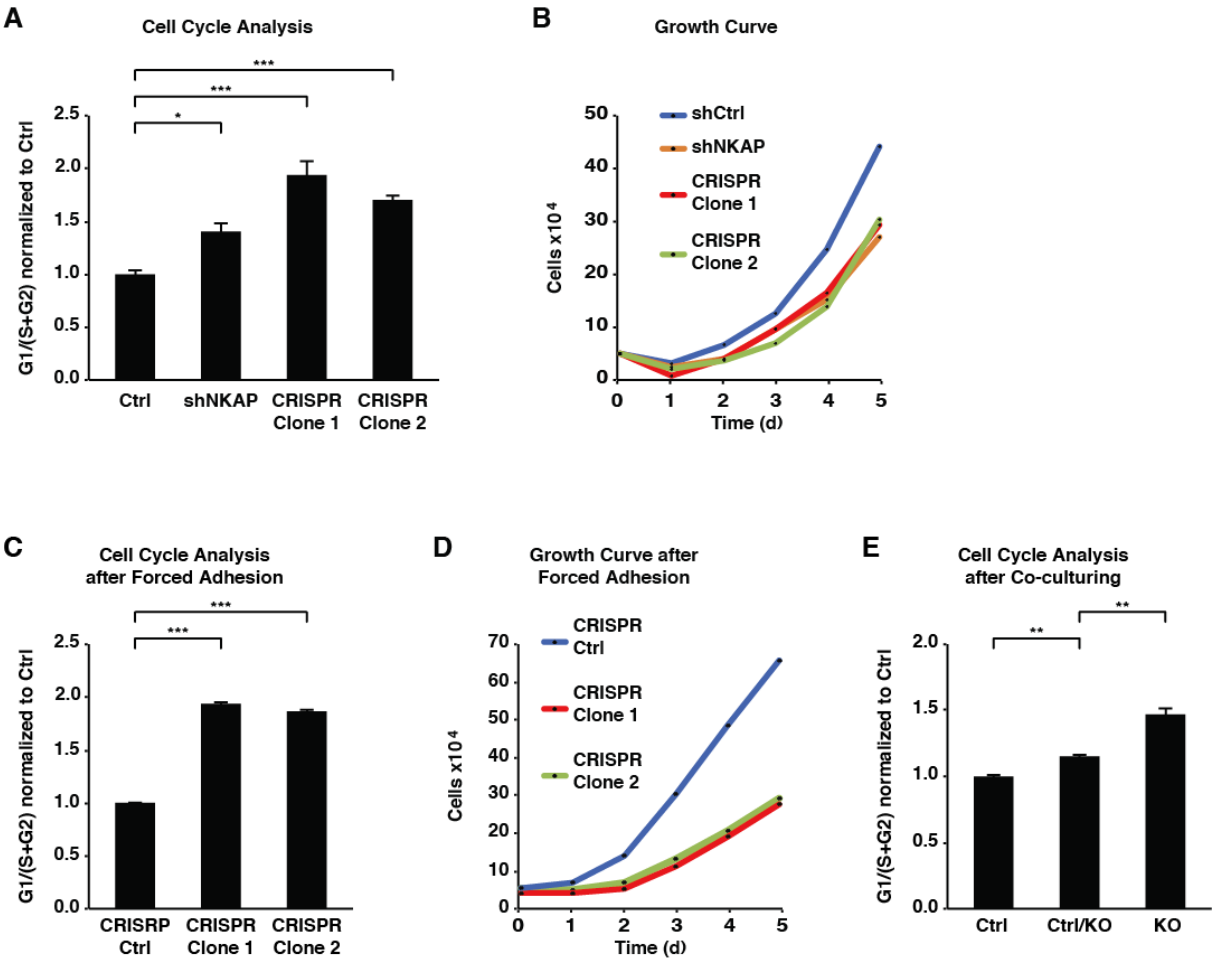

Figure 18. NKAP depletion induces a G1/G0 cell cycle arrest. (A) After EdU and propidium iodide incorporation, a cell cycle analysis of NKAP knockout, knockdown and control M010817 cells was performed using flow cytometry. **(B)** To assess the proliferative potential of NKAP knockout, knockdown and control M010817 cells, a growth curve analysis was performed over 5 days. **(C)** After NKAP knockout and control M010817 cells were seeded in fibronectin-coated dishes their cell cycle profile was determined according to the descriptions in (A). **(D)** KNAP knockout and control M010817 cells were cultured in fibronectin-coated dishes and a growth curve analysis was performed over 5 days. **(E)** NKAP knockout and control M010817 cells were co-cultured in a 1:1 ratio and their cell cycle profile was assessed as described in (A). **(A, C, E)** For statistical analysis the unpaired student's t-test was applied and the data are depicted as mean ± s.e.m. of n=3.

6.1.9. Cell intrinsic mechanisms induce the cell cycle arrest in NKAP depleted cells

Cell replication is a tightly controlled process that relies on intrinsic as well as extrinsic signaling cues. To address whether the cell cycle arrest is due to decreased secretion of growth promoting signaling molecules, I planned to determine the cell cycle profile of co-cultured NKAP wild type and knockout M010817 cells. Hence, NKAP wild type and knockout cells were co-incubated in a 1:1 ratio for two days prior to cell cycle analysis. If co-culturing rescues the proliferation defect in NKAP knockout cells, the mixed and the pure wild type population present with similar cell cycle profiles. However, if

co-culturing has no effect on NKAP knockout cells, the cell cycle profile appears as an intermediate product of both, wild type and knockout cells. The cell cycle distribution is thereby biased towards the faster proliferating wild type population (63%), which outnumbers the knockout population (37%) after two days in culture. The results of the cell cycle analysis however revealed that the cell cycle profile of co-cultured wild type and knockout cells is significantly distinct from purely cultured M010817 wild type cells. Moreover, considering the growth advantage of NKAP wild type M010817 cells, the estimated G1/(S+G2) ratio of 1.17 (1+0.37·(1.47-1) perfectly coincides with the effectively measured G1/(S+G2) ratio of 1.15 (Figure 18E). Consequently, these results demonstrate that co-culturing does not rescue the cell cycle arrest and suggest that NKAP depletion impedes cell proliferation through cell intrinsic mechanisms and not through reduced secretion of growth promoting factors.

6.1.10. NKAP deficiency enhances metastasis formation *in vivo*

To examine the effect of NKAP deficiency under *in vivo* conditions, I subcutaneously injected M010817 NKAP knockout cells into immune-compromised *NOD.Cg-Prkdc*^{scid} *Il2rg*^{tm1Wjl}*/SzJ* (NSG) mice. I sacrificed the mice 4 weeks after injection and determined the weight of the primary tumors. Despite the *in vitro* induced G1/G0 cell cycle arrest after NKAP depletion, there was no significant difference in tumor growth *in vivo* (Figure 19A-B). Additionally, to assess the metastatic potential of NKAP deficient cells, I collected the lungs of injected animals and analyzed the metastatic burden by RT-qPCR. Therefore, I measured the relative mRNA expression of two independent human housekeeping genes (GAPDH, PPIA) in homogenized lung tissue and normalized against the murine housekeeping gene USF1. An earlier report has described a similar approach to quantify human circulating tumor cells (CTCs) in the blood system of previously injected mice [Gorges_2012]. In order to determine the metastatic load in mouse lungs, I used the same primers for the human housekeeping genes as suggested in the report. To evaluate the specificity of the primers, I additionally analyzed the lungs of non-injected mice. Hence, the specificity of the primers was clearly confirmed, as GAPDH and PPIA expression levels in injected animals were significantly higher as compared to uninjected animals. Ultimately, the results of the RT-qPCR analysis revealed that GAPDH and PPIA expression was

significantly elevated in mice injected with NKAP depleted cells (Figure 19C-D). Thereby, the extent of the metastatic burden does not coincide with the size of the primary tumor, as *in vivo* tumor growth remained unaffected upon NKAP depletion.

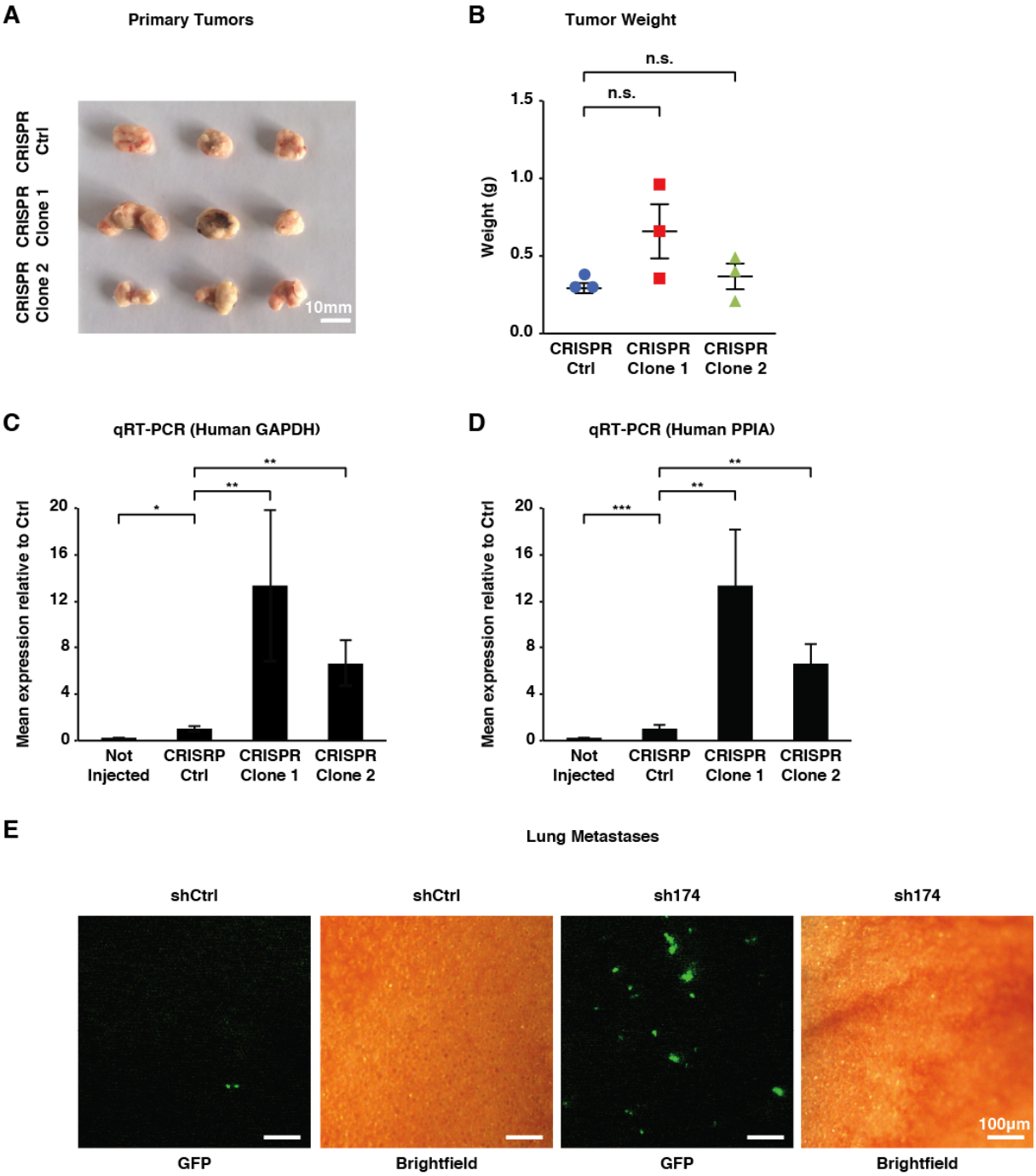

Figure 19. NKAP depletion increases the metastatic potential *in vivo*. (A) Macroscopic image of primary tumors 4 weeks after subcutaneous injection of 300'000 NKAP knockout and control M010817 cells in NSG mice (n=3). Scale bar, 10 mm. **(B)** Weights of the tumors depicted in (A). **(C-D)** To examine the metastatic burden in the lungs of mice described in (A), RT-qPCR was used to determine human GAPDH and human PPIA levels in homogenized lung tissue. Relative mRNA expression levels were normalized to murine USF1. **(E)** Superficial GFP-positive lesions and corresponding bright-field images from lungs of mice injected with NKAP

knockdown and control M010817 cells. Scale bars, 100 μm. **(B, C, D)** For statistical analysis the unpaired student's t-test was applied and the data are depicted as mean ± s.e.m. of n=3.

In a second experiment, NKAP knockdown cells labeled with a GFP reporter were injected into NSG mice to qualitatively assess the incidence of metastatic cells in the lung. Therefore, I isolated the lungs of previously injected mice four weeks after injection and visualized superficially located metastases using a fluorescence-coupled binocular. Corroborating the results described above, the number of metastases in mice that were injected with NKAP knockdown cells was dramatically increased (Figure 19E). However, the exact number of metastatic lesions per lung could not be determined, as with depth the emitted GFP signal slowly merges with the surrounding background noise.

6.1.11. NKAP associates with EMT, cell adhesion and cytoskeleton remodeling

To determine downstream effector genes that are differentially expressed upon NKAP depletion, I performed RNA sequencing (RNA-seq) to compare the gene expression profile of NKAP knockout, knockdown and control M010817 cells. In total 2954 genes were differentially expressed in NKAP knockout cells, and 1863 genes had altered expression in NKAP knockdown cells when compared to control cells (fold change >1.4-fold, FDR corrected $P<0.05$). Overlapping the two signatures revealed 910 commonly regulated genes (Figure 20A). To further assess the pathways that are functionally affected upon NKAP depletion, I conducted a gene ontology pathway enrichment analysis using the MetaCore™ platform (Figure 20B). Interestingly, the MetaCore™ analysis proposed enriched pathways associated with EMT, cell adhesion, and cytoskeleton remodeling. However, most genes engaged in the proposed pathways, change their expression in a way that stands in contrast to the observed phenotype. A prominent example following this paradoxical phenomenon is fibronectin 1 (FN1), an extracellular protein that helps cells attach to the surrounding matrix. Although fibronectin is four times up regulated in NKAP deficient cells, their adhesion capacity remains low. Thereby, up regulation of FN1 might be a compensation mechanism to overcome the adhesion defect induced by NKAP depletion. The reason for decreased adhesion however could not be determined by RNA-seq.

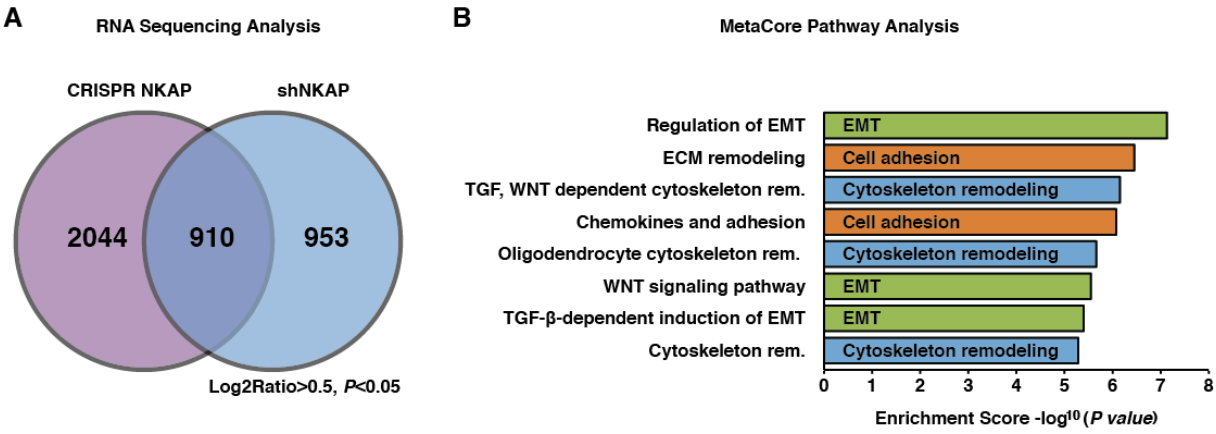

Figure 20. NKAP deficiency affects EMT, cell adhesion and cytoskeleton remodeling. (A) RNA sequencing was performed to establish a comparative transcriptomic analysis of NKAP knockout, knockdown and control cells. The overlap reveals 910 differentially expressed genes (log2Ratio>0.5, P<0.05, FDR≤0.05). **(B)** These genes (910) were further analyzed using the MetaCore™ pathway enrichment algorithm. The top eight hits are represented in the table.

6.1.12. NKAP over expression in M010817 cells is weak

In order to revert the phenotype observed in NKAP depleted cells, I generated a lentiviral over expression construct containing an HA_NKAP fusion protein under the control of the CMV promoter. The vector further comprises an eGFP reporter regulated by the SV40 promoter. Next, M010817 NKAP knockout and control cells were infected and selected with Puromycin to obtain a pure population. In addition, infected cells were sorted for high GFP to guarantee accurate expression of the exogenous protein. However, exogenous protein levels were fairly weak, despite all the measures taken and abundant eGFP expression, as confirmed by immunoblot analysis (Figure 21A). Hence, this indicates that high NKAP expression is poorly tolerated, and M010817 cells are either able to silence the CMV promoter or high NKAP expression induces apoptosis.

6.1.13. NKAP over expression only partly rescues the NKAP depletion phenotype *in vivo*

Although exogenous NKAP levels were low, the range of expression was similar to the endogenous protein. Therefore, I planned to address whether exogenous NKAP expression is able to revert the *in vivo* phenotype evoked by NKAP depletion. To this end, I subcutaneously injected NKAP reconstituted M010817 cells, described in the previous section, into NSG mice and harvested primary tumors and lungs for further evaluation four weeks post injection. In accordance with previous findings, NKAP reconstitution had no effect on tumor growth (data not shown). However, the metastatic burden was substantially reduced upon NKAP over expression (Figure 21B-C). Although a clear trend is observable, the differences were not significant due to the high variability in the non-reconstituted control group. Nonetheless, these results clearly demonstrate that the increased metastatic proclivity of M010817 cells is indeed a consequence of NKAP depletion and that NKAP reconstitution at least partly reverts this phenotype.

6.1.14. NKAP appears with a punctuated pattern within the nucleus

As shown by Western blot analysis, the achieved expression levels for exogenous NKAP were low in M010817 cells. However, the method does not allow a conclusion about the expression intensity on a single cell level. Hence, it might be that NKAP is expressed in all cells on a similarly low level or it might be that NKAP is high in a small subset of the population, while it is absent in the rest. To address this question, I performed an immunocytochemistry staining of M010817 cells over expressing HA_NKAP using a monoclonal anti-HA antibody. The anti-HA staining nicely illustrates the localization of the exogenous HA_NKAP protein to the nucleus in a punctuated manner (Figure 21D). However, although all cells were strongly GFP positive, only a small fraction expressed the HA-tagged protein, whereas in residual cells the expression was completely absent (data not shown). Hence, M010817 cells are able to silence the CMV promoter, independently of the GFP reporter, in order to shut down NKAP expression.

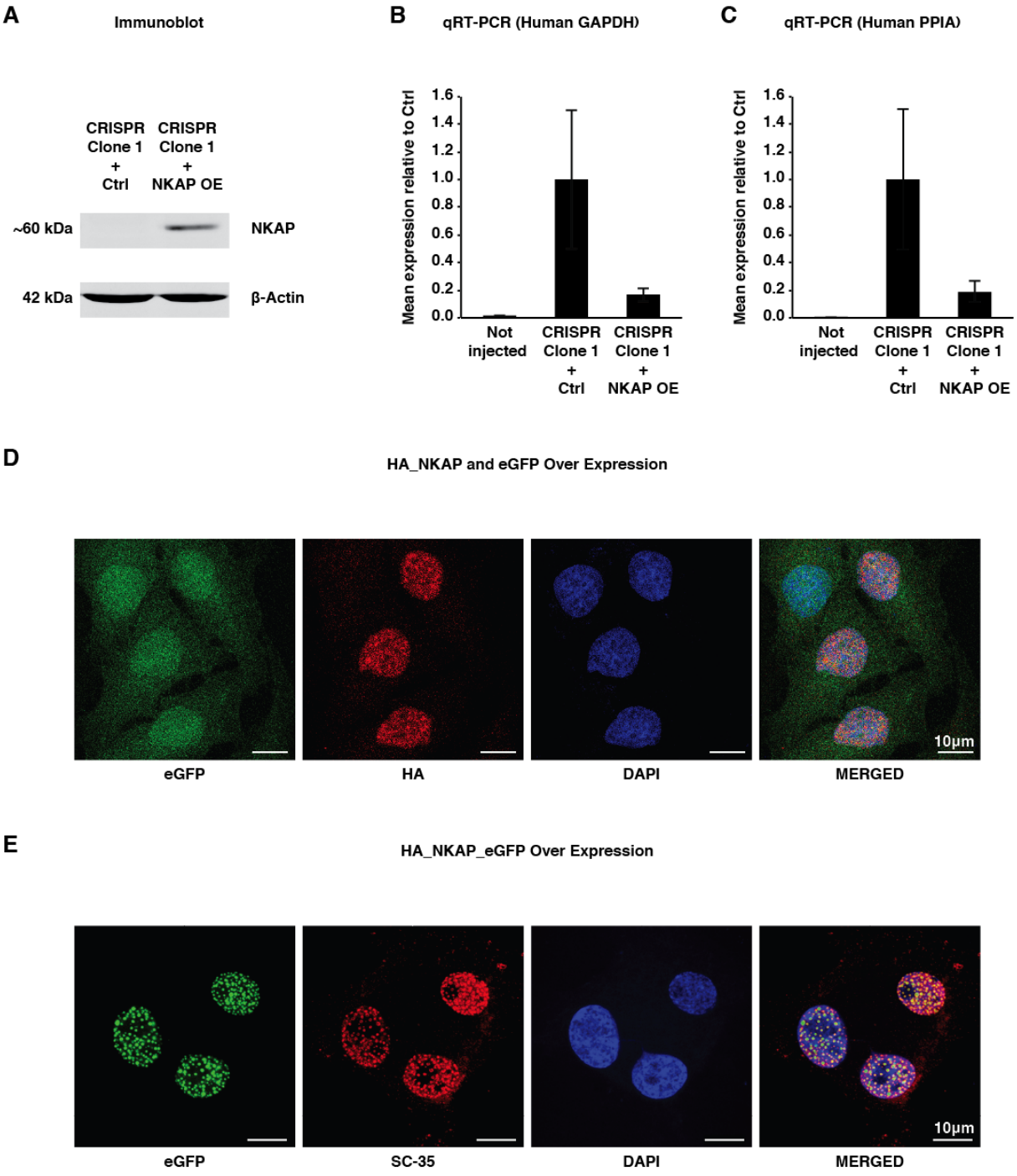

Figure 21. NKAP localizes to nuclear speckles. (A) To revert the NKAP depletion-mediated phenotype, NKAP knockout M010817 cells were reconstituted with a HA_NKAP fusion protein and a eGFP reporter. The expression of the exogenous protein was confirmed by immunoblotting. **(B)** Reconstituted cells were subcutaneously injected into NSG mice and the metastatic burden was assessed as described in (Figure 19C-D). **(C)** Immunofluorescent staining for the HA-tag and internal eGFP expression in reconstituted NKAP knockout M010817 cells. Scale bars, 10 µm. **(D)** Immunofluorescent staining for SC-35 and internal eGFP expression in NKAP knockout M010817 cells reconstituted with a HA_NKAP_eGFP fusion protein. Scale bars, 10 µm. **(B, C)** For statistical analysis the unpaired student's t-test was applied and the data are depicted as mean ± s.e.m. of n=3.

6.1.15. NKAP localizes to the nuclear speckles

Since M010817 cells were able to silence NKAP expression independently of the eGFP reporter, I created a HA_NKAP_eGFP fusion protein with the intention to directly link the intensity of the GFP signal with protein expression. Furthermore, the eGFP tag allows the exact subcellular localization of the protein. Accordingly, I transfected M010817 NKAP knockout and control cells with a lentiviral construct containing the fusion protein under the control of an SV40 promoter. I subjected the transfected cells to Puromycin selection and sorted for high GFP expression as described above. A previous study performed in HEK cells suggests NKAP as a component of the RNA processing machinery and has shown its localization to the nuclear speckles [Burgute_2014]. To test whether NKAP behaves similar in M010817 cells, I conducted an immunofluorescence staining to co-label GFP positive cells with the nuclear speckle marker serine/arginine-rich splicing factor 2 (SRSF2). SRSF2 is required for the formation of the earliest splicing complex and interacts with various spliceosomal components [Fu_1993]. The staining revealed the accumulation of the eGFP reporter in multiple small nuclear spots that exclusively colocalize with SRSF2 (Figure 21E). Consequently, these findings illustrate that the exogenously expressed NKAP fusion protein localizes to nuclear speckles in M010817 cells, thereby confirming previous data that suggest NKAP as a speckle protein involved in RNA processing [Burgute_2014]. Usually, speckles appear as irregularly shaped nuclear structures localized in the interchromatin space [Spector_2011]. However, the SRSF2 antibody staining supports previous data demonstrating that nuclear speckles increase in number and appear as homogenous, round spots upon NKAP over expression [Burgute_2014]. Thus, it is assumed that excessive NKAP synthesis leads to the accumulation of the protein in nuclear speckles, which have been proposed as a storage place for RNA processing factors. Interestingly, inhibition of the transcription machinery leads to a similar accumulation of nuclear speckle proteins in enlarged rounded spots [Melcak_2000].

Unfortunately, the exogenous fusion protein was only present in the minority of the cell population, and the number of GFP positive cells decreased drastically over time in culture. This clearly indicates

that M010817 cells poorly tolerate NKAP over expression and silencing is required for the maintenance of the cellular integrity.

6.1.16. NKAP interacts with nuclear speckle components

A previous report demonstrated the interaction of NKAP with components of the NOTCH co-repressor complex such as CIR and HDAC3. Interestingly, both factors partially localize to nuclear speckles [Pajerowski_2009]. A later study showed that NKAP co-precipitates with RNA binding proteins, i.e. hnRNPs, RNA helicases and splicing factors [Burgute_2014]. To gain more insights into the mechanistic function of NKAP in M010817 cells, I sought to investigate its interaction partners. Therefore, I performed a co-immunoprecipitation study in collaboration with Sergio Leone (group of PD Dr. Raffaella Santoro) in HA_NKAP expressing M010817 cells using a monoclonal anti-HA antibody. Subsequently, the eluate was processed for LC-MS/MS analysis. The results of the mass spectrometry analysis revealed that the majority of the proteins identified associate with nuclear speckles and include hnRNPs, RNA helicases, splicing factors, and other RNA-binding proteins (Table 1). Interestingly, NKAP also co-precipitated with stress response factors that at least partly exert their function in nuclear speckles. Consequently, the data obtained by mass spectrometry confirm earlier co-immunoprecipitation studies and demonstrate that NKAP interacts with nuclear speckle and RNA processing proteins in M010817 cells. Although, the interaction with CIR and HDAC3 was not affirmed, NKAP co-precipitated with pinin (PNN). PNN binds to the transcriptional repressor C-terminal binding protein (CtBP), a component of the NOTCH co-repressor complex, and thereby prevents CtBP-mediated transcriptional repression. Hence, NKAPs' interaction with PNN suggests a connection with the NOTCH co-repressor complex, however the functional significance of this interaction remains speculative.

A

BioSample	Gene Name	Function
9	HSPB1	Stress response protein
8	HNRNPA2B1	Heterogeneous nuclear ribonucleoprotein
7	PHB	Cell cycle regulator
6	DHX9	RNA helicase
6	HNRNPM	Heterogeneous nuclear ribonucleoprotein
5	HNRNPK	Heterogeneous nuclear ribonucleoprotein
5	HNRNPU	Heterogeneous nuclear ribonucleoprotein
5	HNRNPC	Heterogeneous nuclear ribonucleoprotein
5	HNRNPL	Heterogeneous nuclear ribonucleoprotein
4	DDX5	RNA helicase
4	HSPA1A	Stress response protein
3	HNRNPA1	Heterogeneous nuclear ribonucleoprotein
3	HNRNPA3	Heterogeneous nuclear ribonucleoprotein
2	NKAP	RNA processing protein
2	DDX17	RNA helicase
2	DDX21	RNA helicase
2	NONO	Paraspeckle protein
2	PARP1	Stress response protein
2	SRSF3	RNA-binding protein
2	SYNCRIP	Heterogeneous nuclear ribonucleoprotein
2	RBMX	RNA-binding protein
2	SFPQ	Splicing factor
2	HNRNPD	Heterogeneous nuclear ribonucleoprotein
2	RALY	RNA-binding protein
2	DDX39A	RNA helicase
2	CRYAB	Stress response protein
1	DDX3X	RNA helicase
1	MATR3	Paraspeckle protein
1	HNRNPH1	Heterogeneous nuclear ribonucleoprotein
1	SUMO2	Stress response protein
1	PNN	RNA processing protein

Table 01. NKAP interacts with nuclear speckle proteins involved in RNA processing. (A) To determine NKAP interaction partners, a co-immunoprecipitation study was performed in HA_NKAP over expressing M010817 cells using a monoclonal anti-HA-antibody. Subsequently, the eluate was processed for LC-MS/MS analysis. The table depicts NKAP interaction partners localized in nuclear speckles.

6.1.17. CIR knockdown does not phenocopy NKAP depletion

As mentioned before, CIR localizes to nuclear speckles and interacts with NKAP, as confirmed by co-immunoprecipitation [Pajerowski_2009]. Likewise to NKAP, CIR regulates transcription as a compo-

nent of the NOTCH co-repressor complex [Hsieh_1999]. However, CIR has also been proposed to modulate splice site selection during alternative splicing of pre-mRNAs [Maita_2004]. To further investigate the relationship between NKAP and the NOTCH co-repressor complex, I decided to address the role of CIR in M010817 cells. Therefore, I transiently depleted CIR expression in M010817 cells using two different siRNAs. Subsequently, I performed an adhesion assay and determined the cell cycle profile using EdU incorporation. As confirmed by RT-qPCR, the siRNAs achieved an 80%, and 72% reduction in CIR expression, respectively (Figure 22A). However, transient CIR depletion had neither an effect on cell adhesion nor on the cell cycle, implying that CIR deficiency does not mimic the NKAP phenotype in M010817 cells (Figure 22B-D). Consequently, these data suggest that NKAP's role in cellular attachment and cell cycle progression is not mediated by CIR.

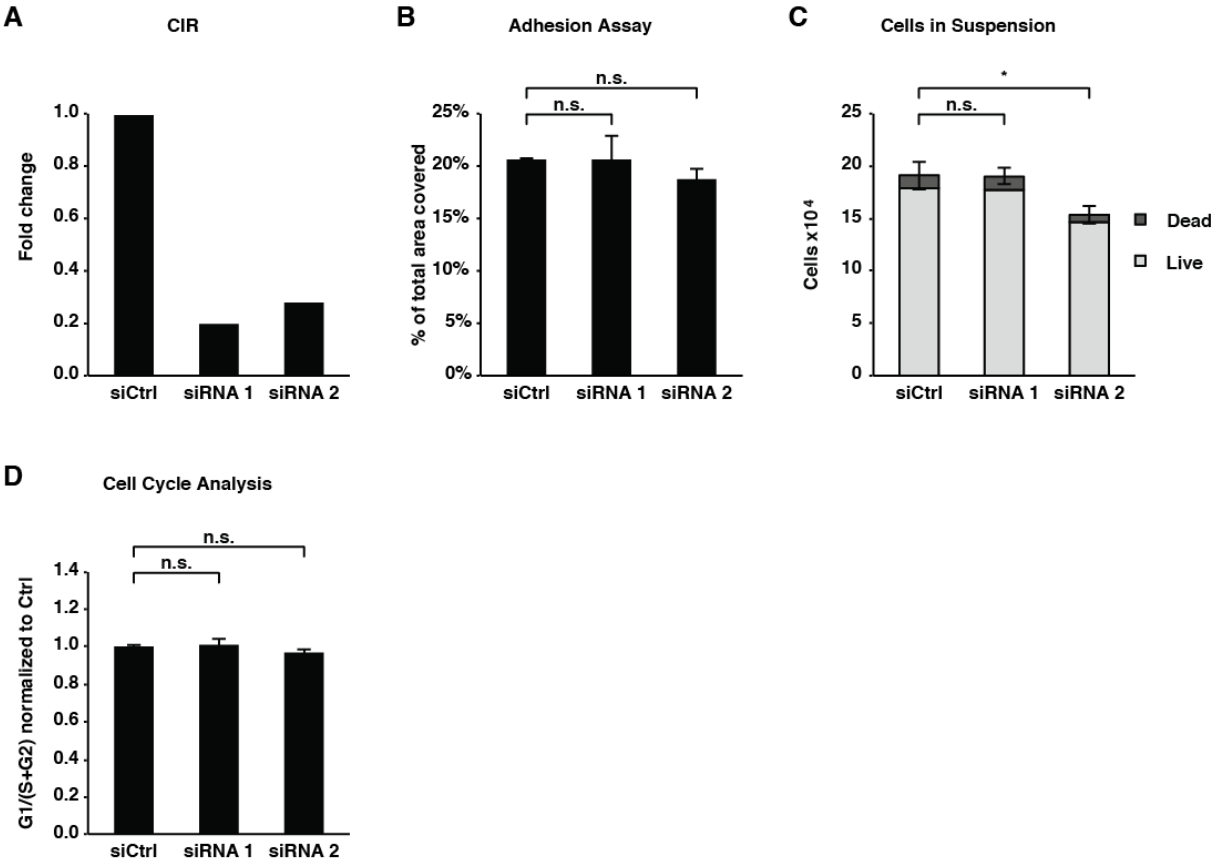

Figure 22. CIR deficiency does not phenocopy NKAP depletion. (A) M010817 cells were transiently transfected with two siRNAs (55 nM) targeting CIR. The knockdown was confirmed using RT-qPCR. **(B-C)** To assess the adhesive capacity of transiently transfected cells described in (A), an adhesion assay was performed as described in (Figure 17B-C). **(D)** To determine the cell cycle profile of CIR knockdown M010817 cells (A), a cell cycle analysis was performed according to previous instructions (Figure 18A). **(B-D)** For statistical analysis the unpaired student's t-test was applied and the data are depicted as mean ± s.e.m. of n=3.

6.1.18. NKAP depletion reduces translational activity

This and earlier studies have shown NKAP's subcellular localization to nuclear speckles, where it interacts with a plethora of RNA processing factors. Hence, it is well conceivable that NKAP is involved in the co- or post-transcriptional processing of pre-mature RNA. If NKAP depletion truly affects RNA processing, unprocessed RNA would accumulate, whereas the concentration of mature RNA would decrease. Consequently, translation drops in response to reduced substrate levels. To test this hypothesis, I pulsed M010817 NKAP knockout and control cells with O-propargyl-puromycin (OP-puro) and assessed the incorporation rate using fluorescence activated cell analysis. OP-puro is a functional analog of puromycin and is efficiently incorporated into newly synthesized peptides. Subsequently, OP-puro is fluorescently labeled, whereas the intensity of the signal directly correlates with the translational activity. As a negative control I used M010817 control cells pre-incubated with cycloheximide, a potent protein synthesis inhibitor. As a result, the median OP-puro incorporation was 5 times (P>0.001) reduced in cycloheximide treated cells, confirming the specificity of the signal (Figure 23A-B). The FACS analysis further revealed that the OP-puro incorporation was 2.4-fold and 1.6-fold decreased in both NKAP knockout clones tested. These results demonstrate that NKAP depletion leads to impaired transcriptional activity, which suggests that NKAP is required in co- or post-transcriptional processes.

6.1.19. NKAP expression levels are tightly regulated to allow optimal transcriptional activity

As described earlier, exogenous NKAP was only expressed in a small fraction of the cell population, whereas it was silenced in the residual fraction. To test whether the translational potential is restored in M010817 cells expressing the exogenous HA_NKAP_eGFP fusion protein, I examined their translational activity using OP-puro incorporation followed by flow cytometric analysis. To assess the difference between silenced and strong NKAP expression, I compared the OP-puro incorporation rate of lowest (10%) and highest (10%) GFP-expressing cells. Surprisingly, the translational activity was only slightly increased (P=0.02) in high NKAP expressing cells when compared to the low group (Figure

23C). Furthermore, I compared their OP-puro incorporation to a third group with intermediate GFP expression (10%, optimized). Strikingly, M010817 cells with intermediate NKAP levels showed a dramatic increase in translational activity when compared to the low and high group. Hence, these results demonstrate that NKAP levels are tightly regulated and that aberrant NKAP expression leads to impaired translational activity.

6.1.20. Reduced adhesion is a consequence of impaired protein synthesis

With the results described in the previous sections, it became evident that NKAP deficiency interferes with the translational activity. During the course of the preparation procedure for the adhesion assay, cells were routinely incubated with trypsin to allow dissociation from the culture dish. Trypsin is a serine protease that hydrolyses cell surface proteins, thereby inducing cellular detachment from the substrate. Consequently, cells have to replenish their arsenal of surface proteins in order to guarantee reattachment to the culture dish. However, if translational activity is impaired, cells attach in a temporally deferred manner due to delayed protein synthesis. To test this assumption, I incubated M010817 NKAP knockout and control cells with PBS-EDTA to allow mild detachment from the culture dish without destroying the surface proteome. Subsequently, I conducted an adhesion assay as described earlier in this study [6.1.5.]. Strikingly, the adhesion in the NKAP knockout clone 1 was completely restored upon PBS-EDTA treatment, while the adhesive capacity of the NKAP knockout clone 2 was dramatically improved (P=0.03) (Figure 23D-E). Hence, these data clearly illustrate that impaired cellular adhesion in NKAP depleted cells is a consequence of delayed protein replenishment on the cell surface after trypsinization due to the compromised translational activity.

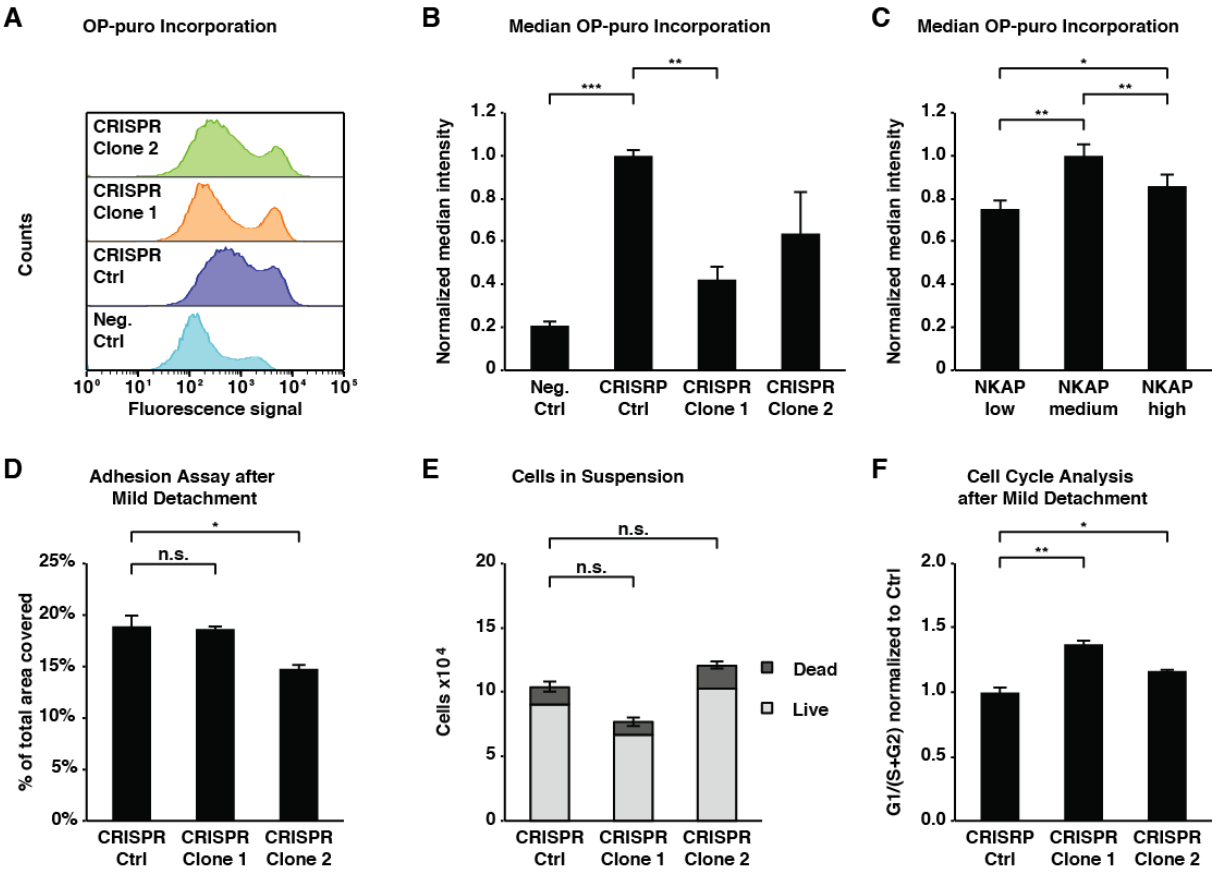

Figure 23. NKAP deficiency reduces translation activity. (A-B) Translational activity in NKAP knockout and control M010817 cells was assessed after OP-puro incorporation using flow cytometry. As a negative control, M010817 control cells were treated with 50 µg/ml cycloheximide. **(C)** NKAP knockout cells reconstituted with the HA_NKAP_eGFP fusion protein were separated according to their GFP expression into a low, medium and high group. Subsequently, their translational activity was assessed as described in (A-B). **(D-E)** The adhesion capacity of NKAP knockout and control M010817 cells was assessed after mild detachment using PBS-EDTA. The adhesion assay was performed according to the descriptions in (Figure 17A-B). **(F)** The cell cycle of NKAP knockout and control M010817 was determined after mild detachment using PBS-EDTA as described previously in (Figure 18A). **(B-F)** For statistical analysis the unpaired student's t-test was applied and the data are depicted as mean ± s.e.m. of n=3.

6.1.21. Delayed replenishment of the surface proteome partly induces the cell cycle arrest

Since delayed replenishment of the surface proteome due to reduced translational activity led to impaired cellular attachment after trypsinization, I sought to investigate whether this might also be the reason for the observed cell cycle arrest. Therefore, I plated NKAP deficient M010817 cells after PBS-EDTA treatment in order to examine their cell cycle profile using EdU incorporation and subsequent flow cytometric analysis. The cell cycle analysis revealed a drastic enhancement of the cell cycle profile in NKAP depleted cells, though the results were still significant when compared to control

cells (Figure 23F). Consequently, these results imply that decelerated recovery after trypsinization is partly responsible for the G1 cell cycle arrest observed in NKAP deficient M010817 cells. Nonetheless, the cell cycle arrest was not completely restored after PBS-EDTA treatment, which indicates that NKAP depletion also has an internal effect on cell proliferation.

6.2. Contributions

In the course of my PhD study rewiring the role of NKAP in melanoma, I conducted the vast majority of the above-described *in vivo* and *in vitro* experiments. In brief, my contributions to the study comprise xenograft experiments using NSG mice, molecular cloning, generation of NKAP knockdown, knockout and overexpressing melanoma cell cultures, immunochemical imaging studies including immunocytochemistry and Western blot analysis, RT-qPCR analysis, and cell culture experiments including growth curve and cell cycle analysis, adhesion assays, Boyden chamber invasion assays, and translational activity assays. Further on, my contributions to the study comprehend the usage of computational and statistical data processing applications such as FlowJo 7.6, CellProfiler 2.0, Imaris, GraphPad PRISM 5, ApE 2.0.44, Microsoft Office 2011, Adobe Photoshop CS5, Adobe Illustrator CS5, and Adobe InDesign CS5. Furthermore, my contributions include the experimental design, and the writing of this report. Finally, I created the graphical abstract of two recently published reports by our group [Zingg_2015; Baggiolini_2016]. For these contributions I was included as co-author in the publications.

The experimental procedures described in the following paragraph were conducted in collaboration with colleagues and co-workers. Co-immunoprecipitation studies were performed together with Sergio Leone (group of PD Dr. Raffaella Santoro). Western blots were conducted in cooperation with Yudong Zhang. Xenograft studies using NSG mice were performed in collaboration with Dr. Gaetana Restivo. Assessing the metastatic burden in lung tissues using RT-qPCR analysis was conducted with the help of Johanna Diener. *In vitro* cell culture assays were done together with Ana Antunes and Annika Klug. TCGA data evaluation was performed with the help of Dr. Phil Cheng (group of Prof. Mitchell Levesque). Confocal imaging was done in collaboration with Luis Zurkirchen, and CellProfiler analysis was performed in cooperation with Kim Ferrari (group of Prof. Bruno Weber).

7. Discussion

Initially, NKAP has been described as an activator of NF-KB, while later reports proposed NKAP as a component of the NOTCH co-repressor complex regulating T cell development and survival and maintenance of hematopoietic stem cells [Chen_2003; Pajerowski_2009; Pajerowski_2010]. However a recent study identified NKAP as a nuclear speckle protein involved in RNA processing and splicing. During my doctoral thesis I investigated the role of NKAP in melanoma and demonstrate that NKAP depletion inhibits translational activity and thereby increases the metastatic behavior in melanoma.

7.1.1. The neural crest associated factor NKAP plays a role in melanoma

Previous studies in our lab have shown the reactivation of neural crest specific factors during the course of melanomagenesis [Civenni_2009; Shakhova_2012; Zingg_2015]. The goal of my PhD thesis was to determine a novel neural crest associated transcriptional regulator involved in melanoma. In a preliminary study, the transcriptional profile of early-differentiated neural crest derivatives was compared to untreated neural crest stem cells. The whole-genome transcriptome array was initially performed to identify novel transcription factors that drive early processes during neural crest differentiation. Whether this approach generally suits the requirements to identify novel key drivers in melanomagenesis remains to be seen. However, fast responding transcriptional adaptations might very well be reflected during certain aspects of melanoma progression, endowing cells with high plasticity. Therefore, comparing the transcriptional profile of early-differentiated neural crest derivatives to their undifferentiated counterparts represents a valid approach to identify novel neural crest associated factors in melanoma. Hence, on the basis of the whole-genome transcriptome array I determined 7 transcriptional regulators, which were associated with neural crest stem cells and tested their functional involvement in melanoma using an RNAi screening approach. The results revealed that 6 out of 7 genes were expressed in melanoma, which emphasizes the hypothesis that many neural crest associated genes find reuse in melanoma. The results further demonstrate that NKAP depletion induced a strong G1 cell cycle arrest. However, the remaining factors had no consistent impact on the cell cycle,

suggesting their function in a different cell biological process. Noteworthy, the achieved knockdowns for NF-YA and NF-YB using RNAi were insufficient and the generation of NF-YB knockout cells using CRISPR-CAS9 was not successful, highlighting their indispensible role in melanoma. Ultimately, the results of the RNAi screening approach prompted me to interrogate NKAPs function in melanoma.

7.1.2. Functional manipulations were limited to the human melanoma cell culture M010817

To investigate NKAP's role in melanoma I generated stable NKAP knockdown and knockout cells using the human melanoma cell culture M010817. M010817 is a fast proliferating cell culture, endowed with metastatic potential that tolerates a single cell expansion, which is necessary to create a knockout clone. To exclude possible side effects elicited by the clonal selection, I mostly performed the experiments using 2 NKAP knockout clones and stably transfected NKAP knockdown cells. As expected, the evoked phenotypes were usually more pronounced in the NKAP knockout clones when compared to the knockdown cells. In addition, I reconstituted knockout cells with a fluorescently tagged NKAP fusion protein to revert the phenotype observed after NKAP depletion. However, to strengthen the results obtained in M010817 it was the goal to establish further NKAP knockdown and knockout cell cultures. Unfortunately, only few cell cultures tolerated a single cell expansion, whereas in others the achieved knockdown efficiency was insufficient. Furthermore, the number of available cell cultures was strongly restricted, due to their limited metastatic behavior *in vivo*. Surprisingly, invasive melanoma cell cultures generally presented with a low metastatic proclivity after subcutaneous injection in NSG mice. Therefore, most experiments performed in this study were restricted to the human melanoma cell culture M010817.

7.1.3. NKAP localizes to nuclear speckles and interacts with RNA processing factors

A previous report has demonstrated NKAP as a SR-related nuclear speckle protein involved in RNA processing and splicing [Burgute_2014]. In this study the exclusive localization to nuclear speckles

was confirmed using a fluorescently labeled NKAP fusion protein. Furthermore, co-immunoprecipitation followed by mass spectrometry revealed that NKAP interacts with a plethora of RNA processing factors and other nuclear speckle proteins. Hence, it was not surprising that NKAP depletion drastically interfered with translational activity, highlighting its presumed role in RNA processing. However, the exact mechanisms leading to decreased protein synthesis remain unclear. It is possible that likewise to the SR proteins SRSF1 and SRSF2, NKAP depletion reduces the production of nascent RNA [Lin_2009]. On the other side, it has already been published that NKAP deficiency reduces the levels of processed mRNA [Burgute_2014]. Hence, it remains to be shown whether reduced translation in NKAP depleted melanoma cells is a consequence of decreased RNA synthesis or a consequence of impaired RNA processing.

7.1.4. Aberrant NKAP expression leads to impaired translational activity

As a first observation, NKAP depleted melanoma cells attached in a temporally deferred manner after trypsinization when compared to control cells. What initially appeared as induction of EMT, later turned out to be a consequence of delayed replenishment of adhesion molecules on the cell surface after trypsinization due to impaired protein synthesis. Hence, when applying a mild dissociation method without trypsin, NKAP deficient cells presented with normal adhesion properties. Apart from the results obtained from the OP-puro incorporation assay, these findings further support that NKAP functions as a pivotal factor in co- or post-transcriptional processes.

However, NKAP reconstitution using a fluorescently tagged fusion protein was not able to revert the adhesion phenotype in NKAP depleted cells. Evidently, the cells poorly tolerated excessive NKAP expression and silenced the exogenous gene to allow the maintenance of the cellular integrity. These data found further supporting evidence as cells with high NKAP levels only presented a slight increase in translational activity when compared to low NKAP expressing cells. However, the translational activity culminated with intermediate NKAP levels, suggesting that NKAP is a tightly regulated protein, which is critical for protein synthesis. While NKAP depletion results in reduced translational

activity presumably due to decreased RNA levels, it is conceivable that excessive NKAP expression impairs translation as a consequence of perturbed RNA processing. Hence, NKAP represents an important factor that allows the fine-tuning of translation, whereas only well-regulated NKAP levels guarantee optimal conditions for protein synthesis.

As shown earlier, inhibition of RNA polymerase II (pol II) leads to the accumulation of RNA processing factors in enlarged nuclear speckles. In a similar way, nuclear speckles lose their irregular shape in response to NKAP over expression and appear as homogenous, round spots. It is assumed that excessive NKAP production leads to the accumulation of the protein in nuclear speckles. Nonetheless, it is also possible that NKAP over expression causes perturbations in the RNA maturation process, which secondarily leads to a general accumulation of speckle proteins including NKAP. However, further experiments will be necessary to answer this question.

Interestingly, a previous study using a luciferase reporter assay demonstrated that NKAP acts as a transcriptional repressor. The study examined the ability of a GAL4DBD-NKAP fusion protein to repress transcription from a luciferase reporter containing four copies of a GAL4-binding sequence upstream of the SV40 promoter [Pajerowski_2009]. As a result, the reporter activity was reduced and NKAP assigned a transcriptional repressor. However, the authors did not address whether the reporter activity was reduced in response to impaired RNA processing, which concomitantly results in decreased translational activity. Hence, it is conceivable that excessive NKAP expression perturbed the RNA maturation process, leading to decreased translation of the reporter protein. Along this line, if NKAP solely acts as a transcriptional repressor, translation would increase upon NKAP ablation. However, the contrary is the case, NKAP depletion induces a strong reduction in translational activity, suggesting NKAP as an activator of co- and post-transcriptional processes.

Previously, NKAP has been identified as an activator of NF-KB [Chen_2003]. In this study the authors found that NKAP activated NF-KB in a dose dependent manner using a NF-KB reporter assay. However, another report revealed that translational repression mediates activation of NF-KB by phos-

phorylated translation initiation factor 2 (eIF2α) [Deng_2004]. Hence, it can be assumed that with increasing NKAP expression translation was continuously impaired leading to the activation of the NF-KB pathway. However, it remains to be confirmed whether excessive NKAP levels lead to increased phosphorylation of eIF2α. Nonetheless, it would be an act of negligence to presume that impaired translation generally activates the NF-KB pathway. Thus, despite reduced translational activity, the RNAseq data provide no evidence that NKAP depletion leads to the up regulation of known NF-KB downstream targets (data not shown). Consequently, these findings propose that excessive NKAP expression induces a stress response during the RNA maturation process, whereas NKAP depletion simply reduces the levels of processed RNAs, without inducing a stress response.

All in all, the results of this study propose that NKAP is a tightly regulated protein, which is required in co- or post-transcriptional processes. Nonetheless, further investigations will be required to unravel the exact mechanistic function of NKAP in RNA processing and splicing.

7.1.5. RNAseq data reveal compensational adaptations in response to decreased adhesion

In order to determine potential NKAP downstream effectors, RNAseq and subsequently a MetaCore™ pathway enrichment analysis was performed. The results revealed enriched pathways associated with EMT, cell adhesion and cytoskeleton remodeling. Nonetheless, most genes engaged in the proposed pathways, altered their expression in a way that stands in contrast to the observed phenotype. Unfortunately, it is likely that many of the identified genes altered their expression as a compensation mechanism in response to decreased adhesion. Therefore, to better examine NKAP downstream effectors, RNAseq should be repeated in cells that are passaged without trypsinization.

7.1.6. NKAP is not involved in alternative splicing

To address if NKAP is involved in alternative splicing, I analyzed the RNAseq data using the DEXseq algorithm to identify differentially expressed exons between NKAP knockdown, knockout and control

cells (data not shown). However, the results revealed only 152 commonly regulated genes with differentially expressed exons in NKAP knockout and knockdown cells. Thus, these results rather suggest that alternative splicing is not affected by NKAP and therefore not the reason for the dramatic reduction in translational activity upon NKAP depletion. However, these data allow no conclusion about NKAP's involvement in constitutive splicing.

7.1.7. CIR ablation does not phenocopy NKAP deficiency

As demonstrated in a previous study, NKAP interacts with components of the NOTCH co-repressor complex, such as CIR [Pajerowski_2009]. However, CIR ablation neither affected the cell cycle nor the adhesive property of M010817 cells. These results illustrate that CIR knockdown does not phenocopy NKAP depletion. Moreover, NKAP did not co-immunoprecipitate with CIR in M010817 cells, suggesting that this interaction does not play a role in M010817 and might be cell type specific. As stated previously, the results of this study do not support the assumption that NKAP acts as a transcriptional repressor. Nonetheless, the interactions with components of the NOTCH co-repressor complex might be relevant in a different context. Thus, it can be hypothesized that CIR, as a component of the NOTCH co-repressor complex, locally binds to NKAP in order to interfere with its function as an RNA processing factor. Consequently, this interaction represents an additional repressive mechanism on a post-transcriptional level. However, further experiments will be required to verify this hypothesis.

7.1.8. Despite reduced proliferation *in vitro*, tumor growth of NKAP depleted cells is not affected *in vivo*

Interestingly, despite the *in vitro* observed G1/G0 cell cycle arrest, there was no significant difference between NKAP knockout and control M010817 cells regarding size and weight of the primary tumor after subcutaneous injection into NSG mice. Hence, it might be that *in vitro* cultured NKAP knockout cells are not able to produce enough autocrine growth factors as a consequence of impaired translation, and therefore proliferation is reduced. On the other side, subcutaneously injected NKAP knockout

cells encounter additional growth promoting factors from the surrounding tumor stroma, which helps them to overcome their proliferation deficit observed *in vitro*.

7.1.9. NKAP depletion increases the metastatic behavior *in vivo*

In addition to the tumor growth analysis, I assessed the metastatic burden in the lungs of mice that were subcutaneously injected with M010817 NKAP knockout cells. Strikingly, despite unaffected tumor growth, the metastatic potential was drastically increased upon NKAP ablation as compared to control cells. These findings were further supported retrieving clinical data from the TCGA database. Hence, while differential NKAP expression in primary tumors had no effect on patient survival, patients with low NKAP expression in lymph node and distant metastases revealed a significantly shorter survival. Summing up, these results indicate that NKAP depletion-mediated translational inhibition leads to increased metastatic proclivity in melanoma. Nonetheless, the exact underlying mechanisms linking translational inhibition with increased metastasis formation in melanoma remain to be resolved.

Interestingly, a recent study demonstrated that global repression of protein synthesis induces an alternative translational program, which promotes stem cell function and tumorigenesis [Blanco_2016]. Therefore, the authors genetically depleted Nop2/Sun domain family, member 2 (NSUN2), a methyltransferase catalyzing the methylation of tRNA precursors, in a tumor mouse model and found that protein synthesis was globally repressed. However, distinct transcripts escaped this repression and established an alternative translational program that stimulates stem cell functions and tumorigenesis. Surprisingly, these alterations render the cells more sensitive to cytotoxic stress.

As a matter of fact, these findings are of particular relevance in the context of NKAP deficient melanomas, as it has been shown that stem cell-like features are associated with increased invasiveness [Civenni_2011; Goding_2011; Vandamme_2014]. Hence, it might be that NKAP depletion-mediated translational inhibition activates an alternative translational stem cell program, which concomitantly

increases the metastatic behavior. However, further inquiries are necessary to prove that this translational escape mechanism also exists in melanoma and that NKAP depleted cells are associated with increased stemness. In a second step, further investigations would have to address whether NKAP deficiency renders melanoma cells more sensitive to cytotoxic stress.

7.1.10. From neural crest stem cells to melanoma

As mentioned above, it has been shown that repressed protein synthesis induces stem cell function and tumorigenesis. Moreover, it has been demonstrated that translation is generally reduced in stem cells when compared to more restricted cells [Blanco_2016]. Therefore, it was surprising to find NKAP up regulated in neural crest stem cells when compared to their early-differentiated derivatives. However, a translation profile has not yet been assessed, and therefore statements about the translation status of neural crest cells are purely speculative. Thus, it might be that during early differentiation translation drops transiently, in order to increase again during terminal differentiation. Furthermore, it is unclear whether NKAP acts context dependent, as the functional relevance of the interaction partners has not yet been resolved. It is conceivable that with different interaction partners NKAP gains temporal and spatial specificity. Therefore, it might be interesting to address the role of the NOTCH co-repressor complex with respect to NKAP function in a developmental context.

7.1.11. Conclusion

In summary, the results of my doctoral thesis demonstrate that the neural crest-associated factor NKAP plays an important role in melanoma. Initially, NKAP was identified in a genome-wide transcriptome analysis comparing neural crest stem cells to their early-differentiated derivatives. On the basis of this array, it was the goal of my PhD study to identify a novel transcriptional regulator involved in melanoma. Therefore, I performed NKAP loss-of-function and gain-of-function experiments using a human melanoma cell culture. The results revealed that NKAP localizes to nuclear speckles and interacts with RNA processing factors. The results further illustrated that NKAP depletion induces

a drastic reduction in protein synthesis, whereas NKAP overexpression is poorly tolerated by the cells and also decreases the translational activity. Consequently, these data show that aberrant NKAP expression results in impaired translational activity and indicate that NKAP is a tightly regulated protein required in co- or post-transcriptional processes. Nonetheless, it will be essential to show whether reduced translation is a consequence of decreased RNA synthesis or a consequence of impaired RNA processing. Strikingly, xenotransplantation experiments revealed that NKAP ablation increases the metastatic behavior of injected cells, although tumor growth is not affected. These results were further underlined with clinical data retrieved from the TCGA database, highlighting that low NKAP levels in lymph node and distant metastases are associated with poor survival in melanoma patients. Consequently, these data suggest that NKAP depletion-mediated translational inhibition increases the metastatic potential in melanoma. However, whether the initiation of an alternative translational stemness program elevates the metastatic proclivity in melanoma requires further investigations.

8. Materials and methods

8.1. *In vivo* analysis

8.1.1. Xenograft experiments

Prior to injections, human melanoma cells were resuspended in 100 µl melanoma growth medium and 100 µl BD Matrigel™ Matrix (354234 BD Biosciences). If not stated otherwise, 300'000 cells were injected subcutaneously into the right side of the back of adult *NOD.Cg-Prkdc^{scid} Il2rg^{tm1Wjl}/SzJ* (NSG) mice (Dr. Leonard D. Shultz, The Jackson Laboratory). The mice were sacrificed around 4-5 weeks after injection or when signs of pain, like hunched back, apathy, weight loss, scrubby fur or abnormal behavior, were observed. After dissection, primary tumors were weighed and the size was determined by measuring two diameters, perpendicular to each other, using a caliper. In order to assess the tumor volume we applied the following formula $V = \frac{\pi}{6} f\ (length \cdot width)^{3/2}$ [Feldmann_2009]. The xenograft studies were evaluated and approved by the cantonal veterinary office Zurich.

8.1.2. Quantitative analysis of lung metastases

In order to quantitatively assess the metastatic burden, the expression of human mRNA was measured in the lungs of injected mice. In short, dissected lungs were collected in 1.5 ml TRIzol® Reagent (15596-026 Invitrogen) and frozen at -80°C. After tissue homogenization and cell lysis, phenol-chloroform-isoamyl alcohol mixture (77617 Sigma-Aldrich) was used for phase separation. Subsequently, Isopropanol was added for precipitation followed by a washing step with Ethanol. In order to increase the grade of purification the extracted RNA was subjected to the RNeasy Mini Kit (74106 Qiagen) including RNase-free DNase (79254 Qiagen) treatment according to the manufacturer's protocol. The RNA concentration was determined using a NanoDrop ND-1000 photospectrometer (NanoDrop Technologies). The Maxima First Strand cDNA Synthesis Kit (K1672 Thermo Fisher Scientific) was applied for the reverse transcription of 1 µg mRNA followed by an RNase H (EN0201

Thermo Fisher Scientific) digest in accordance with the supplier's guidelines. Real-time quantitative PCR was performed on a LightCycler® 480 Instrument II using the LightCycler® 480 SYBR Green I Master (4887352001 Roche). Each sample was analyzed in technical triplicates and the primers used are listed in [Table 2]. Relative mRNA expression of human GAPDH and human PPIA was normalized against murine housekeeping transcript USF1.

Table 02. RT-qPCR primers

Gene	***Species***	**Forward sequence**	**Reverse sequence**
GAPDH	*Human*	ATCATCCCTGCCTCTACTGG	GTCAGGTCCACCACTGACAC
PPIA	*Human*	TTCATCTGCACTGCCAGGAC	TCGAGTTGTCCACAGTCAGC
USF1	*Mouse*	CAGGGCTCAGAGGCACTACT	GCTCCCTCCCTGCAATACTT

8.2. *In vitro* analysis

8.2.1. Molecular cloning

Vectors and inserts were subjected to 0.5 U/µl restriction enzymes [Table 3] in the corresponding reaction buffer. The digest was performed in 20 µl reaction volume for 1 h at 37°C. The reaction mix was separated in a 1% agarose gel (A8963,1000 AppliChem) by gel electrophoresis using a Mini-Sub cell GT electrophoresis cell (Bio-Rad). The desired DNA fragments were excised from the gel followed by a gel purification using the QIAquick Gel Extraction Kit (28706 Qiagen) according to the manufacturer's recommendations. In a 10 µl reaction volume, 200 ng of vector were ligated for 2 h at 37°C with the corresponding amount of insert using 0.5 U/µl T4 Ligase (EL0011 Thermo Fisher Scientific). Library Efficiency® DH5α™ Competent Cells (18263012 Thermo Fisher Scientific) or, in case of Gateway® cloning, OneShot® OmniMAX™ 2 T1^{R} Chemically Competent *E. Coli* (C854003 Thermo Fisher Scientific) were transformed by heat shock with 5 µl of the ligation mix according to standard protocols. Transformed bacteria were plated under 50 µl/ml Ampicillin (A0166 Sigma-Aldrich®) or 100 µl/ml Kanamycin (K1377 Sigma-Aldrich®) selection on Luria Broth (LB) agar plates overnight at 37°C. Single colonies were cultured in 3 ml liquid LB medium supplemented with 50

µl/ml Ampicillin (A0166 Sigma-Aldrich®) or 100 µl/ml Kanamycin (K1377 Sigma-Aldrich®) overnight at 37°C under constant shaking (220 rpm). The plasmid was purified using the QIAamp DNA Mini Kit (51306 Qiagen) according to the supplier's recommendations. The DNA concentration was determined using a NanoDrop ND-1000 photospectrometer (NanoDrop Technologies). The plasmid was sent for Sanger sequencing (Microsynth AG) to confirm the sequence. In order to achieve high yield transfection-grade plasmid DNA, transformed bacteria were grown in 200 ml LB medium supplemented with 50 µl/ml Ampicillin (A0166 Sigma-Aldrich®) or 100 µl/ml Kanamycin (K1377 Sigma-Aldrich®) overnight at 37°C under constant shaking (220 rpm). The NucleoBond® Xtra Maxi (740414.50 Macherey-Nagel) kit was applied for plasmid extraction.

Table 03. Restriction Enzymes

U/µl	*Name*	Catalog #	Manufacturer
0.5	*BamHI*	ER0055	Thermo Fisher Scientific
0.5	*ClaI*	ER0141	Thermo Fisher Scientific
0.5	*HindIII*	ER0501	Thermo Fisher Scientific
0.5	*KpnI*	ER0521	Thermo Fisher Scientific
0.5	*SacI*	ER1135	Thermo Fisher Scientific

8.2.2. Cell culture

Human melanoma-derived cell cultures were established from surplus material from primary cutaneous melanoma and melanoma cell culture excised by surgery. Written consent obtained from all patients was approved by the local institutional review boards (EK647 & EK800). The utilized human melanoma cell cultures listed in [Table 4] were kindly provided by the URPP biobank, UZH and were previously characterized [Zipser_2011]. HEK293T cells were purchased from ATCC. Human melanoma cell cultures were cultured in melanoma growth medium consistent of RPMI 1640 (42401 Thermo Fisher Scientific) supplemented with 10% heat inactivated fetal bovine serum (HI FBS, 16140 Thermo Fisher Scientific), 4 mM L-Glutamine (25030 Thermo Fisher Scientific), Penicillin-Streptomycin (50 U/ml; 50 µg/ml, 15070 Thermo Fisher Scientific) and Gibco™ Amphotericin B (0.5 µg/ml, 15290 Thermo Fisher Scientific) as previously described [Shakhova_2012; Zipser_2011].

HEK293T cells were cultured in Dulbecco's Modified Eagle Medium (DMEM, 11965 Thermo Fisher Scientific) supplemented with 10% HI FBS (16140 Thermo Fisher Scientific) and Penicillin-Streptomycin (50 U/ml; 50 µg/ml, 15070 Thermo Fisher Scientific). All cells were maintained at 37°C and 5% CO_2.

Table 04. Human Melanoma Cell Cultures

Cell Culture	*Gender*	Age	Mutation	Phenotype
M980513	*F*	29	BRAF V600E	Proliferative
M000921	*F*	52	BRAF V600E	Proliferative
M010817	*F*	37	N-RAS Q61R	Proliferative
M050829	*M*	39	N-RAS Q61L	Intermediate
M121224	*M*	37	BRAF V600E / N-RAS Q61K	Invasive
M130219	*M*	48	N-RAS Q61R	Invasive
M130427	*M*	48	N-RAS Q61R	Proliferative
M130429	*M*	48	N-RAS Q61R	Proliferative

8.2.3. NKAP gene silencing by RNA interference in human melanoma cell cultures

In order to temporarily deplete LIN9, LIN28A, NF-YA, NF-YB, NF-YC, NKAP and SSBP2, human melanoma cell cultures were transfected with small interfering RNA (siRNA) using FlexiTube GeneSolution (Qiagen) packages containing 4 preselected siRNAs [Table 5]. For transfection 25 nM siRNA were applied in combination with jetPRIME® transfection reagent (114-07 Polyplus Transfection) according to the manufacturer's protocol. The melanoma growth medium was exchanged 24 h post-transfection. Unless otherwise stated, the cells were further processed and evaluated 72 h after transfection. As control siRNA, the AllStars Negative Control siRNA (SI03650318 Qiagen) was used.

In order to achieve a stable NKAP knockdown, a small hairpin RNA (shRNA) expressing lentiviral construct was generated using the MuLE (Multiple Lentiviral Expression) system. Therefore, the shRNA sequence [Table 5] together with the U6 promoter was isolated from the TRC1-pLKO-puro vector (Mission® Sigma-Aldrich) and introduced into the pMuLE ENTR H1 L1-R5 (#62101 Addgene) using ClaI and SacI restriction sites. The correct order of the sequence was confirmed by

Sanger sequencing (Microsynth AG). The Gateway® LR Clonase® II Enzyme Mix (11791100 Thermo Fisher Scientific) was used to combine the shRNA expressing entry vector with the pMuLE ENTR SV40 eGFP L5-L2 (#62144 Addgene) and the pLenti X1 Puro DEST (694-6) (#17297 Addgene) vector according to published instructions [Albers_2015]. For lentivirus production HEK293T cells were chemically transfected with 10 µg shRNA expression plasmid and 5 µg psPAX2 (#12260 Addgene) and 2.5 µg pMD2.G (#12259 Addgene) using 12.5 mM $CaCl_2$ in Hepes Buffered Saline (HBS) according to standard protocols. The medium was exchanged 24 h post-transfection and the virus containing suspension was collected 48 h, 72 h and 96 h after transfection. For lentiviral infection melanoma cell cultures were incubated in 50% melanoma growth medium and 50% virus containing medium for 24 h. To increase the infection rate, we supplemented the mix with 5 µg/ml Polybrene® (SC-134220 Santa Cruz). As soon as the GFP marker was expressed, the selection procedure was started with 3 µg/ml Puromycin (ant-pr-1 Invitrogen) for 1 week. Furthermore, cells were sorted for high GFP expression using the BD FACSAria™ III 5L (BD Biosciences) in order to increase the knockdown efficiency and to adjust GFP expression over all conditions.

Table 05. RNA interference

Function	*Gene*	Clone ID	Target sequence	Provider
shRNA	*NKAP*	TRCN0000143174	GCATCATTTGAATGCTCAGGT	Sigma-Aldrich
shRNA	*NKAP*	TRCN0000145475	GCTGAAGAACCATCAGATTTA	Sigma-Aldrich
siRNA	*CIR*	SI04266199	CAGGGCATAACAACAGTGATT	Qiagen
siRNA	*CIR*	SI04253501	AACGTGTAAAGAATGGCCTTA	Qiagen
siRNA	*CIR*	SI04242553	CAGTAGTGAGAGTGAGAGTAA	Qiagen
siRNA	*CIR*	SI04175864	GTCCTGGTAGTTACAAGCAAA	Qiagen
siRNA	*LIN9*	SI02779539	ACGAGTGGTTCTATTCAAATA	Qiagen
siRNA	*LIN9*	SI02649003	TAGGCTTCCAACACCAAATAA	Qiagen
siRNA	*LIN9*	SI02649010	TTCCTTTAGATGTCTCATAAA	Qiagen
siRNA	*LIN9*	SI03034031	AAGCTTATCTAACACGTGGAA	Qiagen
siRNA	*LIN28A*	SI03126123	AACGGGACAAATGCAATAGAA	Qiagen
siRNA	*LIN28A*	SI04214938	CACCAGATTAGGTTAGGCCTA	Qiagen
siRNA	*LIN28A*	SI04321919	TAAAGACTTATTGGTACGCAA	Qiagen
siRNA	*LIN28A*	SI04365221	CACGCTGTGAGATCACCGCAA	Qiagen
siRNA	*NF-YA*	SI00658238	TAGAGGGTTATTAAACCTTGA	Qiagen
siRNA	*NF-YA*	SI05392576	CCGCGAGTCGTTCATTTAACA	Qiagen
siRNA	*NF-YA*	SI05392583	ACGGCCGGCACTTGCACTTAA	Qiagen

siRNA	*NF-YA*	SI05392590	AAGCTAGACCTTTGCCTATTA	Qiagen
siRNA	*NF-YB*	SI04168836	CAGGTGCATAATATCCTAATT	Qiagen
siRNA	*NF-YB*	SI04216485	CTCTGCAATAAACTAAACGTA	Qiagen
siRNA	*NF-YB*	SI04312868	CTGGGTTACCAAATATGCAAA	Qiagen
siRNA	*NF-YB*	SI04341372	TTGCATGATAACCTAGCTAGA	Qiagen
siRNA	*NF-YC*	SI00658301	CAGCCTGTATCAGGCACTCAA	Qiagen
siRNA	*NF-YC*	SI04152169	CTCATCGATATTGTTCCAAGA	Qiagen
siRNA	*NF-YC*	SI04201673	CAGCTCTACCAGATCCAGCAA	Qiagen
siRNA	*NF-YC*	SI05140933	CAGCTGCAGTATATCCGCTTA	Qiagen
siRNA	*NKAP*	SI03164056	CACGCTCGCGGTCGCGTTCTA	Qiagen
siRNA	*NKAP*	SI04331929	AAGAAGAAGTCTAGCCGTTCA	Qiagen
siRNA	*NKAP*	SI04345348	AACTCTGGCCATGCTCTGTTA	Qiagen
siRNA	*NKAP*	SI04360412	TTGGCCTAGCCTCCTCGACAA	Qiagen
siRNA	*SSBP2*	SI04141242	CGGGTCCAAATGTGATTCAAA	Qiagen
siRNA	*SSBP2*	SI04154864	CACCAGGATTCTTACATTCTT	Qiagen
siRNA	*SSBP2*	SI04240985	CAGCCCTTCACAGAACTACTA	Qiagen
siRNA	*SSBP2*	SI04323452	TGCAATCATGGATAGGAATAA	Qiagen

8.2.4 CRISPR/CAS9-mediated NKAP knockout in human melanoma cell cultures

The CRISPR/CAS9 technique was applied to completely ablate NKAP expression in human melanoma cell cultures. Therefore, the online available Optimized CRISPR Design tool (http://crispr.mit.edu/) was used to identify a 20 bp long sequence (TGATGAACATACACCAGTGG; quality score 69) targeting exon 1 of the NKAP gene. Single-stranded oligonucleotides [Table 6] were synthesized (Microsynth AG) and annealed in a TProfessional Basic thermal cycler (Biometra) under a slowly cooling temperature gradient from 95°C to 4°C. Double-stranded oligonucleotides were ligated into the single guide RNA (sgRNA) expressing MLM3636 (#43860 Addgene) vector using Golden Gate cloning. Human melanoma cell cultures were transfected with 10 µg MLM3636 and 10 µg pCAG-T7-Cas9-P2A-EGFP (kindly provided by the group of Dr. Pawel Pelczar, USZ) by electroporation (30 ms, 1 pulse, 1300 V) using a MicroPorator^{TM} (Digital Bio). Electroporation was carried out in melanoma growth medium devoid of antibiotic or antifungal additives. GFP positive cells were seeded as single cells into 96-well plates 3 days after transfection using a BD FACSAria^{TM} III 5L (BD Biosciences). In order to select NKAP depleted clones, genomic DNA was isolated according to standard protocols using proteinase K (3115828001 Roche) enriched lysis buffer and subsequent iso-

propanol precipitation. The region encompassing the sgRNA target site was amplified in a PCR reaction using the primers indicated in [Table 6] and send for Sanger sequencing (Microsynth AG). The PCR reaction was performed in a T3000 ThermoCycler (Biometra) using the AmpliTaq Gold® 360 Master Mix (4398881 Applied Biosystems™) according to the manufacturer's guidelines. Additionally, the absence of the protein was confirmed by immunoblot analysis in compliance with previously described settings.

Table 06. CRISPR/CAS9

sgRNA oligonucleotides	**Sequence**
Forward Primer	ACACCTGATGAACATACACCAGTGGG
Reverse Primer	AAAACCCACTGGTGTATGTTCATCAG
Genomic PCR NKAP exon1	**Sequence**
Forward Primer	ATCTTTCCTATGGTTCCTGTTTCTC
Reverse Primer	CTTTCTCCTTTTCTTGGACCTTTC

8.2.5. Generation of stably expressing HA_NKAP_eGFP human melanoma cell cultures

The lentiviral overexpression construct for the HA_NKAP_eGFP fusion protein is based on the NKAP full-length sequence isolated from human melanocyte template cDNA. In brief, mRNA was extracted from human melanocytes using the RNeasy Mini Kit (74106 Qiagen) including RNase-free DNase (79254 Qiagen) treatment according to the manufacturer's protocol. The Transcriptor High Fidelity cDNA Synthesis Kit (5081955001 Roche) was applied for the reverse transcription of 1 µg mRNA in accordance with the supplier's guidelines. In a PCR reaction, the NKAP full-length sequence was amplified from template cDNA using the primers indicated in [Table 7]. The PCR reaction was performed in a T3000 ThermoCycler (Biometra) utilizing the Expand High Fidelity PCR system (11732650001 Roche). In a previous step, the HA-tag (TACCCCTACGACGTCCCCGACTACGCCGGATCC) was isolated from the pcDNA_HA vector (kindly provided by the group of PD Dr. Raffaella Santoro) and introduced N-terminal to the eGFP of the pMuLE ENTR SV40 eGFP L5-L2 (#62144 Addgene) using HindIII and BamHI restriction sites. The NKAP full-length cDNA was then inserted between the HA-tag and the eGFP sequence using BamHI and EcoRI restriction sites. The

correct order of the sequence was confirmed by Sanger sequencing (Microsynth AG). The Gateway® LR Clonase® II Enzyme Mix (11791100 Thermo Fisher Scientific) was used to combine the HA_NKAP_eGFP overexpression vector with the empty pMuLE ENTR CMV L1-R5 (#62090 Addgene) vector and the pLenti X1 Puro DEST (694-6) (#17297 Addgene) according to published instructions [Albers_2015]. The lentivirus production and subsequent infection of melanoma cell cultures was performed as described above.

Table 07. Overexpression primers

Function	Sequence
Forward Primer	TATATAGGATCCATGGCTCCGGTGTCC
Reverse Primer	GCTCGCTCGAGTTATTTGTCATCCTTC

8.2.6. Proliferation assays and cell cycle analysis

In order to address cell growth, 50'000 human melanoma cells were seeded in 6-well plates and the cell number was determined daily over 5 days using a Neubauer chamber. To determine the cell cycle profile, human melanoma cells were pulsed for 30 min with 10 μM 5-Ethynyl-2'-deoxyuridine (EdU) and stained with the Click-iT® EdU Alexa Fluor® 647 Imaging Kit (C10340 Thermo Fisher Scientific). The cells were analyzed by counting 30'000 events using a BD FACSCanto™ II (BD Biosciences) flow cytometer. Data evaluation was performed on the FlowJo 7.6 software.

8.2.7. Adhesion assay

To assess to adhesive capacity of human melanoma cell cultures, 500'000 cells were seeded in 6-well plates (140675 Thermo Fisher Scientific) in melanoma growth medium and incubated for 12 hours at 37°C. The number of cells in suspension was determined with Countess Cell Counting Chamber Slides (Thermo Fisher Scientific) using an EVE™ Automatic Cell Counter (NanoEnTek). Adherent cells were stained with 0.5 % (v/w) Crystal Violet (C3886 Sigma-Aldrich) in 20% Ethanol for 5 min at room temperature. In order to quantify the area covered by cells, 5 randomized pictures per well

were recorded with a DMI 6000B (Leica) microscope and evaluated using the CellProfiler 2.0 software [Carpenter_2006].

8.2.8. Boyden chamber invasion assay

As a preparation to the invasion assay human melanoma cells were starved for 48 h in melanoma growth medium containing only 1% HI FBS (16140 Thermo Fisher Scientific). Subsequently, 150'000 cells were subjected to Corning® BioCoat™ Matrigel® Invasion Chamber inserts containing HI FBS-free melanoma growth medium. Cells were incubated for 22 h to allow migration along the nutrient gradient, where melanoma growth medium containing 10% HI FBS acted as chemoattractant. Invaded cells were fixed in 3.7% formaldehyde (F8775-25ML Sigma-Aldrich) for 10 min at room temperature and stained with Hoechst 33342 (145533 Sigma-Aldrich). Excised membranes were mounted on cover slides, and cells were visualized using a DMI 6000B (Leica) microscope. Cell numbers were quantified by the CellProfiler 2.0 software [Carpenter_2006].

8.2.9. Immunocytochemistry

Cells were seeded on Nunc™ Thermanox™ Coverslips 25 mm (174985 Thermo Fisher Scientific) in 6-well plates and fixed in 3.6% formaldehyde (F8775-25ML Sigma-Aldrich) for 10 min at room temperature. Cells were permeabilized with 0.2% Tween®20 (P2287 Sigma-Aldrich) in phosphate buffered saline (PBS; 10010-056 Thermo Fisher Scientific) for 1 h at room temperature and blocked with 1% bovine serum albumin (BSA; A9418-5G Sigma-Aldrich) in PBS (10010-056 Thermo Fisher Scientific) for 1 h at room temperature. Immunofluorescent staining was performed using primary antibodies [Table 8] in PBS with 1% BSA over night at 4°C and secondary antibodies [Table 9] were applied in PBS with 1% BSA for 1 h at room temperature. Nuclei were visualized with Hoechst 33342 (145533 Sigma-Aldrich). Cover slips were mounted on glass slides and images were recorded using a DMI 6000B (Leica) microscope or an SP8 (Leica) Confocal Laser Scanning Microscope.

Table 08. Primary antibodies

Antigen	*Species*	Type	Dilution	Catalog #	Company
GFP	*Chicken*	Polyclonal	1:200	GFP-1020	Aves Labs. Inc.
HA-tag	*Mouse*	Monoclonal	1:400	ab1424	Abcam
Human NKAP	*Goat*	Polyclonal	1:250	sc-161948	Santa Cruz
Human SC35	*Mouse*	Monoclonal	1:400	ab11826	Abcam

Table 09. Secondary antibodies

Antibody	Dilution	Catalog #	Company
Alexa Fluor® 546 Goat anti-Mouse IgG (H+L)	1:400	A-11030	Thermo Fisher Scientific
Alexa Fluor® 555 Donkey anti-Goat IgG (H+L)	1:250	A21432	Thermo Fisher Scientific
Alexa Fluor® 647-AffiniPure Donkey anti-Mouse IgG (H+L)	1:250	715-605-150	Jackson ImmunoResearch
Alexa Fluor® 647-AffiniPure Goat anti-Chicken IgY (IgG)(H+L)	1:250	103-605-155	Jackson ImmunoResearch
Cy3-AffiniPure Goat anti-Mouse IgG (H+L)	1:250	115-165-003	Jackson ImmunoResearch

8.2.10. Protein isolation and immunoblot analysis

Cells were resuspended in 400 µl RIPA Lysis and Extraction Buffer (89900 Thermo Fisher Scientific) supplemented with Halt Phosphatase/ Protease Inhibitor Cocktail (78420/87786 Thermo Fisher Scientific) and either processed immediately or stored at -80°C. Protein concentration was determined using the Pierce™ BCA Protein Assay Kit (23225 Thermo Fisher Scientific) in accordance with the manufacturer's recommendations. The protein solution was prepared by adding 4x Laemmli Sample Buffer (1610747 Bio-Rad) followed by denaturation at 95°C for 5 min. If not stated differently, 50 µg of protein were subjected to a 4-20% Mini-PROTEAN® TGX™ Precast Protein Gel (4561094 Bio-Rad) and separated by sodium dodecyl sulfate polyacrylamide gel electrophoresis (SDS-PAGE) using Tris/Glycine/SDS (1610732 Bio-Rad) running buffer and a Mini-PROTEAN® Tetra Vertical Electrophoresis Cell (1658004 Bio-Rad). Proteins were transferred on 0.45 µm nitrocellulose membranes (1620215 Bio-Rad) by blotting for 1 h at 110 V in Tris/Glycine transfer buffer (1620734 Bio-Rad)

using a Mini Trans-Blot® Cell (1703930 Bio-Rad). Membranes were blocked in Odyssey blocking buffer (927-40100 LI-COR) for 1 h at room temperature. Primary antibodies [Table 10] were applied in Odyssey blocking buffer (927-40100 LI-COR) overnight at 4°C. The membrane was incubated with secondary antibodies [Table 11] in Odyssey blocking buffer (927-40100 LI-COR) for 1 h at room temperature. Membranes were scanned and processed using the Odyssey imaging system (LI-COR).

Table 10. Primary antibodies

Antigen	***Species***	**Type**	**Dilution**	**Catalog #**	**Company**
HA-tag	*Mouse*	Monoclonal	1:2'000	ab1424	Abcam
Human NKAP	*Goat*	Polyclonal	1:250	sc-161948	Santa Cruz
Human β-ACTIN	*Mouse*	Monoclonal	1:10'000	a5316	Sigma-Aldrich
Human β-ACTIN	*Rabbit*	Monoclonal	1:10'000	4970	Cell Signaling

Table 11. Secondary antibodies

Antibody	**Dilution**	**Catalog #**	**Company**
IRDye 680 LT Donkey anti-Mouse IgG (H+L)	1:10'000	926-68022	LI-COR
IRDye 680 LT Donkey anti-Rabbit IgG (H+L)	1:10'000	926-68023	LI-COR
IRDye 800 CW Donkey anti-Goat IgG (H+L)	1:10'000	926-32214	LI-COR
IRDye 800 CW Donkey anti-Mouse IgG (H+L)	1:10'000	926-32212	LI-COR

8.2.11. RNA isolation and real-time quantitative PCR

RNA was extracted from cells using the RNeasy Mini Kit (74106 Qiagen) including RNase-free DNase (79254 Qiagen) treatment according to the manufacturer's protocol. RNA concentration was determined by the NanoDrop ND-1000 photospectrometer (NanoDrop Technologies) and 1 µg RNA was subjected to reverse transcriptase reaction using the Maxima First Strand cDNA Synthesis Kit (K1672 Thermo Fisher Scientific) followed by a RNase H (EN0201 Thermo Fisher Scientific) treatment in accordance with the supplier's guidelines. Real-time quantitative PCR was performed on a LightCycler® 480 Instrument II using the LightCycler® 480 SYBR Green I Master (4887352001 Roche). Each sample was analyzed in technical triplicates and the primers used are listed in [Table 12]. Relative mRNA expression was normalized against human housekeeping transcript RPL28.

Table 12. RT-qPCR primers

Gene	*Species*	Forward sequence	Reverse sequence
CIR	*Human*	GAAAGGAGCCCCACGAGAAA	AGTGGGAACCGAACTTGCAT
LIN28A	*Human*	CGGGCATCTGTAAGTGGTTC	CAGACCCTTGGCTGACTTCT
LIN9	*Human*	GGAACGAAAGTTACAGCACGA	CAAGCCCTGTCCTATCAAAAGT
NF-YA	*Human*	GAGCCCCTGTATGTGAATGC	TGTCATGGCTTCTTCGTCAC
NF-YB	*Human*	GGAAAGATCGCAAAAGATGC	GTCTTCCGCTTCTCCTGATG
NF-YC	*Human*	AGACAGAGGTCCAGCAAGGA	GGCTGATTGGCTGACTGAAT
NKAP	*Human*	TGAAGATAGCGACAGTGACTCT	CAGCCTTTGTTCGATCCTTCC
RPL28	*Human*	GCAATTGGTTCCGCTACAAC	TGTTCTTGCGGATCATGTGT
SSBP2	*Human*	CTCCTGGGAATTATGTAGGTCCT	AGAGCCATTCATGTGATGTGAC

8.2.12. RNA sequencing and gene expression profiling

RNA sequencing including sample preparation was performed by the Functional Genomic Center Zurich (FGCZ). In short, the quantity and quality of the isolated RNA was determined with a Qubit® (1.0) Fluorometer (Thermo Fisher Scientific) and a Bioanalyzer 2100 (Agilent). The TruSeq Stranded mRNA Sample Prep Kit (Illumina) was used in the succeeding steps. Briefly, total RNA samples (1 μg) were poly(A) enriched and fragmented with divalent cations and elevated temperature. Fragmented RNA was subjected to reverse transcription with addition of Actinomycin that allows RNA but not DNA dependent synthesis. In order to achieve strand specificity, dUTP was incorporated instead of dTTP during second strand synthesis. A single 'A' nucleotide is added to the 3' ends prior to ligation of the TruSeq adapters, which comprise the index for multiplexing. In a PCR reaction, fragments featuring TruSeq adapters were enriched. The quality and quantity of the enriched libraries were validated by RT qPCR using a LightCycler 96 (Roche) and the Bioanalyzer 2100 (Agilent). The TruSeq SR Cluster Kit v3-cBot-HS (Illumina) was used for cluster generation using 8 pM of pooled normalized libraries on cBOT. Sequencing was performed on the HiSeq 2500 single end 125 bp (Illumina) using the TruSeq SBS Kit v3-HS (Illumina). Gene ontology pathway enrichment analysis was performed with MetaCore^{TM} (Thomson Reuters).

8.2.13. Pull-down assays and mass spectrometry

Cell nuclei were isolated using buffer A (10 mM Hepes pH 7.6, 1.5 mM $MgCl_2$, 10 mM KCl, 0.5 mM DTT) and a Dounce homogenizer. Subsequently, nuclei were resuspended in buffer 1 (0.3 M sucrose, 15 mM TRIS-HCl pH 7.5, 60 mM KCl, 15 mM NaCl, 5 mM $MgCl_2$, 0.1 mM EDTA, 0.5 mM DTT, 0.5% NP40, 1% sodium deoxycholate). Nuclei were subjected to MNase (30 U) treatment in MNase buffer (0.3 M sucrose, 85 mM TRIS-HCl pH 7.5, 3 mM $MgCl_2$, 2mM $CaCl_2$) and sonicated for 10 sec. From the resulting supernatant 0.5 mg protein was immunoprecipitated overnight at 4°C using anti-HA-Agarose (A2095 Sigma-Aldrich). Proteins were eluted with 100 µg/ml Influenza Hemagglutinin (HA) peptide (12149 Sigma-Aldrich). Proteins were precipitated with 20% trichloroacetic acid (TCA) and washed with cold acetone. Dried pellets were dissolved in 30 µl buffer (10 mM TRIS, 2 mM $CaCl_2$ pH 8.2), 10 µl acetonitrile, 5 µl trypsin (100 ng/µl in 10 mM HCl) and 5 µl RapiGest™ (Waters Inc.). After centrifugation, dried pellets were dissolved in 0.1% formic acid. Mass spectrometry was performed at the FGCZ. After transferring the proteins to autosampler vials, 2 µl injection volume was analyzed by liquid chromatography tandem mass spectrometry (LC-MS/MS) using a nanoACQUITY UPLC® system (Waters Inc.) connected to a Q Exactive™ Hybrid Quadrupole-Orbitrape™ Mass Spectrometer (Thermo Fisher Scientific). Database analysis was performed using the Mascot Search Engine (Matrix Science). Scaffold 4 (Proteome Software) was used to visualize search results for the SwissProt_2015_11 database assuming a trypsin digest.

8.2.14. Translational activity assay

In order to address translational activity, human melanoma cells were pulsed for 30 min with 20 µM O-propargyl-puromycin (OP-puro) and stained with the Click-iT® Plus OPP Alexa Fluor® 647 Protein Synthesis Assay Kit (C10458 Thermo Fisher Scientific). As a negative control human melanoma cells were pre-incubated with 50 µg/ml cycloheximide (C1988-1G Sigma-Aldrich). The cells were analyzed by counting 30'000 events using a BD FACSCanto™ II (BD Biosciences) flow cytometer. Data evaluation was performed on the FlowJo 7.6 software.

8.3. *In silico* analysis

8.3.1. TCGA analysis

RNA sequencing and clinical data for melanoma patients were retrieved from The Cancer Genome Atlas (TCGA; http://cancergenome.nih.gov/). Statistical data analysis was performed as previously described using the TCGA Browser v0.9 online tool (tcgabrowser.ethz.ch:3839/TEST/) [Cheng_2015]. For differential expression and survival analysis in primary tumors or lymph nodes and distant metastases the dataset was segregated into NKAP high (top 15%) and low (bottom 15%) expressing patient samples.

8.3.2. Statistical analysis

For xenograft experiments at least 3 mice were injected. The unpaired Student's t-test was used to statistically evaluate the size and weight of primary tumors as well as the metastatic burden in lung tissue. *In vitro* experiments were performed as triplicates. In order to compare to groups the unpaired Student's t-test was applied. $P<0.05$ was considered as significant. Statistical analysis was done with GraphPad PRISM (Graphpad Software Inc.).

9. References

Abdel-Malek Z, Swope VB, Suzuki I, et al. Mitogenic and melanogenic stimulation of normal human melanocytes by melanotropic peptides. *Proc Natl Acad Sci USA*. 1995;92(5):1789-1793. doi:10.1073/pnas.92.5.1789.

Ackermann J, Frutschi M, Kaloulis K, Mckee T, Trumpp A, Beermann F. Metastasizing Melanoma Formation Caused by Expression of Activated N-Ras Q61K on an INK4a-Deficient Background. *Cancer Res.* 2005;(10):4005-4011.

Adegbidi H, Yedomon H, Atadokpede F, Ango-padonou F. Skin cancers at the National University Hospital of Cotonou from 1985 to 2004. *Journal of Dermatology.* 2007:26-29.

Agnarsdóttir, M. MITF Expression in Cutaneous Malignant Melanoma. *J Mol Biomark Diagn*. 2012;3(4). doi:10.4172/2155-9929.1000129.

Aitken J, Welch J, Duffy D, et al. CDKN2A Variants in a Population-Based Sample of Queensland Families With Melanoma. J Natl Cancer Inst. 1999;91(5):446-52.

Aksan I, Goding CR. Targeting the Microphthalmia Basic Helix-Loop-Helix – Leucine Zipper Transcription Factor to a Subset of E-Box Elements In Vitro and In Vivo. *Molecular and Cellular Biology.* 1998;18(12):6930-6938.

Albers J, Danzer C, Rechsteiner M, et al. A versatile modular vector system for rapid combinatorial mammalian genetics. *J Clin Invest.* 2015;125(4):1603-1619. doi:10.1172/JCI79743DS1.

Alegre ML, Frauwirth KA, Thompson CB. T-cell regulation by CD28 and CTLA-4. *Nat Rev Immunol*. 2001;1(3):220-228. doi:10.1038/35105024.

Alexaki VI, Javelaud D, Van Kempen LCL, et al. GLI2-mediated melanoma invasion and metastasis. *J Natl Cancer Inst*. 2010;102(15):1148-1159. doi:10.1093/jnci/djq257.

Alexandrov LB, Nik-Zainal S, Wedge DC, et al. Signatures of mutational processes in human cancer. *Nature*. 2013;500(7463):415-421. doi:10.1038/nature12477.

Amiel J, Attié T, Jan D, et al. Heterozygous endothelin receptor B (EDNRB) mutations in isolated Hirschsprung disease. *Hum Mol Genet*. 1996;5(3):355-357. doi:10.1093/hmg/5.3.355.

Anaka M, Hudson C, Lo P-H, et al. Intratumoral genetic heterogeneity in metastatic melanoma is accompanied by variation in malignant behaviors. *BMC Med Genomics*. 2013;6(1):40. doi:10.1186/1755-8794-6-40.

Anderson DJ. Stem cells and pattern formation in the nervous system: The possible versus the actual. *Neuron*. 2001;30(1):19-35. doi:10.1016/S0896-6273(01)00260-4.

Anderson DJ, Axel R. A bipotential neuroendocrine precursor whose choice of cell fate is determined by NGF and glucocorticoids. *Cell*. 1986;47(6):1079-1090. doi:10.1016/0092-8674(86)90823-8.

Anderson RB. Matrix metalloproteinase-2 is involved in the migration and network formation of enteric neural crest-derived cells. *Int J Dev Biol*. 2010;54(1):63-69. doi:10.1387/ijdb.082667ra.

Aoki H, Moro O. Involvement of microphthalmia-associated transcription factor (MITF) in expression of human melanocortin-1 receptor (MC1R). *Life Sci*. 2002;71(18):2171-2179. doi:10.1016/S0024-3205(02)01996-3.

Ascierto PA, Minor D, Ribas A, et al. Phase II trial (BREAK-2) of the BRAF inhibitor dabrafenib (GSK2118436) in patients with metastatic melanoma. *J Clin Oncol*. 2013;31(26):3205-3211. doi:10.1200/JCO.2013.49.8691.

Asuquo ME, Udosen AM, Ikpeme IA, et al. Cutaneous squamous cell carcinoma in Calabar, southern Nigeria. *Clin Exp Dermatol*. 2009;34(8):870-873. doi:10.1111/j.1365-2230.2009.03243.x.

Avetisyan M, Schill EM, Heuckeroth RO. Building a second brain in the bowel. *J Clin Invest*. 2015;125(3):899-907. doi:10.1172/JCI76307.

Azimi F, Scolyer RA, Rumcheva P, et al. Tumor-infiltrating lymphocyte grade is an independent predictor of sentinel lymph node status and survival in patients with cutaneous melanoma. *J Clin Oncol*. 2012;30(21):2678-2683. doi:10.1200/JCO.2011.37.8539.

Bachmann IM, Halvorsen OJ, Collett K, et al. EZH2 expression is associated with high proliferation rate and aggressive tumor subgroups in cutaneous melanoma and cancers of the endometrium, prostate, and breast. *J Clin Oncol*. 2006;24(2):268-273. doi:10.1200/JCO.2005.01.5180.

Bachmann IM, Straume O, Puntervoll HE, Kalvenes MB, Akslen LA. Importance of P-cadherin, β-catenin, and Wnt5a/Frizzled for progression of melanocytic tumors and prognosis in cutaneous melanoma. *Clin Cancer Res*. 2005;11(24):8606-8614. doi:10.1158/1078-0432.CCR-05-0011.

Baggiolini A, Varum S, Mateos JM, et al. Premigratory and migratory neural crest cells are multipotent in vivo. *Cell Stem Cell*. 2015;16(3):314-322. doi:10.1016/j.stem.2015.02.017.

Bajetta E, Del Vecchio M, Nova P, et al. Multicenter phase III randomized trial of polychemotherapy (CVD regimen) versus the same chemotherapy (CT) plus subcutaneous interleukin-2 and interferon-α2b in metastatic melanoma. *Ann Oncol*. 2006;17(4):571-577. doi:10.1093/annonc/mdl007.

Bajetta E, Del Vecchio M, Bernard-Marty C, et al. Metastatic melanoma: Chemotherapy. *Semin Oncol*. 2002;29(5):427-445. doi:10.1053/sonc.2002.35238.

Balch CM, Urist MM, Karakousis CP, et al. Efficacy of 2-cm surgical margins for intermediate-thickness melanomas (1 to 4 mm). Results of a multi-institutional randomized surgical trial. *Ann Surg*. 1993;218(3):262-7-9. doi:10.1097/00006534-199506000-00070.

Balch CM, Soong S, Atkins MB, et al. An Evidence-based Staging System for Cutaneous Melanoma. *CA Cancer J Clin*. 2004;54(3):131-149.

Baltz AG, Munschauer M, Schwanhäusser B, et al. The mRNA-Bound Proteome and Its Global Occupancy Profile on Protein-Coding Transcripts. *Mol Cell*. 2012;46(5):674-690. doi:10.1016/j.molcel.2012.05.021.

Banerjee SS, Eyden B. Divergent differentiation in malignant melanomas: A review. *Histopathology*. 2008;52(2):119-129. doi:10.1111/j.1365-2559.2007.02823.x.

Barash Y, Calarco J a, Gao W, et al. Deciphering the splicing code. *Nature*. 2010;465(7294):53-59. doi:10.1038/nature09000.

Bardeesy N, Bastian BC, Hezel A, Pinkel D, DePinho RA, Chin L. Dual inactivation of RB and p53 pathways in RAS-induced melanomas. *Mol Cell Biol*. 2001;21(6):2144-2153. doi:10.1128/MCB.21.6.2144-2153.2001.

Barden H, Levine S. Histochemical observations on rodent brain melanin. *Brain Res Bull*. 1983;10(6):847-851. doi:10.1016/0361-9230(83)90218-6.

Barrangou R, Fremaux C, Deveau H, Richards M, et al. CRISPR provides acquired resistance against viruses in prokaryotes. *Sciences.* 2007 Mar 23;315(5819):1709-12.

Barrio MG, Nieto MA. Overexpression of Snail family members highlights their ability to promote chick neural crest formation. *Development.* 2002;1593:1583-1593.

Basch ML, Bronner-Fraser M, García-Castro MI. Specification of the neural crest occurs during gastrulation and requires Pax7. *Nature*. 2006;441(7090):218-222. doi:10.1038/nature04684.

Bastian BC, Kashani-Sabet M, Hamm H, et al. Gene amplifications characterize acral melanoma and permit the

detection of occult tumor cells in the surrounding skin. *Cancer Res*. 2000;60(7):1968-1973.

Bauer J, Curtin JA, Pinkel D, Bastian BC. Congenital melanocytic nevi frequently harbor NRAS mutations but no BRAF mutations. *J Invest Dermatol.* 2007 Jan;127(1):179-82.

Bautista NC, Cohen S, Anders KH. Benign Melanocytic Nevus Cells in Axillary Lymph Nodes. A Prospective Incidence and Immunohistochemical Study With Literature Review. *Am J Clin Pathol.* 1994 (Jul); 102(1):102-108.

Baxter LL, Pavan WJ. Pmel17 expression is Mitf-dependent and reveals cranial melanoblast migration during murine development. *Gene Expr Patterns*. 2003;3(6):703-707. doi:10.1016/j.modgep.2003.07.002.

Bedogni B. Notch signaling in melanoma: Interacting pathways and stromal influences that enhance Notch targeting. *Pigment Cell Melanoma Res*. 2014;27(2):162-168. doi:10.1111/pcmr.12194.

Bedogni B, Warneke JA, Nickoloff BJ, Giaccia AJ, Powell MB. Notch1 is an effector of Akt and hypoxia in melanoma development. *J Clin Invest*. 2008;118(11):3660-3670. doi:10.1172/JCI36157.

Bellmeyer A, Krase J, Lindgren J, LaBonne C. The protooncogene c-Myc is an essential regulator of neural crest formation in Xenopus. *Dev Cell*. 2003;4(6):827-839. doi:10.1016/S1534-5807(03)00160-6.

Benaud CM, Dickson RB. Adhesion-regulated G1 cell cycle arrest in epithelial cells requires the downregulation of c-Myc. *Oncogene*. 2001 Jul 27;20(33):4554-67.

Bennett DC. Genetics of melanoma progression: The rise and fall of cell senescence. *Pigment Cell Melanoma Res*. 2016;29(2):122-140. doi:10.1111/pcmr.12422.

Bennett DC. How to make a melanoma: What do we know of the primary clonal events? *Pigment Cell Melanoma Res*. 2008;21(1):27-38. doi:10.1111/j.1755-148X.2007.00433.x.

Berger MF, Hodis E, Heffernan TP, et al. Melanoma genome sequencing reveals frequent PREX2 mutations. *Nature*. 2012;485(7399):502-506. doi:10.1038/nature11071.

Berget SM, Moore C, Sharp PA. Spliced segments at the 5' terminus of adenovirus 2 late mRNA. *Proc Natl Acad Sci U S A*. 1977;74(8):3171-3175. doi:10.1073/pnas.74.8.3171.

Bertolotto C, Lesueur F, Giuliano S, et al. 6. A SUMOylation-defective MITF germline mutation predisposes to melanoma and renal carcinoma. *Nature*. 2011;480(7375):94-98. doi:10.1038/nature10539.

Betancur P, Bronner-Fraser M, Sauka-Spengler T. Assembling Neural Crest Regulatory Circuits into a Gene Regulatory Network. *Annu Rev Cell Dev Biol*. 2010;26:581-603. doi:10.1146/annurev.cellbio.042308.113245.

Betancur P, Bronner-Fraser M, Sauka-Spengler T. Genomic code for Sox10 activation reveals a key regulatory enhancer for cranial neural crest. *Proc Natl Acad Sci USA*. 2010;107(8):3570-3575. doi:10.1073/pnas.0906596107.

Bevona C, Goggins W, Quinn T, Fullerton J, Tsao H. Cutaneous Melanomas Associated With Nevi. Arch Dermatol. 2003 Dec; 139(12):1620-4.

Bhatia S, Tykodi SS, Thompson JA. Treatment of metastatic melanoma: an overview. *Oncology (Williston Park)*. 2009;23(6):488-496.

Bixby S, Kruger GM, Mosher JT, Joseph NM, Morrison SJ. Cell-intrinsic differences between stem cells from different regions of the peripheral nervous system regulate the generation of neural diversity. *Neuron*. 2002;35(4):643-656. doi:10.1016/S0896-6273(02)00825-5.

Black DL. Mechanisms of Alternative Pre-Messenger RNA Splicing. *Annu Rev Biochem*. 2003;72(1):291-336. doi:10.1146/annurev.biochem.72.121801.161720.

Blanco S, Bandiera R, Popis M, et al. Stem cell function and stress response are controlled by protein synthesis. *Nature*. 2016;534(7607):335-340. doi:10.1038/nature18282.

Bockman DE, Kirby ML. Dependence of thymus development on derivatives of the neural crest. *Science.* 1984 Feb 3;223(4635):498-500.

Boiko AD, Razorenova O V, van de Rijn M, et al. Human melanoma-initiating cells express neural crest nerve growth factor receptor CD271. *Nature*. 2010;466(7302):133-137. doi:10.1038/nature09161.

Bolande RP. The neurocristopathies: A unifying concept of disease arising in neural crest maldevelopment. *Human Pathology*. 1974;5(4):409-429.

Bolande RP. Neurocristopathy: its growth and development in 20 years. *Pediatr Pathol Lab Med*. 1997;17(1):1-25. doi:10.3109/15513819709168343.

Bondurand N, Pingault V, Goerich DE, et al. Interaction among SOX10, PAX3 and MITF, three genes altered in Waardenburg syndrome. *Hum Mol Genet*. 2000;9(13):1907-1917. doi:10.1093/hmg/9.13.1907.

Bondurand N, Dastot-Le Moal F, Stanchina L, et al. Deletions at the SOX10 gene locus cause Waardenburg syndrome types 2 and 4. *Am J Hum Genet*. 2007;81(6):1169-1185. doi:10.1086/522090.

Bondurand N, Girard M, Pingault V, Lemort N, Dubourg O, Goossens M. Human Connexin 32, a gap junction protein altered in the X-linked form of Charcot–Marie–Tooth disease, is directly regulated by the transcription factor SOX10. *Human Molecular Genetics.* 2001;10(24):2783-2796.

Box NF, Terzian T. The role of p53 in pigmentation, tanning and melanoma. *Pigment Cell Melanoma Res*. 2008;21(5):525-533. doi:10.1111/j.1755-148X.2008.00495.x.

Boyman O, Sprent J. The role of interleukin-2 during homeostasis and activation of the immune system. *Nat Rev Immunol*. 2012;12(3):180-190. doi:10.1038/nri3156.

Brash DE, Haseltine WA. UV-induced mutation hotspots occur at DNA damage hotspots. *Nature*. 1982;298(5870):189-192. doi:10.1038/298189a0.

Brede G, Solheim J, Prydz H. PSKH1, a novel splice factor compartment-associated serine kinase. *Nucleic Acids Res*. 2002;30(23):5301-5309. doi:10.1093/nar/gkf648.

Breslow A. Thickness, Cross-Sectional Areas and Depth of Invasion in the Prognosis of Cutaneous Melanoma. Ann Surg. 1970 (Nov); 172(5):902-908.

Bridgewater LC, Crombrugghe B De. Chondrocyte-specific Enhancer Elements in the Col11a2 Gene Resemble the Col2a1 Tissue-specific Enhancer. *The Journal of Biologica Chemistry*. 1998;273(24):14998-15006.

Bronner-Fraser M. Analysis of the Early Stages of Trunk Neural Crest Migration in Avian Embryos Using Monoclonal Antibody HNK-1. *Developmental Biology.* 1986;55:44-55.

Brou C, Logeat F, Gupta N, et al. A Novel Proteolytic Cleavage Involved in Notch Signaling. *Mol Cell*. 2000;5(2):207-216. doi:10.1016/S1097-2765(00)80417-7.

Buchbinder EI, Desai A. CTLA-4 and PD-1 Pathways. *Am J Clin Oncol*. 2016;39(1):98-106. doi:10.1097/COC.0000000000000239.

Bulliard J, Cox B, Elwood MJ. Comparison of the site distribution of melanoma in New Zealand and Canada. *Int J Cancer.* 1997;72: 235(February):231-235.

Burge CB, Tuschl T, Sharp PA. Splicing of Precursors to mRNAs by the Spliceosomes. *The RNA World, 2nd ed.* 1999

Burgute BD, Peche VS, Steckelberg A-L, et al. NKAP is a novel RS-related protein that interacts with RNA and RNA binding proteins. *Nucleic Acids Res*. 2014;42(5):3177-3193. doi:10.1093/nar/gkt1311.

Burstyn-Cohen T, Kalcheim C. Association between the cell cycle and neural crest delamination through specific regulation of G1/S transition. *Dev Cell*. 2002;3(3):383-395. doi:10.1016/S1534-

5807(02)00221-6.

Butler P. Quantitation of Cell Shedding into Efferent Blood of Mammary. *Cancer Res.* 1975;35(March):512-516.

Cáceres JF, Misteli T, Screaton GR, Spector DL, Krainer AR. Role of the Modular Domains of SR Proteins in Subnuclear Localization and Alternative Splicing Specificity. *J Cell Biol*. 1997;138(2):225-238.

Cano A, Pérez-Moreno MA, Rodrigo I, et al. The transcription factor snail controls epithelial-mesenchymal transitions by repressing E-cadherin expression. *Nat Cell Biol*. 2000;2(2):76-83. doi:10.1038/35000025.

Cantley LC, Neel BG. New insights into tumor suppression: PTEN suppresses tumor formation by restraining the phosphoinositide 3-kinase/AKT pathway. *Proc Natl Acad Sci*. 1999;96(8):4240-4245. doi:10.1073/pnas.96.8.4240.

Caramel J, Papadogeorgakis E, Hill L, et al. A Switch in the Expression of Embryonic EMT-Inducers Drives the Development of Malignant Melanoma. *Cancer Cell*. 2013;24(4):466-480. doi:10.1016/j.ccr.2013.08.018.

Carpenter AE, Jones TR, Lamprecht MR, et al. CellProfiler: image analysis software for identifying and quantifying cell phenotypes. *Genome Biol*. 2006;7(10):R100. doi:10.1186/gb-2006-7-10-r100.

Carreira S, Goodall J, Aksan I, et al. Mitf cooperates with Rb1 and activates p21Cip1 expression to regulate cell cycle progression. *Nature*. 2005;433(7027):764-769. doi:10.1038/nature03269.

Carreira S, Goodall J, Denat L, et al. Mitf regulation of Dia1 controls melanoma proliferation and invasiveness. *Genes & Development*. 2006:3426-3439. doi:10.1101/gad.406406.changes.

Carreira S, Liu B, Goding CR. The gene encoding the T-box factor Tbx2 is a target for the microphthalmia-associated transcription factor in melanocytes. *J Biol Chem*. 2000;275(29):21920-21927. doi:10.1074/jbc.M000035200.

Carson K, Wen D, Li P, Lana AM, et al. Nodal Nevi and Cutaneous Melanomas. *Am J Surg Pathol.* 1996;20(July):834-840.

Chandeck C, Mooi WJ. Oncogene-induced cellular senescence. *Adv Anat Pathol*. 2010;17(1):42-48. doi:10.1097/PAP.0b013e3181c66f4e.

Chang AE, Karnell LH, Menck HR. The National Cancer Data Base Report on Cutaneous and A Summary of 84 , 836 Cases from the Past Decade. *Cancer.* 1998 OCt 15;83(8):1664-1678.

Chang YM, Barrett JH, Bishop TD, et al. Sun exposure and melanoma risk at different latitudes: A pooled analysis of 5700 cases and 7216 controls. *Int J Epidemiol*. 2009;38(3):814-830. doi:10.1093/ije/dyp166.

Chapman PB, Hauschild A, Robert C, et al. Improved survival with vemurafenib in melanoma with BRAF V600E mutation. *N Eng J Med*. 2011;364(26):2507-2516. doi:10.1056/NEJMoa1103782.

Chen DS, Irving BA, Hodi FS. Molecular pathways: Next-generation immunotherapy-inhibiting programmed death-ligand 1 and programmed death-1. *Clin Cancer Res*. 2012;18(24):6580-6587. doi:10.1158/1078-0432.CCR-12-1362.

Chen D, Li Z, Yang Q, Zhang J, Zhai Z, Shu HB. Identification of a nuclear protein that promotes NF- KB activation. *Biochem Biophys Res Commun*. 2003;310(3):720-724. doi:10.1016/j.bbrc.2003.09.074.

Chen H, Weng QU, Fisher DE. UV signalling pathways within the skin. *J Invest Dermatol.* 2015;134(8):2080-2085. doi:10.1038/jid.2014.161.UV.

Chen L. Co-inhibitory molecules of the B7-CD28 family in the control of T-cell immunity. *Nat Rev Immunol*. 2004;4(May):336-347. doi:10.1038/nri1349.

Cheng P, Shakhova O, Widmer DS, Eichhoff OM, et al. Methylation-dependent SOX9 expression mediates invasion in human melanoma cells and is a negative prognostic factor in advanced melanoma. *Genome Biol.* 2015 Feb 22;16:42.

Cheung M, Chaboissier MC, Mynett A, Hirst E, Schedl A, Briscoe J. The transcriptional control of trunk neural crest induction, survival, and delamination. *Dev Cell*. 2005;8(2):179-192. doi:10.1016/j.devcel.2004.12.010.

Chien AJ, Moore EC, Lonsdorf AS, et al. Activated Wnt/beta-catenin signaling in melanoma is associated with decreased proliferation in patient tumors and a murine melanoma model. *Proc Natl Acad Sci USA*. 2009;106(4):1193-1198. doi:10.1073/pnas.0811902106.

Chow LT, Gelinas RE, Broker TR, Roberts RJ. An amazing sequence arrangement at the 5' ends of adenovirus 2 messenger RNA. *Cell*. 1977;12(1):1-8. doi:10.1016/0092-8674(77)90180-5.

Ciferri C, Lander GC, Maiolica A, Herzog F, Aebersold R, Nogales E. Molecular architecture of human polycomb repressive complex 2. *Elife*. 2012;2012(1):1-22. doi:10.7554/eLife.00005.

Civenni G, Walter A, Kobert N, et al. Human CD271-positive melanoma stem cells associated with metastasis establish tumor heterogeneity and long-term growth. *Cancer Res*. 2011;71(8):3098-3109. doi:10.1158/0008-5472.CAN-10-3997.

Clark WH, From L, Bernardino E, Mihm MC. The Histogenesis Malignant and Biologic Behavior of Primary Human Melanomas of the Skin. *Cancer Res*. 1969;(March)29:705-726

Clark WH, Elder DE, Guerry D 4th, Epstein MN, et al. A study of tumor progression: the precursor lesions of superficial spreading and nodular melanoma. *Hum Pathol.* 1984 Dec;15(12):1147-65.

Clark WH. Tumour progression and the nature of cancer. *Br J Cancer.* 1991 Oct;64(4):631-44.

Cmarko D, Verschure PJ, Martin TE, et al. Ultrastructural analysis of transcription and splicing in the cell nucleus after bromo-UTP microinjection. *Mol Biol Cell*. 1999;10(1):211-223.

Cohen C, Zavala-Pompa A, Sequeira JH, et al. Mitogen-actived Protein Kinase Activation Is an Early Event in Melanoma Progression. *Clin Cancer Res.* 2002;8(December):3728-3733.

Coles EG, Taneyhill LA, Bronner-Fraser M. A critical role for Cadherin6B in regulating avian neural crest emigration. *Dev Biol*. 2007;312(2):533-544. doi:10.1016/j.ydbio.2007.09.056.

Colwill K, Pawson T, Andrews B, et al. The Clk/Sty protein kinase phosphorylates SR splicing factors and regulates their intranuclear distribution. *EMBO J*. 1996;15(2):265-275.

Comijn J, Berx G, Vermassen P, et al. The two-handed E box binding zinc finger protein SIP1 downregulates E-cadherin and induces invasion. *Mol Cell*. 2001;7(6):1267-1278. doi:10.1016/S1097-2765(01)00260-X.

The FANTOM Consortium. The transcriptional network that controls growth arrest and differentiation in a human myeloid leukemia cell line. *Nat Genet.* 2009;41(5):553-562. doi:10.1038/ng.375.

Cooksey CJ, Garratt PJ, Land EJ, et al. Evidence of the Indirect Formation of the Catecholic Intermediate Substrate Responsible for the Autoactivation Kinetics of Tyrosinase. *The Journal of Biological Chemistry.* 1997;272(42):26226-26235.

Cotsarelis G, Sun TT, Lavker RM. Label-retaining cells reside in the bulge area of pilosebaceous unit: Implications for follicular stem cells, hair cycle, and skin carcinogenesis. *Cell*. 1990;61(7):1329-1337. doi:10.1016/0092-8674(90)90696-C.

Cronin JC, Wunderlich J, Loftus SK, et al. Frequent mutations in the MITF pathway in melanoma. *Pigment Cell Melanoma Res*. 2009;22(4):435-444. doi:10.1111/j.1755-148X.2009.00578.x.

Cruz J, Reis-Filho JS, Lopes JM. Primary cutaneous malignant melanoma with lipoblast-like cells. Arch Pathol Lab Med. 2003 Mar; 127(3):370-1.

Cully M, You H, Levine AJ, Mak TW. Beyond PTEN mutations: the PI3K pathway as an integrator of multiple inputs during tumorigenesis. *Nat Rev Cancer*. 2006;6(3):184-192. doi:10.1038/nrc1819.

Curtin JA, Fridlyand J, Kageshita T, Patel HN, et al. Distinct Sets of Genetic Alterations in Melanoma. *N Engl J Med.* 2005:2135-2147.

Curtin JA, Busam K, Pinkel D, Bastian BC. Somatic activation of KIT in distinct subtypes of melanoma. *J Clin Oncol*. 2006;24(26):4340-4346. doi:10.1200/JCO.2006.06.2984.

d'Ischia M, Wakamatsu K, Cicoira F, et al. Melanins and melanogenesis: From pigment cells to human health and technological applications. *Pigment Cell Melanoma Res*. 2015;28(5):520-544. doi:10.1111/pcmr.12393.

Daguenet E, Baguet A, Degot S, et al. Perispeckles are major assembly sites for the exon junction core complex. *Mol Biol Cell*. 2012;23(9):1765-1782. doi:10.1091/mbc.E12-01-0040.

Damsky W, Theodosakis N, Bosenberg M. Melanoma metastasis: new concepts and evolving paradigms. *Oncogene*. 2013;33(19):2413-2422. doi:10.1038/onc.2013.194.

Damsky WE, Rosenbaum LE, Bosenberg M. Decoding melanoma metastasis. *Cancers (Basel)*. 2011;3(1):126-163. doi:10.3390/cancers3010126.

Davy A, Soriano P. Ephrin-B2 forward signaling regulates somite patterning and neural crest cell development. *Dev Biol.* 2007 Apr 1;304(1):182-93.

Debby-Brafman A, Burstyn-Cohen T. F-Spondin, Expressed in Somite Regions Avoided by Neural Crest Cells, Mediates Inhibition of Distinct Somite Domains to Neural Crest Migration. *Neuron*, 1999;22:475-488.

DeDavid M, Orlow SJ, Provost N, et al. A study of large congenital melanocytic nevi and associated malignant melanomas: Review of cases in the New York University Registry and the world literature. *J Am Acad Dermatol*. 1997;36(3):409-416. doi:10.1016/S0190-9622(97)80217-4.

DeDavid M, Orlow SJ, Provost N, et al. Neurocutaneous melanosis: Clinical features of large congenital melanocytic nevi in patients with manifest central nervous system melanosis. *J Am Acad Dermatol*. 1996;35(4):529-538. doi:10.1016/S0190-9622(96)90674-X.

Delmas V, Beermann F, Martinozzi S, Carreira S, et al. b-Catenin induces immortalization of melanocytes by suppressing p16INK4a expression and cooperates with N-Ras in melanoma development. *Genes & Development*. 2007; 21:2923-2935.

Deng J, Lu PD, Zhang Y, et al. Translational repression mediates activation of nuclear factor kappa B by phosphorylated translation initiation factor 2. *Cell Biol*. 2004;24(23):10161-10168. doi:10.1128/MCB.24.23.10161.

Disky A, Campos D, Benchikhi H. Case report : Mucosal melanoma of the lip and the cheek. *Dermatol Online J.* 2008 Aug 15;14(8):20

Dorsky RI, Raible DW, Moon RT. Direct regulation of nacre, a zebrafish MITF homolog required for pigment cell formation, by the Wnt pathway. *Genes & Development.* 2000;(206):158-162.

Dorsky RI, Moon RT, Raible DW. Control of neural crest cell fate by the Wnt signalling pathway. *Nature*. 1998;396(6709):370-373. doi:10.1038/24620.

Druckenbrod NR, Epstein ML. Age-dependent changes in the gut environment restrict the invasion of the hindgut by enteric neural progenitors. *Development*. 2009;136(18):3195-3203. doi:10.1242/dev.031302.

Du J, Fisher DE. Identification of Aim-1 as the underwhite mouse mutant and its transcriptional regulation by MITF. *J Biol Chem*. 2002;277(1):402-406. doi:10.1074/jbc.M110229200.

Du J, Miller AJ, Widlund HR, Horstmann MA, Ramaswamy S, Fisher DE. MLANA/MART1 and SILV/PMEL17/GP100 are transcriptionally regulated by MITF in melanocytes and melanoma. *Am J Pathol*. 2003;163(1):333-343. doi:10.1016/S0002-9440(10)63657-7.

Du J, Widlund HR, Horstmann MA, et al. Critical role of CDK2 for melanoma growth linked to its melanocyte-specific transcriptional regulation by MITF. *Cancer Cell*. 2004;6(6):565-576. doi:10.1016/j.ccr.2004.10.014.

Duband JL, Thiery JP. Distribution of laminin and collagens during avian neural crest development. *Development*. 1987;101:461-478.

Duncan LM. The Classification of Cutaneous Melanoma. *Hematol Oncol Clin North Am*. 2009;23(3):501-513. doi:10.1016/j.hoc.2009.03.013.

Dutt S, Kléber M, Matasci M, Sommer L, Zimmermann DR. Versican V0 and V1 guide migratory neural crest cells. *J Biol Chem*. 2006;281(17):12123-12131. doi:10.1074/jbc.M510834200.

Edelmann L, Pandita RK, Spiteri E, et al. A common molecular basis for rearrangement disorders on chromosome 22q11. *Hum Mol Genet*. 1999;8(7):1157-1167. doi:10.1093/hmg/8.7.1157.

Edge R, D'Ischia M, Land EJ, et al. Dopaquinone redox exchange with dihydroxyindole and dihydroxyindole carboxylic acid. *Pigment Cell Res*. 2006;19(5):443-450. doi:10.1111/j.1600-0749.2006.00327.x.

Eggermont AMM, Kirkwood JM. Re-evaluating the role of dacarbazine in metastatic melanoma: What have we learned in 30 years? *Eur J Cancer*. 2004;40(12):1825-1836. doi:10.1016/j.ejca.2004.04.030.

Eichhoff OM, Weeraratna A, Zipser MC, et al. Differential LEF1 and TCF4 expression is involved in melanoma cell phenotype switching. *Pigment Cell Melanoma Res*. 2011;24(4):631-642. doi:10.1111/j.1755-148X.2011.00871.x.

Elwood MJ, Jopson J. Melanoma and sun exposure: An overview of published studies. *Int J Cancer*. 1997;73(2):198-203. doi:10.1002/(SICI)1097-0215(19971009)73:2<198::AID-IJC6>3.0.CO;2-R.

Emison ES, Garcia-Barcelo M, Grice EA, et al. Differential contributions of rare and common, coding and noncoding ret mutations to multifactorial hirschsprung disease liability. *Am J Hum Genet*. 2010;87(1):60-74. doi:10.1016/j.ajhg.2010.06.007.

Endo Y, Osumi N, Wakamatsu Y. Bimodal functions of Notch-mediated signaling are involved in neural crest formation during avian ectoderm development. *Development*. 2002;129(4):863-873. http://dev.biologists.org/content/129/4/863.abstract.

Enomoto H, Araki T, Jackman A, et al. GFR alpha1-deficient mice have deficits in the enteric nervous system and kidneys. *Neuron*. 1998;21(2):317-324. doi:10.1016/S0896-6273(00)80541-3.

Erdag G, Schaefer JT, Smolkin ME, et al. Immunotype and immunohistologic characteristics of tumor-infiltrating immune cells are associated with clinical outcome in metastatic melanoma. *Cancer Res*. 2012;72(5):1070-1080. doi:10.1158/0008-5472.CAN-11-3218.

Erdei E, Torres SM. A new understanding in the epidemiology of melanoma. *Expert Rev Anticancer Ther*. 2010;10(11):1811-1823. doi:10.1586/era.10.170.

Erickson CA, Goins TL. Avian neural crest cells can migrate in the dorsolateral path only if they are specified as melanocytes. *Development*. 1995;121(3):915-924.

Erickson CA, Duong TD, Tosney KW. Descriptive and experimental analysis of the dispersion of neural crest cells along the dorsolateral path and their entry into ectoderm in the chick embryo. *Dev Biol*. 1992;151(1):251-272. doi:10.1016/0012-1606(92)90231-5.

Eroglu Z, Ribas A. Combination therapy with BRAF and MEK inhibitors for melanoma: latest evidence and place in therapy. *Ther Adv Med Oncol*. 2016;8(1):48-56. doi:10.1177/1758834015616934.

Fackenthal JD, Godley LA. Aberrant RNA splicing and its functional consequences in cancer cells. *Dis Model*

Mech. 2008;1(1):37-42. doi:10.1242/dmm.000331.

Fan T, Jiang S, Chung N, et al. EZH2-dependent suppression of a cellular senescence phenotype in melanoma cells by inhibition of p21/CDN1A expression. *Mol Cancer Res.* 2012;9(4):418-429. doi:10.1158/1541-7786.MCR-10-0511.

Farolfi A, Ridolfi L, Guidoboni M, et al. Ipilimumab in advanced melanoma: reports of long-lasting responses. *Melanoma Res*. 2012;22(3):263-270. doi:10.1097/CMR.0b013e328353e65c.

Faure C, Chalazonitis A, Rhéaume C, et al. Gangliogenesis in the enteric nervous system: Roles of the polysialylation of the neural cell adhesion molecule and its regulation by bone morphogenetic protein-4. *Dev Dyn*. 2007;236(1):44-59. doi:10.1002/dvdy.20943.

Fecher LA, Amaravadi RK, Flaherty KT. The MAPK pathway in melanoma. *Curr Opin Oncol*. 2008;20(2):183-189. doi:10.1097/CCO.0b013e3282f5271c.

Fedorow H, Tribl F, Halliday G, Gerlach M, Riederer P, Double KL. Neuromelanin in human dopamine neurons: Comparison with peripheral melanins and relevance to Parkinson's disease. *Prog Neurobiol*. 2005;75(2):109-124. doi:10.1016/j.pneurobio.2005.02.001.

Feldman JP, Goldwasser R. Quantitative Methods Inquires A mathematical model for tumor volume evaluation V = π. *Methods*. m:455-462.

Ferlay J, Steliarova-Foucher E, Lortet-Tieulent J, et al. Cancer incidence and mortality patterns in Europe: Estimates for 40 countries in 2012. *Eur J Cancer*. 2013;49(6):1374-1403. doi:10.1016/j.ejca.2012.12.027.

Fernández L, Lapunzina P, Arjona D, et al. Comparative study of three diagnostic approaches (FISH, STRs and MLPA) in 30 patients with 22q11.2 deletion syndrome. *Clin Genet*. 2005;68(4):373-378. doi:10.1111/j.1399-0004.2005.00493.x.

Fidler IJ, Metastasis: quantitative analysis of distribution and fate of tumor emboli labeled with 125 I-5-iodo-2'-deoxyuridine. *J Natl Cancer Inst.* 1970 Oct;45(4):773-82.

Fife BT, Bluestone JA. Control of peripheral T-cell tolerance and autoimmunity via the CTLA-4 and PD-1 pathways. *Immunol Rev.* 2008:166-182.

Flaherty KT, Infante JR, Daud A, et al. Combined BRAF and MEK inhibition in melanoma with BRAF V600 mutations. *N Engl J Med*. 2012;367(18):1694-1703. doi:10.1056/NEJMoa1210093.

Flaherty KT, Robert C, Hersey P, et al. Improved Survival with MEK Inhibition in BRAF-Mutated Melanoma. *N Engl J Med*. 2012;367(2):107-114. doi:10.1056/NEJMoa1203421.

Fu XD. The superfamily of arginine/serine-rich splicing factors. *RNA*. 1995;1(7):663-680.

Fu XD. Specific commitment of different pre-mRNAs to splicing by single SR proteins. *Nature*. 1993;365(6441):82-85. doi:10.1038/365082a0.

Fuchs S, Herzog D, Sumara G, et al. Stage-Specific Control of Neural Crest Stem Cell Proliferation by the Small Rho GTPases Cdc42 and Rac1. *Cell Stem Cell*. 2009;4(3):236-247. doi:10.1016/j.stem.2009.01.017.

Furness JB. The Enteric Nervous System. *Wiley-Blackwell.* 2005 (November). ISBN: 978-1-4051-3376-0

Gammill LS, Roffers-Agarwal J. Division of labor during trunk neural crest development. *Dev Biol*. 2010;344(2):555-565. doi:10.1016/j.ydbio.2010.04.009.

Gandini S, Sera F, Cattaruzza MS, et al. Meta-analysis of risk factors for cutaneous melanoma: I. Common and atypical naevi. *Eur J Cancer*. 2005;41(1):28-44. doi:10.1016/j.ejca.2004.10.015.

Gandini S, Sera F, Cattaruzza MS, et al. Meta-analysis of risk factors for cutaneous melanoma: II. Sun exposure. *Eur J Cancer*. 2005;41(1):45-60. doi:10.1016/j.ejca.2004.10.016.

Garcia-Castro MI, Marcelle C, Bronner-Fraser M. Ectodermal Wnt function as a neural crest inducer. *Science.* 2002 Aug 2;297(5582):848-51.

Garibyan L, Fisher DE. How sunlight causes melanoma. *Curr Oncol Rep.* 2010 Sep;12(5):319-326.

Garraway LA, Widlund HR, Rubin MA, et al. Integrative genomic analyses identify MITF as a lineage survival oncogene amplified in malignant melanoma. *Nature*. 2005;436(7047):117-122. doi:10.1038/nature03664.

George L, Chaverra M, Todd V, Lansford R, Lefcort F. Nociceptive sensory neurons derive from contralaterally migrating, fate-restricted neural crest cells. *Nat Neurosci*. 2007;10(10):1287-1293. doi:10.1038/nn1962.

Giehl K. Oncogenic Ras in tumour progression and metastasis. *Biol Chem*. 2005;386(3):193-205. doi:10.1515/BC.2005.025.

Gilchrest BA, Eller MS, Geller AC, Yaar M. The pathogenesis of melanoma induced by ultraviolet radiation. N Engl J Med. 1999 Apr 29;340(17):1341-8

Giot L, Bader JS, Brouwer C, et al. A Protein Interaction Map of Drosophila melanogaster. *Science*. 2003;302(5651):1727-36.

Giuliani N, Lunghi P, Morandi F, et al. Downmodulation of ERK protein kinase activity inhibits VEGF secretion by human myeloma cells and myeloma-induced angiogenesis. *Leukemia*. 2004;18(3):628-635. doi:10.1038/sj.leu.2403269.

Giuliano AE, Moseley HS, Morton DL. Clinical aspects of unknown primary melanoma. *Ann Surg*. 1980;191(1):98-104.

Glavic A, Silva F, Aybar MJ, Bastidas F, Mayor R. Interplay between Notch signaling and the homeoprotein Xiro1 is required for neural crest induction in Xenopus embryos. *Development*. 2004;131(2):347-359. doi:10.1242/dev.00945.

Goding CR. A picture of Mitf in melanoma immortality. *Oncogene*. 2011;30(20):2304-2306. doi:10.1038/onc.2010.641.

Goding CR. Mitf from neural crest to melanoma : signal transduction and transcription in the melanocyte lineage. *Genes & Development.* 2000:1712-1728.

Goel VK, Ibrahim N, Jiang G, Singhai M, et al. Melanocytic nevus-like hyperplasia and melanoma in transgenic BRAFV600E mice. *Oncogene*. 2009 June 11; 28(23):2289-2298.

Gogas H, Bafaloukos D, Bedikian AY. The role of taxanes in the treatment of metastatic melanoma. Melanoma Res. 2004 Oct;14(5):415-420.

Goldstein AM, Jeffery P, Chidambaram A, Fraser MC, Tucker MA. Genotype – Phenotype Relationships in U . S . Melanoma-Prone Families With CDKN2A and CDK4 Mutations. *J Natl Cancer Inst.* 2000;92(12):1006-10.

Goldstein AM, Chan M, Harland M, et al. High-risk melanoma susceptibility genes and pancreatic cancer, neural system tumors, and uveal melanoma across GenoMEL. *Cancer Res*. 2006;66(20):9818-9828. doi:10.1158/0008-5472.CAN-06-0494.

Gordon WR, Arnett KL, Blacklow SC. The molecular logic of Notch signaling: a structural and biochemical perspective. *J Cell Sci*. 2009;121(Pt 19):3109-3119. doi:10.1242/jcs.035683.The.

Gorges TM, Tinhofer I, Drosch M, et al. Circulating tumour cells escape from EpCAM-based detection due to epithelial-to-mesenchymal transition. *BMC Cancer*. 2012;12:178.

Graham A, Begbie J, McGonnell I. Significance of the Cranial Neural Crest. *Dev Dyn*. 2004;229(1):5-13. doi:10.1002/dvdy.10442.

Graveley BR. Sorting out the complexity of SR protein functions. *RNA*. 2000 Sep;6(9):1197-1211.

Gray-Schopfer VC, Cheong SC, Chong H, et al. Cellular senescence in naevi and immortalisation in melanoma: a role for p16? *Br J Cancer*. 2006;95(4):496-505. doi:10.1038/sj.bjc.6603283.

Gray-Schopfer VC, Wellbrock C, Marais R. Melanoma biology and new targeted therapy. *Nature*. 2007;445(7130):851-857. doi:10.1038/nature05661.

Greco G, Panzella L, Verotta L, Ischia M, Napolitano A. Uncovering the Structure of Human Red Hair Pheomelanin : Benzothiazolylthiazinodihydroisoquinolines As Key Building Blocks. *Journal of Natural Products*. 2011:675-682.

Greenstein A, Giaid A, Richardson JA, Emoto N, Hammer RE. Interaction of Endothelin-3 with Endothelin-B Receptor Is Essential for Development of Epidermal Melanocytes and Enteric Neurons. *Cell.* 1994;79:1277-1285.

Greenwood AL, Turner EE, Anderson DJ. Identification of dividing, determined sensory neuron precursors in the mammalian neural crest. *Development.* 1999;3559:3545-3559.

Grichnik JM. Genomic instability and tumor stem cells. *J Invest Dermatol*. 2006;126(6):1214-1216. doi:10.1038/sj.jid.5700240.

Griseri P, Vos Y, Giorda R, et al. Complex pathogenesis of Hirschsprung's disease in a patient with hydrocephalus, vesico-ureteral reflux and a balanced translocation t(3;17)(p12;q11). *Eur J Hum Genet*. 2009;17(4):483-490. doi:10.1038/ejhg.2008.191.

Guillemot F, Lo LC, Johnson JE, Auerbach A, Anderson DJ, Joyner AL. Mammalian achaete-scute homolog 1 is required for the early development of olfactory and autonomic neurons. *Cell*. 1993;75(3):463-476. doi:10.1016/0092-8674(93)90381-Y.

Gupta PB, Kuperwasser C, Brunet J, et al. The melanocyte differentiation program predisposes to metastasis following neoplastic transformation. *Nat Genet.* 2005;37(10):1047-1054.

Hacıhamdioglu B. 22q11 deletion syndrome : current perspective. *The Application of Clinical Genetics.* 2015:123-132.

Hagedorn L, Suter U, Sommer L. P0 and PMP22 mark a multipotent neural crest-derived cell type that displays community effects in response to TGF-β family factors. *Development.* 1999;3794:3781-3794.

Hall BK. The neural crest as a fourth germ layer and vertebrates as quadroblastic not triploblastic. *Evolution & Development.* 2000;5:3-5.

Hall LL, Smith KP, Byron M, Lawrence JB. The molecular anatomy of a speckle. Anat Rec A Discov Mol Cell Evol Biol. 2006 July; 288(7):664-675.

Hardy KM, Kirschmann DA, Seftor EA, et al. Regulation of the embryonic morphogen nodal by Notch4 facilitates manifestation of the aggressive melanoma phenotype. *Cancer Res*. 2010;70(24):10340-10350. doi:10.1158/0008-5472.CAN-10-0705.

Hari L, Brault V, Kléber M, et al. Lineage-specific requirements of β-catenin in neural crest development. *J Cell Biol*. 2002;159(5):867-880. doi:10.1083/jcb.200209039.

Harris ML, Hall R, Erickson C a. Directing pathfinding along the dorsolateral path - the role of EDNRB2 and EphB2 in overcoming inhibition. *Development*. 2008;135(24):4113-4122. doi:10.1242/dev.023119.

Hartman ML, Czyz M. Pro-Survival Role of MITF in Melanoma. *J Invest Dermatol*. 2015;135(2):352-358. doi:10.1038/jid.2014.319.

Hartman ML, Czyz M. Anti-apoptotic proteins on guard of melanoma cell survival. *Cancer Lett*. 2013;331(1):24-34. doi:10.1016/j.canlet.2013.01.010.

Hauschild A, Grob JJ, Demidov L V., et al. Dabrafenib in BRAF-mutated metastatic melanoma: A multicentre,

open-label, phase 3 randomised controlled trial. *Lancet*. 2012;380(9839):358-365. doi:10.1016/S0140-6736(12)60868-X.

Hayat MJ, Howlader N, Reichman ME, Edwards BK. Cancer statistics, trends, and multiple primary cancer analyses from the Surveillance, Epidemiology, and End Results (SEER) Program. *Oncologist*. 2007;12(1):20-37. doi:10.1634/theoncologist.12-1-20.

He C, Zhou F, Zuo Z, Cheng H, Zhou R. A global view of cancer-specific transcript variants by subtractive transcriptome-wide analysis. *PLoS One*. 2009;4(3). doi:10.1371/journal.pone.0004732.

Heanue T a, Pachnis V. Enteric nervous system development and Hirschsprung's disease: advances in genetic and stem cell studies. *Nat Rev Neurosci*. 2007;8(6):466-479. doi:10.1038/nrn2137.

Hedley ML, Amrein H, Maniatis T. An amino acid sequence motif sufficient for subnuclear localization of an arginine/serine-rich splicing factor. *Proc Natl Acad Sci USA*. 1995;92(December 1995):11524-11528. doi:10.1073/pnas.92.25.11524.

Hegele A, Kamburov A, Grossmann A, et al. Dynamic Protein-Protein Interaction Wiring of the Human Spliceosome. *Mol Cell*. 2012;45(4):567-580. doi:10.1016/j.molcel.2011.12.034.

Hoang MP, Sinkre P, Albores-saavedra J. Extraordinary Case Report Rhabdomyosarcoma Arising in a Congenital Melanocytic Nevus. 2002;24(1):26-29.

Hodi SF, O'Day SJ, Mcdermott DF, et al. Improved Survival with Ipilimumab in Patients with Metastatic Melanoma. *N Engl J Med*. 2010;363(8):711-723. doi:10.1056/NEJMoa1003466.

Hodis E, Watson IR, Kryukov G V., et al. A landscape of driver mutations in melanoma. *Cell*. 2012;150(2):251-263. doi:10.1016/j.cell.2012.06.024.

Hoek KS, Schlegel NC, Brafford P, et al. Metastatic potential of melanomas defined by specific gene expression profiles with no BRAF signature. *Pigment Cell Res*. 2006;19(4):290-302. doi:10.1111/j.1600-0749.2006.00322.x.

Hoek KS, Schlegel NC, Eichhoff OM, et al. Novel MITF targets identified using a two-step DNA microarray strategy. *Pigment Cell Melanoma Res*. 2008;21(6):665-676. doi:10.1111/j.1755-148X.2008.00505.x.

Hong CS, Saint-Jaennet JP. The activity of Pax3 and Zic1 regulates three distinct cell fates at the neural crest plate border. *Mol Biol Cell.* 2007 Jun;18(6):2192-202.

Houben R, Becker JC, Kappel A, et al. Constitutive activation of the Ras-Raf signaling pathway in metastatic melanoma is associated with poor prognosis. *J Carcinog*. 2004;3(1):6. doi:10.1186/1477-3163-3-6.

Houghton AN, Polsky D. Focus on melanoma. *Cancer Cell*. 2002;2(4):275-278. doi:10.1016/S1535-6108(02)00161-7.

Howard JD, Moriarty WF, Park J, et al. Notch signaling mediates melanoma-endothelial cell communication and melanoma cell migration. *Pigment Cell Melanoma Res*. 2013;26:697-707. doi:10.1111/pcmr.12131.

Hsieh JJ, Zhou S, Chen L, Young DB, Hayward SD. CIR, a corepressor linking the DNA binding factor CBF1 to the histone deacetylase complex. *Proc Natl Acad Sci USA*. 1999;96(1):23-28. doi:10.1073/pnas.96.1.23.

Hsu F-C, Pajerowski AG, Nelson-Holte M, Sundsbak R, Shapiro VS. NKAP is required for T cell maturation and acquisition of functional competency. *J Exp Med*. 2011;208(6):1291-1304. doi:10.1084/jem.20101874.

Hsu M, Meier FE, Nesbit M, Hsu J, Belle P Van, Elder DE. E-cadherin expression in melanoma cells restores keratinocyte-mediated growth control and down-regulates expression of invasion-related adhesion receptors. *Am J Pathol.* 2000;156(5):1515-1525.

Hu-Lieskovan S, Mok S, Moreno BH, et al. Improved antitumor activity of immunotherapy with BRAF and MEK inhibitors in BRAF V600E melanoma. *Sci Transl Med.* 2015 March 18;7(279):279ra41.

doi:10.1126/scitranslmed.aaa4691.

Hüsemann Y, Geigl JB, Schubert F, et al. Systemic Spread Is an Early Step in Breast Cancer. *Cancer Cell*. 2008;13(1):58-68. doi:10.1016/j.ccr.2007.12.003.

Hussussian CJ, Struewing JP, Goldstein a M, et al. Germline p16 mutations in familial melanoma. *Nat Genet*. 1994;8:15-21. doi:10.1038/ng0994-15.

Ignatius MS, Moose HE, El-Hodiri HM, Henion PD. Colgate/hdac1 repression of foxd3 expression is required to permit mitfa-depenent melanogenesis. *NIH Public Access*. Vol 313.; 2009. doi:10.1016/j.ydbio.2007.10.045.colgate/hdac1.

Ijuin K, Nakanishi K, Ito K. Different downstream pathways for Notch signaling are required for gliogenic and chondrogenic specification of mouse mesencephalic neural crest cells. *Mech Dev*. 2008;125(5-6):462-474. doi:10.1016/j.mod.2008.01.008.

Jarriault S, Brou C, Logeat F, Schroeter EH, Kopan R, Israel A. Signalling downstream of activated mammalian Notch. *Nature*. 1995;377(6547):355-358. doi:10.1038/377355a0.

Javelaud D, Alexaki VI, Pierrat MJ, et al. GLI2 and M-MITF transcription factors control exclusive gene expression programs and inversely regulate invasion in human melanoma cells. *Pigment Cell Melanoma Res*. 2011;24(5):932-943. doi:10.1111/j.1755-148X.2011.00893.x.

Jemal A, Bray F, Ferlay J. Global Cancer Statistics: 2011. *CA Cancer J Clin*. 1999;49(2):1,33-64. doi:10.3322/caac.20107.

Ji M, Andrisani OM. High-Level Activation of Cyclic AMP Signaling Attenuates Bone Morphogenetic Protein 2-Induced Sympathoadrenal Lineage Development and Promotes Melanogenesis in Neural Crest Cultures. 2005;25(12):5134-5145. doi:10.1128/MCB.25.12.5134.

Jia L, Cheng L, Raper J. Slit/Robo signaling is necessary to confine early neural crest cells to the ventral migratory pathway in the trunk. *Dev Biol*. 2005;282(2):411-421. doi:10.1016/j.ydbio.2005.03.021.

Jin EJ, Erickson C a, Takada S, Burrus LW. Wnt and BMP signaling govern lineage segregation of melanocytes in the avian embryo. *Dev Biol*. 2001;233(1):22-37. doi:10.1006/dbio.2001.0222.

Jinek M, East A, Cheng A, Lin S, Ma E, Doudna J. RNA-programmed genome editing in human cells. *Elife*. 2013;2013(2):1-9. doi:10.7554/eLife.00471.

Johannessen CM, Johnson LA, Piccioni F, et al. A melanocyte lineage program confers resistance to MAP kinase pathway inhibition. *Nature*. 2013;504(7478):138-142. doi:10.1038/nature12688.

John N, Cinelli P, Wegner M, Sommer L. Transforming growth factor β-mediated sox10 suppression controls mesenchymal progenitor generation in neural crest stem cells. *Stem Cells*. 2011;29(4):689-699. doi:10.1002/stem.607.

Jurica MS, Moore MJ. Pre-mRNA Splicing: Awash in a Sea of Proteins. *Mol Cell.* 2003;12:5-14.

Kageshita T, Hamby C V, Ishihara T, Matsumoto K, Ono T. Loss of b-catenin expression associated with disease progression in malignant melanoma. *Br J Dermatol.* 2001:210-216.

Kalluri R, Weinberg R a. Review series The basics of epithelial-mesenchymal transition. *J Clin Invest*. 2009;119(6):1420-1428. doi:10.1172/JCI39104.1420.

Kapur RP. Practical pathology and genetics of Hirschsprung's disease. *Semin Pediatr Surg*. 2009;18(4):212-223. doi:10.1053/j.sempedsurg.2009.07.003.

Kasemeier-Kulesa JC, Kulesa PM, Lefcort F. Imaging neural crest cell dynamics during formation of dorsal root ganglia and sympathetic ganglia. *Development*. 2005;132(2):235-245. doi:10.1242/dev.01553.

Katalinic A, Kunze U, Schäfer T. Epidemiology of cutaneous melanoma and non-melanoma skin cancer in Schleswig-Holstein, Germany: incidence, clinical subtypes, tumour stages and localization

(epidemiology of skin cancer). *British Journal of Dermatology*. 2003:149; 1200-1206.

Kee Y, Bronner-fraser M. To proliferate or to die : role of Id3 in cell cycle progression and survival of neural crest progenitors. *Genes & Development.* 2005:744-755. doi:10.1101/gad.1257405.et.

Kelsh RN. Sorting out Sox10 functions in neural crest development. *BioEssays*. 2006;28(8):788-798. doi:10.1002/bies.20445.

Keyte A, Hutson MR. The Neural Crest in Cardiac Congenital Anomalies. *Differentiation*. 2012(July);84(1):25-40. doi:10.1016/j.diff.2012.04.005.

Kim J, Lo L, Dormand E, Anderson DJ. SOX10 maintains multipotency and inhibits neuronal differentiation of neural crest stem cells. *Neuron*. 2003;38(1):17-31. doi:10.1016/S0896-6273(03)00163-6.

Kincannon J, Boutzale C. The Physiology of Pigmented Nevi. *Pediatrics.* 1999(Oct);104(4Pt2):1042-5.

King R, Googe PB, Weilbaecher KN, Mihm MC, Fisher DE. Microphthalmia Transcription Factor Expression in Cutaneous Benign , Malignant Melanocytic , and Nonmelanocytic Tumors. *Am J Surg Pathol.* 2001;25(1):51-57.

Kirby ML, Gale TF, Stewart DE. Neural crest cells contribute to normal aorticopulmonary septation. Science. 1983 Jun 3; 220(4601):1059-61.

Kirby ML, Waldo KL. Role of neural crest in congenital heart disease. *Circulation.* 1990 Aug;82(2):332-40.

Kléber M, Lee HY, Wurdak H, et al. Neural crest stem cell maintenance by combinatorial Wnt and BMP signaling. *J Cell Biol*. 2005;169(2):309-320. doi:10.1083/jcb.200411095.

Knecht AK, Bronner-Fraser M. Induction of the neural crest: a multigene process. *Nat Rev Genet*. 2002;3(6):453-461. doi:10.1038/nrg819.

Ko TK, Kelly E, Pines J. CrkRS: a novel conserved Cdc2-related protein kinase that colocalises with SC35 speckles. *J Cell Sci*. 2001;114(Pt 14):2591-2603.

Kobrynski LJ, Sullivan KE. Velocardiofacial syndrome, DiGeorge syndrome: the chromosome 22q11.2 deletion syndromes. *Lancet*. 2007;370(9596):1443-1452. doi:10.1016/S0140-6736(07)61601-8.

Konieczkowski DJ, Johannessen CM, Abudayyeh O, et al. A melanoma cell state distinction influences sensitivity to MAPK pathway inhibitors. *Cancer Discov*. 2014;4(7):816-827. doi:10.1158/2159-8290.CD-13-0424.

Kopan R, Ilagan MXG. The Canonical Notch Signaling Pathway: Unfolding the Activation Mechanism. *Cell*. 2009;137(2):216-233. doi:10.1016/j.cell.2009.03.045.

Kortylewski M, Heinrich PC, Kauffmann ME, Bohm M, Mackiewicz a, Behrmann I. Mitogen-activated protein kinases control p27/Kip1 expression and growth of human melanoma cells. *BiochemJ*. 2001;357(0264-6021

Krauthammer M, Kong Y, Bacchiocchi A, et al. Exome sequencing identifies recurrent mutations in NF1 and RASopathy genes in sun-exposed melanomas. *Nat Genet.* 2015;47(9):996-1002. doi:10.1038/ng.3361.Exome.

Kruger GM, Mosher JT, Bixby S, et al. Neural Crest Stem Cells Persist in the Adult Gut but Undergo Changes in Self-Renewal , Neuronal Subtype Potential , and Factor Responsiveness. *Neuron.* 2002;35:657-669.

Kruhlak MJ, Lever MA, Fischle W, Verdin E, Bazett-jones DP, Hendzel MJ. Reduced Mobility of the Alternate Splicing Factor (ASF) through the Nucleoplasm and Steady State Speckle Compartments 7. *J Cell Biol*. 2000;150(1):41-51.

Krull CE, Lansford R, Gale NW, et al. Interactions of Eph-related receptors and ligands confer rostrocaudal pattern to trunk neural crest migration. *Current Biology*. 1997;7:571-580.

Krummel MF, Allison JP. CD28 and CTLA-4 have opposing effects on the response of T cells to stimulation. *J Exp Med*. 1995;182(2):459-465. doi:10.1210/me.2014-1154.

Kubota M, Suita S, Kamimura T, Ito Y, Szurszewski JH. Electrophysiological properties of the aganglionic segment in Hirschsprung's disease. *Surgery*. 2002;131(1SUPPL.):288-293. doi:10.1067/msy.2002.119963.

Kumar R, Angelini S, Czene K, et al. BRAF mutations in metastatic melanoma: a possible association with clinical outcome. *Clin Cancer Res*. 2003;9(9):3362-3368.

Kumasaka M, Sato H, Sato S, Yajima I, Yamamoto H. Isolation and Developmental Expression of Mitf in Xenopus laevis. *Dev Dyn*. 2004;230(1):107-113. doi:10.1002/dvdy.20019.

LaBonne C, Bronner-Fraser M. Snail-related transcriptional repressors are required in Xenopus for both the induction of the neural crest and its subsequent migration. *Dev Biol*. 2000;221(1):195-205. doi:10.1006/dbio.2000.9609.

LaBonne C, Bronner-fraser M. Neural crest induction in Xenopus : evidence for a two-signal model. *Development.* 1998;2414:2403-2414.

Laga AC, Murphy GF. Cellular heterogeneity in vertical growth phase melanoma. *Arch Pathol Lab Med*. 2010;134(12):1750-1757. doi:10.1043/2009-0394-RAR.1.

Lahav R, Ziller C, Dupin E, Le Douarin NM. Endothelin 3 promotes neural crest cell proliferation and mediates a vast increase in melanocyte number in culture. *Proc Natl Acad Sci USA*. 1996;93(9):3892-3897. doi:10.1073/pnas.93.9.3892.

Lake JI, Heuckeroth RO. Enteric nervous system development: migration, differentiation, and disease. *Am J Physiol Gastrointest Liver Physiol*. 2013;305(1):G1-24. doi:10.1152/ajpgi.00452.2012.

Lamond AI, Spector DL. Nuclear speckles: a model for nuclear organelles. *Nat Rev Mol Cell Biol*. 2003;4(8):605-612. doi:10.1038/nrm1172.

Lang D, Lu MM, Huang L, et al. Pax3 functions at a nodal point in melanocyte stem cell differentiation. *Nature*. 2005;433(7028):884-887. doi:10.1038/nature03292.

Lasfar A, Cohen-Solal KA. Resistance to transforming growth factor β-mediated tumor suppression in melanoma: Are multiple mechanisms in place? *Carcinogenesis*. 2010;31(10):1710-1717. doi:10.1093/carcin/bgq155.

Latchman YE, Liang SC, Wu Y, et al. PD-L1-deficient mice show that PD-L1 on T cells , antigen-presenting cells , and host tissues negatively regulates T cells. Proc Natl Acad Sci USA. 2004;101(29).

Lawrence MS, Stojanov P, Polak P, et al. Mutational heterogeneity in cancer and the search for new cancer-associated genes. *Nature*. 2013;499(7457):214-218. doi:10.1038/nature12213.

Lazovich D, Vogel RI, Berwick M, Martin A, Anderson KE, Warshaw EM. Highly Exposed Population. 2011;19(6):1557-1568. doi:10.1158/1055-9965.EPI-09-1249.Indoor.

Le Douarin NM, Dupin E. Multipotentiality of the neural crest. *Curr Opin Genet Dev*. 2003;13(5):529-536. doi:10.1016/j.gde.2003.08.002.

Lee DA, Cohen JA, Twaddell WS, et al. Are all melanomas the same? Spitzoid melanoma is a distinct subtype of melanoma. *Cancer*. 2006;106(4):907-913. doi:10.1002/cncr.21686.

Lefebvre R, Huang W, Harley VR, Goodfellow PN, Crombrugghe BDE. SOX9 Is a Potent Activator of the Chondrocyte-Specific Enhancer of the Proα1(II) Collagen Gene. *Molecular and Cellular Biology*. 1997;17(4):2336-2346.

Lerner MR, Boyle JA, Mount SM, Wolin SL, Steitz JA. Are snRNPs involved in splicing? *Nature.* 1980 Jan 10;283(5743):220-4.

Lewis JL, Bonner J, Modrell M, et al. Reiterated Wnt signaling during zebrafish neural crest development. *Development*. 2004;131(6):1299-1308. doi:10.1242/dev.01007.

Li G, Satyamoorthy K, Herlyn M. N-cadherin-mediated intercellular interactions promote survival and migration of melanoma cells. *Cancer Res*. 2001;61(9):3819-3825.

Li H, Bingham PM. Arginine/serine-rich domains of the su(wa) and tra RNA processing regulators target proteins to a subnuclear compartment implicated in splicing. *Cell*. 1991;67:335-342. doi:10.1016/0092-8674(91)90185-2.

Light W, Vernon AE, Lasorella A, Iavarone A, LaBonne C. Xenopus Id3 is required downstream of Myc for the formation of multipotent neural crest progenitor cells. *Development*. 2005;132(8):1831-1841. doi:10.1242/dev.01734.

Lin JY, Fisher DE. Melanocyte biology and skin pigmentation. *Nature*. 2007;445(7130):843-850. doi:10.1038/nature05660.

Lin S, Coutinho-Mansfield G, Wang D, Pandit S, Fu X. The splicing factor SC35 has an active role in transcriptional elongation. *Nat Struct Mol Biol*. 2009;15(8):819-826. doi:10.1038/nsmb.1461.The.

Lin WM, Luo S, Muzikansky A, et al. Outcome of patients with de novo versus nevus-associated melanoma. *J Am Acad Dermatol*. 2015;72(1):54-58. doi:10.1016/j.jaad.2014.09.028.

Lister JA, Robertson CP, Lepage T, Johnson SL, Raible DW. Nacre Encodes a Zebrafish Microphthalmia-Related Protein That Regulates Neural-Crest-Derived Pigment Cell Fate. *Development*. 1999;126(17):3757-3767.

Lister JA, Cooper C, Nguyen K, Modrell M, Grant K, Raible DW. Zebrafish Foxd3 is required for development of a subset of neural crest derivatives. *Dev Biol*. 2006;290(1):92-104. doi:10.1016/j.ydbio.2005.11.014.

Liu Y, Sheikh MS. Melanoma: Molecular Pathogenesis and Therapeutic Management. *Mol Cell Pharmacol*. 2014;6(3):228. doi:10.1002/cncr.29075.Familial.

Liu ZJ, Xiao M, Balint K, et al. Notch1 signaling promotes primary melanoma progression by activating mitogen-activated protein kinase/phosphatidylinositol 3-kinase-Akt pathways and up-regulating N-cadherin expression. *Cancer Res*. 2006;66(8):4182-4190. doi:10.1158/0008-5472.CAN-05-3589.

Lo JA, Fisher DE. The melanoma revolution: from UV carcinogenesis to a new era in therapeutics. *Science.* 2014 Nov 21; 346(6212):945-949.

Loercher AE, Tank EMH, Delston RB, Harbour JW. MITF links differentiation with cell cycle arrest in melanocytes by transcriptional activation of INK4A. *J Cell Biol*. 2005;168(1):35-40. doi:10.1083/jcb.200410115.

Long JC, Caceres JF. The SR protein family of splicing factors: master regulators of gene expression. *Biochem J*. 2009;417(1):15-27. doi:10.1042/BJ20081501.

Loring JF, Erickson CA. Neural crest cell migratory pathways in the trunk of the chick embryo. *Dev Biol*. 1987;121(1):220-236. doi:10.1016/0012-1606(87)90154-0.

Lumsden a, Sprawson N, Graham a. Segmental origin and migration of neural crest cells in the hindbrain region of the chick embryo. *Development*. 1991;113(4):1281-1291.

Luo C, Merz PR, Chen Y, et al. MiR-101 inhibits melanoma cell invasion and proliferation by targeting MITF and EZH2. *Cancer Lett*. 2013;341(2):240-247. doi:10.1016/j.canlet.2013.08.021.

Luo C, Tetteh PW, Merz PR, et al. miR-137 inhibits the invasion of melanoma cells through downregulation of multiple oncogenic target genes. *J Invest Dermatol*. 2013;133(3):768-775. doi:10.1038/jid.2012.357.

Luo T, Matsuo-Takasaki M, Lim JH, Sargent TD. Differential regulation of Dlx gene expression by a BMP morphogenetic gradient. *Int J Dev Biol*. 2001;45(4):681-684.

Lynch KW. Regulation of alternative splicing by signal transduction pathways. *Adv Exp Med Biol*. 2007;623:161-174.

Lyon VB. Congenital Melanocytic Nevi. *Pediatr Clin North Am*. 2010;57(5):1155-1176. doi:10.1016/j.pcl.2010.07.005.

Ma Q, Fode C, Guillemot F, Anderson DJ. NEUROGENIN1 and NEUROGENIN2 control two distinct waves of neurogenesis in developing dorsal root ganglia. *Genes Dev*. 1999;13(13):1717-1728. doi:10.1101/gad.13.13.1717.

Mælandsmo GM, Holm R, Nesland JM, Fodstad Ø, Flørenes VA. Reduced β-catenin expression in the cytoplasm of advanced-stage superficial spreading malignant melanoma. *Clin Cancer Res*. 2003;9(9):3383-3388. doi:VL - 9.

Maggadottir SM, Sullivan KE. The Diverse clinical features of chromosome 22q11.2 deletion syndrome (DiGeorge Syndrome). *J Allergy Clin Immunol Pract*. 2013;1(6):589-594. doi:10.1016/j.jaip.2013.08.003.

Maguire LH, Thomas AR, Goldstein AM. Tumors of the neural crest: Common themes in development and cancer. *Dev Dyn*. 2015;244(3):311-322. doi:10.1002/dvdy.24226.

Maita H, Kitaura H, Ariga H, Iguchi-Ariga SMM. CIR, a corepressor of CBF1, binds to PAP-1 and effects alternative splicing. *Exp Cell Res*. 2005;303(2):375-387. doi:10.1016/j.yexcr.2004.10.012.

Mani SA, Guo W, Liao M, et al. The epithelial-mesenchymal transition generates cells with properties of stem cells. *Cell*. 2009;133(4):704-715. doi:10.1016/j.cell.2008.03.027.The.

Manié S, Santoro M, Fusco A, Billaud M. The RET receptor: Function in development and dysfunction in congenital malformation. *Trends Genet*. 2001;17(10):580-589. doi:10.1016/S0168-9525(01)02420-9.

Margueron R, Reinberg D. The Polycomb Complex PRC2 and its Mark in Life. *Nature*. 2011 January 20; 469(7330):343-349.

Marine JC, Jochemsen AG. Mdmx as an essential regulator of p53 activity. *Biochem Biophys Res Commun*. 2005;331(3):750-760. doi:10.1016/j.bbrc.2005.03.151.

Markert CL, Silvers WK. The Effects of Genotype and Cell Environment on Melanoblast Differentiation in the House Mouse. *Genetics*. 1956;41(3):429-450.

Marraffini LA, Sontheimer EJ. CRISPR interference limits horizontal gene transfer in staphylococci by targeting DNA. *Science (80-)*. 2008;322(5909):1843-1845. doi:10.1126/science.1165771.

Matera AG, Wang Z. A day in the life of the spliceosome. *Nat Rev Mol Cell Biol*. 2014;15(2):108-121. doi:10.1038/nrm3742.

Matlin AJ, Clark F, Smith CWJ. Understanding alternative splicing: towards a cellular code. *Nat Rev Mol Cell Biol*. 2005;6(5):386-398. doi:10.1038/nrm1645.

Matsuhisa T, Mori Y. An anchorage-dependent locus in the cell cycle for the growth of 3T3 cells. *Exp Cell Res*. 1981 Oct;135(2):393-8

Mayor R, Guerrero N, Martínez C. Role of FGF and noggin in neural crest induction. *Dev Biol*. 1997;189(1):1-12. doi:10.1006/dbio.1997.8634.

McGovern VJ, Shaw HM, Milton GW. Prognostic significance of a polypoid configuration in melignant melanoma. *Histopathology*. 1983 Sep;7(5):663-72.

McCourt C, Dolan O, Gormley G. Malignant melanoma: a pictorial review. *Ulster Med J*. 2014;83(2):103-110.

McGill GG, Horstmann M, Widlund HR, et al. Bcl2 regulation by the melanocyte master regulator Mitf

modulates lineage survival and melanoma cell viability. *Cell*. 2002;109(6):707-718. doi:10.1016/S0092-8674(02)00762-6.

McHugh JB, Fullen DR, Ma L, Kleer CG, Su LD. Expression of polycomb group protein EZH2 in nevi and melanoma. *J Cutan Pathol*. 2007;34(8):597-600. doi:10.1111/j.1600-0560.2006.00678.x.

Mckeown SJ, Stamp L, Hao MM, Young HM. Hirschsprung disease: A developmental disorder of the enteric nervous system. *Wiley Interdiscip Rev Dev Biol*. 2013;2(1):113-129. doi:10.1002/wdev.57.

McLaughlin CC, Wu XC, Jemal A, Martin HJ, Roche LM, Chen VW. Incidence of noncutaneous melanomas in the U.S. *Cancer*. 2005;103(5):1000-1007. doi:10.1002/cncr.20866.

Mejlvang J, Kriajevska M, Vandewalle C, Chernova T, et al. Direct Repression of Cyclin D1 by SIP1 Attenuates Cell Cycle Progression in Cells Undergoing an Epithelial Mesenchymal Transition. Mol Biol Cell. 2007 Nov; 18(11):4615-4624.

Melcák I, Cermanová S, Jirsová K, Koberna K, Malínský J, Raska I. Nuclear pre-mRNA compartmentalization: trafficking of released transcripts to splicing factor reservoirs. *Mol Biol Cell*. 2000;11(2):497-510.

Melero I, Hervas-Stubbs S, Glennie M, Pardoll DM, Chen L. Immunostimulatory monoclonal antibodies for cancer therapy. *Nat Rev Cancer*. 2007;7(2):95-106. doi:10.1038/nrc2051.

Mellen PL, Morton SJ, Shields CL. American joint committee on cancer staging of uveal melanoma. *Oman J Ophthalmol*. 2013;6(2):116-118. doi:10.4103/0974-620X.116652.

Mellott DO, Burke RD. Divergent roles for Eph and ephrin in avian cranial neural crest. *BMC Dev Biol*. 2008;8:56. doi:10.1186/1471-213X-8-56.

Menon DR, Wels C, Bonyadi Rad E, et al. TGF-β1 and TNF-α differentially regulate Twist1 mediated resistance towards BRAF/MEK inhibition in melanoma. *Pigment Cell Melanoma Res*. 2013;26(6):912-916. doi:10.1111/pcmr.12139.

Meredith P, Riesz J. Radiative relaxation quantum yields for synthetic eumelanin. *Photochem Photobiol*. 2004;79(2):211-216. doi:10.1111/j.1751-1097.2004.tb00012.x.

Meredith P, Sarna T. The physical and chemical properties of eumelanin. *Pigment Cell Res*. 2006;19(6):572-594. doi:10.1111/j.1600-0749.2006.00345.x.

Mermoud JE, Cohen PT, Lamond a I. Regulation of mammalian spliceosome assembly by a protein phosphorylation mechanism. *EMBO J*. 1994;13(23):5679-5688.

Mete O, Bilgic B, Buyukbabani N. A Tumor With Many Faces: Metastatic Malignant Melanoma With Extensive Cartilaginous Differentiation. *Int J Surg Pathol*. 2010;18(3):217-218. doi:10.1177/1066896909359632.

Metzger M, Caldwell C, Barlow AJ, Burns AJ, Thapar N. Enteric Nervous System Stem Cells Derived From Human Gut Mucosa for the Treatment of Aganglionic Gut Disorders. *Gastroenterology*. 2009;136(7):2214-2225.e3. doi:10.1053/j.gastro.2009.02.048.

Meulemans D, Bronner-Fraser M. Gene-regulatory interactions in neural crest evolution and development. *Dev Cell*. 2004;7(3):291-299. doi:10.1016/j.devcel.2004.08.007.

Michaloglou C, Vredeveld LCW, Soengas MS, et al. BRAFE600-associated senescence-like cell cycle arrest of human naevi. *Nature*. 2005;436(August):720-724. doi:10.1038/nature03890.

Miller AJ, Mihm MC. Melanoma. *N Engl J Med.* 2006; 355:51-65

Misteli T, Cáceres JF, Clement JQ, Krainer AR, Wilkinson MF, Spector DL. Serine phosphorylation of SR proteins is required for their recruitment to sites of transcription in vivo. *J Cell Biol*. 1998;143(2):297-307. doi:10.1083/jcb.143.2.297.

Misteli T, Càceres JF, Spector DL. The dynamics of a pre-mRNA splicing factor in living cells. *Nature*.

1997;387:523-527. doi:10.1038/387523a0.

Monsoro-Burq AH, Wang E, Harland R. Msx1 and Pax3 cooperate to mediate FGF8 and WNT signals during Xenopus neural crest induction. *Dev Cell*. 2005;8(2):167-178. doi:10.1016/j.devcel.2004.12.017.

Morel A, Lievre M, Thomas C, Hinkal G, Ansieau S, Puisieux A. Generation of breast cancer stem cells through epithelial-mesenchymal transition. *PLoS One*. 2008;3(8):e2888. doi:10.1371/journal.pone.0002888.

Morrison SJ, Perez SE, Qiao Z, et al. Transient Notch activation initiates an irreversible switch from neurogenesis to gliogenesis by neural crest stem cells. *Cell*. 2000;101:499-510. doi:10.1016/S0092-8674(00)80860-0.

Morrison SJ, White PM, Zock C, Anderson DJ. Prospective identification, isolation by flow cytometry, and in vivo self-renewal of multipotent mammalian neural crest stem cells. *Cell*. 1999;96:737-749. doi:10.1016/S0092-8674(00)80583-8.

Mount SM. A catalogue of splice junction sequences. *Nucleic Acids Res*. 1982;10(2):459-472. doi:10.1093/nar/10.2.459.

Mulé JJ, Shu S, Schwarz SL, Rosenberg SA. Adoptive immunotherapy of established pulmonary metastases with LAK cells and recombinant interleukin-2. *Science.* 1984 Sep 28;225(4669):1487-9.

Müller J, Krijgsman O, Tsoi J, Robert L, et al. Low MITF/AXL ratio predicts early resistance to multiple drugs in melanoma. *Nat Cummun.* 2014; 5:5712.

Mumm JS, Schroeter EH, Saxena MT, et al. A ligand-induced extracellular cleavage regulates gamma-secretase-like proteolytic activation of Notch1. *Mol Cell*. 2000;5:197-206. doi:10.1016/S1097-2765(00)80416-5.

Muthusamy V, Hobbs C, Nogueira C, Cordon-Cardo C, et al. Amplification of CDK4 and MDM2 in malignant melanoma. *Genes Chromosomes Cancer.* 2006 May;45(5):447-54.

Nagoshi N, Shibata S, Kubota Y, et al. Ontogeny and Multipotency of Neural Crest-Derived Stem Cells in Mouse Bone Marrow, Dorsal Root Ganglia, and Whisker Pad. *Cell Stem Cell*. 2008;2(4):392-403. doi:10.1016/j.stem.2008.03.005.

Nagy N, Goldstein AM. Endothelin-3 regulates neural crest cell proliferation and differentiation in the hindgut enteric nervous system. *Dev Biol*. 2006;293(1):203-217. doi:10.1016/j.ydbio.2006.01.032.

Nakamura Y, Sakakibara SI, Miyata T, et al. The bHLH gene Hes1 as a repressor of the neuronal commitment of CNS stem cell. *J Neurosci*. 2000;20(1):283-293.

Nakayama A, Nguyen MTT, Chen CC, Opdecamp K, Hodgkinson CA, Arnheiter H. Mutations in microphthalmia, the mouse homolog of the human deafness gene MITF, affect neuroepithelial and neural crest-derived melanocytes differently. *Mech Dev*. 1998;70(1-2):155-166. doi:10.1016/S0925-4773(97)00188-3.

Naldi L, Altieri A, Imberti GL, Gallus S, Bosetti C, La Vecchia C. Sun exposure, phenotypic characteristics, and cutaneous malignant melanoma. An analysis according to different clinico-pathological variants and anatomic locations (Italy). *Cancer Causes Control*. 2005;16(8):893-899. doi:10.1007/s10552-005-2300-4.

Newgreen D, Thiery JP. Fibronectin in early avian embryos: synthesis and distribution along the migration pathways of neural crest cells. *Cell Tissue Res*. 1980;211(2):269-91.

Nguyen VH, Schmid B, Trout J, Connors S a, Ekker M, Mullins MC. Ventral and lateral regions of the zebrafish gastrula, including the neural crest progenitors, are established by a bmp2b/swirl pathway of genes. *Dev Biol*. 1998;199(1):93-110. doi:10.1006/dbio.1998.8927.

Nichols SE, Reams WM, Plate WONE. The Occurrence and Morphogenesis of Melanocytes in the Connective Tissues of the PET / MCV Mouse. *Journal of Embryology and Experimental Morphology.*

1960;8(March):24-32.

Nikitina N, Sauka-Spengler T, Bronner-Fraser M. Dissecting early regulatory relationships in the lamprey neural crest gene network. *Proc Natl Acad Sci USA*. 2008;105(51):20083-20088. doi:10.1073/pnas.0806009105.

Nikitina N, Bronner-Fraser M. Gene regulatory networks that control the specification of neural-crest cells in the lamprey. *Biochim Biophys Acta - Gene Regul Mech*. 2009;1789(4):274-278. doi:10.1016/j.bbagrm.2008.03.006.

Nilsen TW, Graveley BR. Expansion of the eukaryotic proteome by alternative splicing. *Nature*. 2010;463(7280):457-463. doi:10.1038/nature08909.

Nishimura EK, Jordan SA, Oshima H, et al. Dominant role of the niche in melanocyte stem-cell fate determination. *Nature*. 2002;416(6883):854-860. doi:10.1038/416854a.

Nishimura EK, Suzuki M, Igras V, et al. Key Roles for Transforming Growth Factor-β in Melanocyte Stem Cell Maintenance. *Cell Stem Cell*. 2010;6(2):130-140. doi:10.1016/j.stem.2009.12.010.

Noden DM, Trainor PA. Relations and interactions between cranial mesoderm and neural crest populations. *J Anat.* 2005:575-601.

O'Day SJ, Maio M, Chiarion-Sileni V, et al. Efficacy and safety of ipilimumab monotherapy in patients with pretreated advanced melanoma: A multicenter single-arm phase II study. *Ann Oncol*. 2010;21(8):1712-1717. doi:10.1093/annonc/mdq013.

O'Day SJ, Hamid O, Urba WJ. Targeting cytotoxic T-lymphocyte antigen-4 (CTLA-4): A novel strategy for the treatment of melanoma and other malignancies. *Cancer*. 2007;110(12):2614-2627. doi:10.1002/cncr.23086.

O'Keefe RT, Mayeda A, Sadowski CL, Krainer AR, Spector DL. Disruption of pre-mRNA splicing in vivo results in reorganization of splicing factors. *J Cell Biol*. 1994;124(3):249-260.

O'Reilly FM, Brat DJ, McAlpine BE, Grossniklaus HE, Folpe AL, Arbiser JL. Microphthalmia transcription factor immunohistochemistry: A useful diagnostic marker in the diagnosis and detection of cutaneous melanoma, sentinel lymph node metastases, and extracutaneous melanocytic neoplasms. *J Am Acad Dermatol*. 2001;45(3):414-419. doi:10.1067/mjd.2001.117526.

Ohmholt K, Platz A, Ringborg U, Hansson J. Cytoplasmic and nuclear accumulation of b-catenin is rarely caused by ctnnb1 exon 3 mutations in cutaneous malignant melanoma. *Int J Cancer.* 2001; 92:839-842.

Ohtsuka T, Ishibashi M, Gradwohl G, Nakanishi S, Kageyama R. Hes1 and Hes5 as Notch effectors in mammalian neuronal differentiation. *EMBO J*. 1999;18(8):2196-2207.

Opdecamp K, Nakayama A, Nguyen MT, Hodgkinson CA, Pavan WJ. Melanocyte development in vivo and in neural crest cell cultures : crucial dependence on the Mitf basic-helix-loop-helix-zipper transcription factor. *Development.* 1997;2386:2377-2386.

Osawa M, Egawa G, Mak S-S, et al. Molecular characterization of melanocyte stem cells in their niche. *Development*. 2005;132:5589-5599. doi:10.1242/dev.02161.

Osborne NJ, Begbie J, Chilton JK, Schmidt H, Eickholt BJ. Semaphorin/neuropilin signaling influences the positioning of migratory neural crest cells within the hindbrain region of the chick. *Dev Dyn*. 2005;232(4):939-949. doi:10.1002/dvdy.20258.

Oshima H, Rochat A, Kedzia C, Kobayashi K, Barrandon Y. Morphogenesis and renewal of hair follicles from adult multipotent stem cells. *Cell*. 2001;104(2):233-245. doi:10.1016/S0092-8674(01)00208-2.

Oshimori N, Oristian D, Fuchs E. TGF-β Promotes Heterogeneity and Drug Resistance in Squamous Cell Carcinoma. *Cell.* 2015;160(5):963-976. doi:10.1016/j.cell.2015.01.043.

Otsuka H, Moskowitz M. Arrest of 3T3 in G1 phase in suspension culture. *J Cell Physiol.* 1975 Dec;87(2):213-9.

Packham E a, Brook JD. T-box genes in human disorders. *Hum Mol Genet*. 2003;12 Spec No(1):R37-R44. doi:10.1093/hmg/ddg077.

Pajerowski AG, Nguyen C, Aghajanian H, Shapiro MJ, Shapiro VS. NKAP, a novel modulator of Notch signaling, is required for T cell development. *Immunity*. 2009;30(5):696-707. doi:10.1016/j.immuni.2009.02.011.NKAP.

Pajerowski AG, Shapiro MJ, Gwin K, et al. Adult hematopoietic stem cells require NKAP for maintenance and survival. *Blood*. 2010 Oct 14;116(15):2684-2694. doi:10.1182/blood-2010-02-268391.

Paratore C, Goerich DE, Suter U, Wegner M, Sommer L. Survival and glial fate acquisition of neural crest cells are regulated by an interplay between the transcription factor Sox10 and extrinsic combinatorial signaling. *Development.* 2001;3961:3949-3961.

Pardali K, Moustakas A. Actions of TGF-β as tumor suppressor and pro-metastatic factor in human cancer. *Biochim Biophys Acta - Rev Cancer*. 2007;1775(1):21-62. doi:10.1016/j.bbcan.2006.06.004.

Parente JD, Labareda JMP, Bartolo EAFLF, Santos MFSPF, et al. Cartilaginous melanoma: case report and review of the literature. An Bras Dermatol. 2013 May-Jun;88(3):403-407.

Parkin MD, Bray F, Ferlay J, Pisani P. Estimating the world cancer burden: Globocan 2000. *Int J Cancer*. 2001;94(2):153-156. doi:10.1002/ijc.1440.

Parry R V, Chemnitz JM, Frauwirth K a, et al. CTLA-4 and PD-1 Receptors Inhibit T-Cell Activation by Distinct Mechanisms CTLA-4 and PD-1 Receptors Inhibit T-Cell Activation by Distinct Mechanisms †. *Mol Cell Biol*. 2005;25(21):9543-9553. doi:10.1128/MCB.25.21.9543.

Patel A, Steitz J. Splicing double: insights from the second spliceosome. *Nat Rev Mol Cell Biol*. 2003;4(December):960-970. doi:10.1038/nrm1259.

Peeper DS. Oncogene-induced senescence and melanoma: Where do we stand? *Pigment Cell Melanoma Res*. 2011;24(6):1107-1111. doi:10.1111/j.1755-148X.2011.00933.x.

Peggs KS, Quezada SA, Korman AJ, Allison JP. Principles and use of anti-CTLA4 antibody in human cancer immunotherapy. *Curr Opin Immunol*. 2006;18(2):206-213. doi:10.1016/j.coi.2006.01.011.

Peinado H, Olmeda D, Cano A. Snail, Zeb and bHLH factors in tumour progression: an alliance against the epithelial phenotype? *Nat Rev Cancer*. 2007;7(6):415-428. doi:10.1038/nrc2131.

Peirano RI, Goerich DE, Riethmacher D, Wegner M. Protein Zero Gene Expression Is Regulated by the Glial Transcription Factor Sox10. *Molecular and Cellular Biology.* 2000;20(9):3198-3209.

Perissinotto D, Iacopetti P, Bellina I, et al. Avian neural crest cell migration is diversely regulated by the two major hyaluronan-binding proteoglycans PG-M/versican and aggrecan. *Development.* 2000;2842:2823-2842.

Perrot CY, Javelaud D, Mauviel A. Overlapping activities of TGF-β and Hedgehog signaling in cancer: Therapeutic targets for cancer treatment. *Pharmacol Ther*. 2013;137(2):183-199. doi:10.1016/j.pharmthera.2012.10.002.

Phair RD, Misteli T. High mobility of proteins in the mammalian cell nucleus. *Nature*. 2000;404(6778):604-609. doi:10.1038/35007077.

Picardo M, Dell'Anna ML, Ezzedine K, et al. Vitiligo. *Nat Rev Dis Prim*. 2015;(September 2016):15011. doi:10.1038/nrdp.2015.11.

Pierrat MJ, Marsaud V, Mauviel A, Javelaud D. Expression of microphthalmia-associated transcription factor (MITF), which is critical for melanoma progression, is inhibited by both transcription factor GLI2 and transforming growth factor-β. *J Biol Chem*. 2012;287(22):17996-18004.

doi:10.1074/jbc.M112.358341.

Pingault V, Ente D, Dastot-Le Moal F, Goossens M, Marlin S, Bondurand N. Review and update of mutations causing Waardenburg syndrome. *Hum Mutat*. 2010;31(4):391-406. doi:10.1002/humu.21211.

Pinnix CC, Lee JT, Liu Z, et al. Active Notch1 Confers a Transformed Phenotype to Primary Human Melanocytes. *Cancer Res.* 2010;69(13):5312-5320. doi:10.1158/0008-5472.CAN-08-3767.Active.

Pollock PM, Harper UL, Hansen KS, et al. High frequency of BRAF mutations in nevi. *Nat Genet*. 2003;33(1):19-20. doi:10.1038/ng1054.

Polsky D, Bastian BC, Hazan C, et al. HDM2 Protein Overexpression, but not Gene Amplification, is Related to Tumorigenesis of Cutaneous Melanoma. *Cancer Res.* 2001:7642-7646.

Polyak K, Weinberg RA. Transitions between epithelial and mesenchymal states: acquisition of malignant and stem cell traits. *Nat Rev Cancer*. 2009;9(4):265-273. doi:10.1038/nrc2620.

Pomerantz J, Schreiber-Agus N, Liégeois NJ, et al. The Ink4a tumor suppressor gene product, p19(Arf), interacts with MDM2 and neutralizes MDM2's inhibition of p53. *Cell*. 1998;92(6):713-723. doi:10.1016/S0092-8674(00)81400-2.

Potterf SB, Mollaaghababa R, Hou L, et al. Analysis of SOX10 function in neural crest-derived melanocyte development: SOX10-dependent transcriptional control of dopachrome tautomerase. *Dev Biol*. 2001;237(2):245-257. doi:10.1006/dbio.2001.0372.

Poynter JN, Elder JT, Fullen DR, et al. BRAF and NRAS mutations in melanoma and melanocytic nevi. *Melanoma Res.* 2006(Aug);16(4):267-273.

Puntervoll HE, Yang XR, Vetti HH, et al. Melanoma prone families with CDK4 germline mutation: phenotypic profile and associations with MC1R variants. *J Med Genet*. 2013;50(4):264-270. doi:10.1136/jmedgenet-2012-101455.

Qin J, Stennett L, Bacon P, et al. p53-independent NOXA induction overcomes apoptotic resistance of malignant melanomas. *Mol Cancer Ther.* 2004;3(August):895-902.

Rager EL, Bridgeford EP, Ollila DW. Cutaneous melanoma: Update on prevention, screening, diagnosis, and treatment. *Am Fam Physician*. 2005;72(2):269-276.

Ran FA, Hsu PDP, Wright J, Agarwala V, Scott D a, Zhang F. Genome engineering using the CRISPR-Cas9 system. *Nat Protoc*. 2013;8(11):2281-2308. doi:10.1038/nprot.2013.143.

Ranscht B, Bronner-fraser M. T-cadherin expression alternates with migrating neural crest cells in the trunk of the avian embryo. *Development.* 1991;22:15-22.

Raska I. Nuclear ultrastructures associated with the RNA synthesis and processing. *J Cell Biochem.* 1995 Sep;59(1):11-26.

Ratner N, Miller SJ. A RASopathy gene commonly mutated in cancer: the neurofibromatosis type 1 tumor suppressor. *Nat Rev Cancer.* 2016;15(5):290-301. doi:10.1038/nrc3911.A.

Read AP, Newton VE. Waardenburg syndrome. *J Med Gent*. 1997;34:656-665.

Read J, Wadt KAW, Hayward NK. Melanoma genetics. *J Med Genet*. 2015:1-14. doi:10.1136/jmedgenet-2015-103150.

Redman M, King A, Watson C, et al. What is CRISPR/Cas9? *Arch Dis Child - Educ Pract*. 2016;157:1262-1278. doi:10.1136/ARCHDISCHILD-2016-310459.

Reed JA, McNutt NS, Prieto VG, Albino AP. Expression of transforming growth factor-beta 2 in malignant melanoma correlates with the depth of tumor invasion. Implications for tumor progression. *Am J Pathol*. 1994;145(1):97-104.

Rehimi R, Khalida N, Yusuf F, Dai F, Morosan-Puopolo G, Brand-Saberi B. Stromal-derived factor-1 (SDF-1) expression during early chick development. *Int J Dev Biol*. 2008;52(1):87-92. doi:10.1387/ijdb.072374rr.

Reik W. Stability and flexibility of epigenetic gene regulation in mammalian development. *Nature*. 2007;447(7143):425-432. doi:10.1038/nature05918.

Reintgen DS, Cox EB, McCarty KS Jr, Vollmer RT, Seigler HF. Efficacy of elective lymph node dissection n patients with intermediate thickness primary melanoma. *Ann Surg*. 1983 Sep;198(3):379-85.

Rhim AD, Mirek ET, Aiello NM, et al. EMT and dissemination precede pancreatic tumor formation. *Cell*. 2012;148(1-2):349-361. doi:10.1016/j.cell.2011.11.025.

Ribas A, Kefford R, Marshall MA, et al. Phase III randomized clinical trial comparing tremelimumab with standard-of-care chemotherapy in patients with advanced melanoma. *J Clin Oncol*. 2013;31(5):616-622. doi:10.1200/JCO.2012.44.6112.

Robert C, Karaszewska B, Schachter J, et al. Improved Overall Survival in Melanoma with Combined Dabrafenib and Trametinib. *N Engl J Med*. 2014;372(1):141116004513004. doi:10.1056/NEJMoa1412690.

Robert L, Tsoi J, Wang X, Emerson R, et al. CTLA4 blockade broadens the peripheral T cell receptor repertoire. *Clin Cancer Res.* 2014 May 1; 20(9):2424-2432.

Roesch a. Tumor heterogeneity and plasticity as elusive drivers for resistance to MAPK pathway inhibition in melanoma. *Oncogene*. 2015;34(23):2951-2957. doi:10.1038/onc.2014.249.

Roffers-Agarwal J, Gammill LS. Neuropilin receptors guide distinct phases of sensory and motor neuronal segmentation. *Development*. 2009;136(11):1879-1888. doi:10.1242/dev.032920.

Rudd CE, Schneider H. Unifying concepts in CD28, ICOS and CTLA4 co-receptor signalling. *Nat Rev Immunol*. 2003;3(7):544-556. doi:10.1038/nri1131.

Rudd CE, Taylor A, Schneider H. CD28 and CTLA-4 coreceptor expression and signal transduction. *Immunol Rev*. 2009;229(1):12-26. doi:10.1111/j.1600-065X.2009.00770.x.

Ryan AK, Goodship JA, Wilson DI, et al. Spectrum of clinical features associated with interstitial chromosome 22ql 1 deletions : a European collaborative study. *J Med Genet.* 1997:798-804.

Sacco-Bubulya P, Spector DL. Disassembly of interchromatin granule clusters alters the coordination of transcription and pre-mRNA splicing. *J Cell Biol*. 2002;156(3):425-436. doi:10.1083/jcb.200107017.

Sato T, Sasai N, Sasai Y. Neural crest determination by co-activation of Pax3 and Zic1 genes in Xenopus ectoderm. *Development.* 2005;3:2355-2363. doi:10.1242/dev.01823.

Sauka-Spengler T, Bronner-fraser M. A gene regulatory network orchestrates neural crest formation. *Nature Reviews Molecular Cell Biology* 2008;9(July). doi:10.1038/nrm2428.

Sauvageau M, Sauvageau G. Polycomb Group Proteins: Multi-Faceted Regulators of Somatic Stem Cells and Cancer. *Cell Stem Cell*. 2010 September 3; 7(3):299-313.

Schadendorf D, Hodi FS, Robert C, et al. Pooled Analysis of Long-Term Survival Data From Phase II and Phase III Trials of Ipilimumab in Unresectable or Metastatic Melanoma. J Clin Oncol. 2015 Jun 10;33(17):1889-1994. doi:10.1200/JCO.2014.56.2736.

Schatton T, Scolyer RA, Thompson JF, Mihm MCJ. Tumor-Infiltrating Lymphocytes and Their Significance in Melanoma Prognosis. *Molecular Diagnostics for Melanoma: Methods and Protocols*. 2014: 1102; 287-324.

Schilling TF, Kimmel CB. Segment and cell type lineage restrictions during pharyngeal arch development in the zebrafish embryo. *Development*. 1994;494:483-494.

Schmidt A, Nanney LB, Boyd AS, King LE, Ellis DL. Oestrogen receptor-β expression in melanocytic lesions. *Experimental Dermatology.* 2006:971-980. doi:10.1111/j.1600-0625.2006.00502.x.

Schwartz RN, Stover L, Dutcher JP. Managing Toxicities of High-Dose Interleukin-2. *Cancer Network.* 2002:2-11.

Schwarz D, Varum S, Zemke M, et al. Ezh2 is required for neural crest-derived cartilage and bone formation. *Development.* 2014:867-877. doi:10.1242/dev.094342.

Schwarz Q, Maden CH, Vieira JM, Ruhrberg C. Neuropilin 1 signaling guides neural crest cells to coordinate pathway choice with cell specification. *Proc Natl Acad Sci USA*. 2009;106(15).

Seleye-Fubara D, Etebu EN. Histological review of melanocarcinoma in Port Harcourt. *Nigerian Journal of Clinical Practice.* 2005 (Dec); 8(2):110-113.

Sensi M, Catani M, Castellano G, et al. Human Cutaneous Melanomas Lacking MITF and Melanocyte Differentiation Antigens Express a Functional Axl Receptor Kinase. *J Invest Dermatol*. 2011;131(12):2448-2457. doi:10.1038/jid.2011.218.

Serrano M, Lee H, Chin L, Cordon-cardo C, Beach D, Depinho RA. Role of the INK4a Locus in Tumor Suppression and Cell Mortality. *Cell.* 1996;85:27-37.

Serrano M, Lin AW, Mccurrach ME, Beach D, Lowe SW. Oncogenic ras Provokes Premature Cell Senescence Associated with Accumulation of p53 and p16 INK4a. *Cell.* 1997;88:593-602.

Shah KN, Dalal SJ, Desai MP, Sheth PN, et al. White forelock, pigmentary disorder of irides, and long segment Hirschsprung disease: possible variant of Waardenburg syndrome. *J Petdriatr.* 1981 Sep;99(3):432-5.

Shah NM, Groves AK, Anderson DJ. Alternative Neural Crest Cell Fates Are Instructively Promoted by TGF-β Superfamily Members. *Cell.* 1996;85:331-343.

Shah NM, Marchionni MA, Stroobant P, Anderson DJ. Glial Growth Factor Restricts Mammalian Neural Crest Stem Cells to a Glial Fate. *Cell.* 1994;77:349-360.

Shakhova O. Neural crest stem cells in melanoma development. *Current Opinion in Oncology.* 2014; 26(2): 215-21 doi:10.1097/CCO.0000000000000046.

Shakhova O, Sommer L, Biology D. Neural crest-derived stem cells. *StemBook.* 2010;1-20. doi:10.3824/stembook.1.51.1.

Shakhova O, Zingg D, Schaefer SM, et al. Sox10 promotes the formation and maintenance of giant congenital naevi and melanoma. *Nat Cell Biol*. 2012;14(7):1-9. doi:10.1038/ncb2535.

Sharma S, Kelly TK, Jones PA. Epigenetics in cancer. *Carcinogenesis*. 2010;31(1):27-36. doi:10.1093/carcin/bgp220.

Sharpless NE, Chin L. The INK4a / ARF locus and melanoma. *Oncogene.* 2003:3092-3098. doi:10.1038/sj.onc.1206461.

Simkin JE, Zhang D, Rollo BN, Newgreen DF. Retinoic Acid Upregulates Ret and Induces Chain Migration and Population Expansion in Vagal Neural Crest Cells to Colonise the Embryonic Gut. *PLoS One*. 2013;8(5). doi:10.1371/journal.pone.0064077.

Skotheim RI, Nees M. Alternative splicing in cancer: Noise, functional, or systematic? *Int J Biochem Cell Biol.* 2007;39:1432-1449. doi:10.1016/j.biocel.2007.02.016.

Smalley KS. A pivotal role for ERK in the oncogenic behaviour of malignant melanoma? *Int J Cancer*. 2003;532(October 2002):527-532. doi:10.1002/ijc.10978.

Solit D, Sawyers CL. Drug discovery: How melanomas bypass new therapy. *Nature.* 2010 Dec 16;

468(7326):902-3

Solomon CC, White E, Kristal AR, Vaughan T. Melanoma and lifetime UV radiation. *Cancer Causes and Control.* 2004:893-902.

Sommer L. Context-dependent regulation of fate decisions in multipotent progenitor cells of the peripheral nervous system. Cell and Tissue Research. 2001 Aug;305(2):211-216.

Sommer L, Rao M. Neural stem cells and regulation of cell number. Prog Neurobiol. 2002;66:1-18.

Sotillos S, Roch F, Campuzano S. The metalloprotease-disintegrin Kuzbanian participates in Notch activation during growth and patterning of Drosophila imaginal discs. *Development.* 1997;4779:4769-4779.

Sosman JA, Kim KB, Schuchter L, Gonzalez R, et al. Survival in BRAF V600-mutant advanced melanoma treated with vemurafenib. *N Engl J Med.* 2012 Feb 23; 366(8):707-14.

Spector DL, Ful X, Maniatis T. Associations between distinct pre-mRNA splicing components and the cell nucleus. *EMBO J.* 1991;10(11):3467-3481.

Spector DL, Lamond AI. Nuclear Speckles. Cold Spring Harb Perspect Biol. 2011 Feb;3(2):a000646.

Stahl JM, Sharma A, Cheung M, et al. Deregulated Akt3 Activity Promotes Development of Malignant Melanoma. *Cancer Res.* 2004;(12):7002-7010.

Sveen A, Kilpinen S, Ruusulehto A, Lothe RA, Skotheim RI. Aberrant RNA splicing in cancer ; expression changes and driver mutations of splicing factor genes. *Oncogene.* 2015;35(19):2413-2427. doi:10.1038/onc.2015.318.

Swagata TA, Smita GS, Ashwini M, Ganesh A, Hemangi JR. Acral lentiginous melanoma: report of three cases. *Dermatology E, Journal O.* 2011;7(2):1-11.

Takeda K, Yasumoto K, Takada R, et al. Induction of Melanocyte-specific Transcription Factor by Wnt-3a. *The Journal of Biological Chemistry.* 2000;5(27):14013-14017. doi:10.1074/jbc.C000113200.

Talmadge JE, Fidler IJ. AACR Centennial Series: The Biology of Cancer Metastasis: Historical Perspective. Cancer Res. 2010 July 15;70(14):5649-5669.

Tarin D. The Fallacy of Epithelial Mesenchymal Transition in Neoplasia. *Cancer Res*. 2005;(14):5996-6001.

Tarn WY, Steitz JA. Pre-mRNA splicing: the discovery of a new spliceosome doubles the challenge. *Trends Biochem Sci.* 1997 Apr;22(4):132-7

Tas F. Age-specific Incidence Ratios in Malignant Melanoma in Turkey : Melanoma in Older People is Increasing. *Acta Derm Venereol.* 2011;2007:2000-2001. doi:10.2340/00015555-1076.

TCGA_2015. Genomic Classification of Cutaneous Melanoma Resource Genomic Classification of Cutaneous Melanoma. *Cell.* 2015:1681-1696. doi:10.1016/j.cell.2015.05.044.

Teillet MA, Kalcheim C, Le Douarin NM. Formation of the dorsal root ganglia in the avian embryo: segemental origin and migratory behavior of neural crest progenitor cells. *Dev Biol.* 1987 Apr;120(2):329-47.

Thapa P, Chen MW, Mcwilliams DC, et al. NKAP Regulates Invariant NKT Cell Proliferation and Differentiation into ROR-γt−Expressing NKT17 Cells. *J mmunol.* 2016 Jun 15; 196(12):4987-98. doi:10.4049/jimmunol.1501653.

Thapa P, Das J, Mcwilliams D, et al. The transcriptional repressor NKAP is required for the development of iNKT cells. *Nat Commun.* 2013:1-11. doi:10.1038/ncomms2580.

Theriault LL, Hurley LS. Ultrastructure of Developing Melanosomes in C57 Black and Pallid Mice. *Developmental Biology.* 1970;275:261-275.

Théveneau E, Duband JL, Altabef M. Ets-1 confers cranial features on neural crest delamination. *PLoS One.*

2007 Nov 7;2(11):e1142.

Thiery, J.P., Duband, J.L. & Delouvée, A. Pathways and mechanisms of avian trunk neural crest cell migration and localization. *Developmental Biology*, 1982;93(2), pp.324–343.

Thiry M. The interchromatin granules. *Histol Histopathol*. 1995 Oct;10(4):1035-45.

Thomas NE, Berwick M, Cordeiro-stone M. Could BRAF Mutations in Melanocytic Lesions Arise from DNA Damage Induced by Ultraviolet Radiation ? *J Invest Dermatol*. 2006;126(8):1693-1696. doi:10.1038/sj.jid.5700458.

Tian M, Neil JR, Schiemann WP. Transforming Growth Factor-β and the Hallmarks of Cancer. *Cell Signal.* 2011 June; 23(6):951-962.

Tolcher AW, Messersmith WA, Mikulski SM, et al. Phase I Study of RO4929097, a Gamma Secretase Inhibitor of Notch Signaling, in Patients With Refractory Metastatic or Locally Advanced Solid Tumors. *Journal of Clinical Oncology.* 2016;30(19). doi:10.1200/JCO.2011.36.8282.

Tomita Y, Matsumura K, Wakamatsu Y, et al. Cardiac neural crest cells contribute to the dormant multipotent stem cell in the mammalian heart. *The Journal of Cell Biology.* 2005;170(7):1135-1146. doi:10.1083/jcb.200504061.

Topol L, Jiang X, Choi H, Garrett-beal L, Carolan PJ, Yang Y. Wnt-5a inhibits the canonical Wnt pathway by promoting GSK-3-indepenent beta-catenin degradation. J Cell Biol. 2003;162(5):899-908. doi:10.1083/jcb.200303158.

Tríbulo C, Aybar MJ, Nguyen VH, Mullins MC, Mayor R. Regulation of Msx genes by a Bmp gradient is essential for neural crest specification. *Development.* 2003:6441-6452. doi:10.1242/dev.00878.

Trinkle-Mulcahy L, Ajuh P, Prescott A, et al. Nuclear organisation of NIPP1 , a regulatory subunit of protein phosphatase 1 that associates with pre-mRNA splicing factors. *J Cell Sci.* 1999;168:157-168.

Trinkle-Mulcahy L, Sleeman JE, Lamond AI. Dynamic targeting of protein phosphatase 1 within the nuclei of living mammalian cells. *J Cell Sci.* 2001 Dec;114(Pt23):4219-28.

Tsujimura T, Morii E, Nozaki M, et al. Involvement of Transcription Factor Encoded by the mi Locus in the Expression of c-kit Receptor Tyrosine Kinase in Cultured Mast Cells of Mice. *Blood.* 1996;88(4):1225-1233

Tucker RP, Mckay SE. The expression of tenascin by neural crest cells and glia. *Development.* 1991;1039:1031-1039.

Uesaka T, Enomoto H. Neural Precursor Death Is Central to the Pathogenesis of Intestinal Aganglionosis in Ret Hypomorphic Mice. *The Journal of Neuroscience.* 2010;30(15):5211-5218. doi:10.1523/JNEUROSCI.6244-09.2010.

Van Amelsvoort T, Daly E, Henry J, et al. Brain anatomy in adults with velocardiofacial syndrome with and without schizophrenia. *Arch Gen Psychiatry*. 2004;61:1085-1096.

Vandamme N, Berx G. Melanoma cells revive an embryonic transcriptional network to dictate phenotypic heterogeneity. *Front Oncol*. 2014;4(December):1-6. doi:10.3389/fonc.2014.00352.

Vega S, Morales A V, Ocaña OH, Valdés F, Fabregat I, Nieto MA. Snail blocks the cell cycle and confers resistance to cell death. *Genes Dev*. 2004:1131-1143. doi:10.1101/gad.294104.2002.

Van der Velden HMJ, Van Rossum MM, Blokx WAM, Boezeman JBM, Gerritsen MP. Clinical Characteristics of Cutaneous Melanoma and Second Primary Malignancies in a Dutch Hospital-Based Cohort of Cutaneous Melanoma Patients. *Dermatology Research and Practice.* 2009;2009(Mc). doi:10.1155/2009/479183.

Viana A, Gontijo B. Giant congenital melanocytic nevus. An Bras Dermatol. 2013;88(6):863-878.

Villanueva S, Glavic A, Ruiz P, Mayor R. Posteriorization by FGF , Wnt , and Retinoic Acid Is Required for Neural Crest Induction. *Dev Biol.* 2002;301:289-301. doi:10.1006/dbio.2001.0485.

Vousden KH, Prives C. Review Blinded by the Light : The Growing Complexity of p53. *Cell.* 2009;3:413-431. doi:10.1016/j.cell.2009.04.037.

Wang ET, Sandberg R, Luo S, et al. Alternative isoform regulation in human tissue transcriptomes. *Nature.* 2008;456(November). doi:10.1038/nature07509.

Wang MM. Notch signaling and Notch signaling modifiers. *Int J Biochem Cell Biol*. 2011;43(11):1550-1562. doi:10.1016/j.biocel.2011.08.005.

Ward RJ, Dirks PB. Cancer Stem Cells : At the Headwaters of Tumor Development. *Annu Rev Pathol.* 2007;2:175-89. doi:10.1146/annurev.pathol.2.010506.091847.

Wasmeier C, Alistair N, Bolasco G, et al. Melanosomes at a glance Melanosomes at a Glance. *Journal of Cell Science*. 2008;2008:3995-3999. doi:10.1242/jcs.040667.

Webster MR, Kugel CH III, Weeraratna AT. The Wnts of change : How Wnts regulate phenotype switching in melanoma. *BBA - Rev Cancer*. 2015;1856(2):244-251. doi:10.1016/j.bbcan.2015.10.002.

Weeraratna AT. A Wnt-er Wonderland - The complexity of Wnt signaling in melanoma. *Cancer Metastasis Rev.* 2005:237-250.

Weissinger SE, Keil P, Silvers DN, et al. A diagnostic algorithm to distinguish desmoplastic from spindle cell melanoma. *Modern Pathology.* 2014:524-534. doi:10.1038/modpathol.2013.162.

Werner T, Hammer A, Wahlbuhl M, Bösl MR, Wegner M. Multiple conserved regulatory elements with overlapping functions determine Sox10 expression in mouse embryogenesis. *Nucleic Acid Research.* 2007;35(19):6526-6538. doi:10.1093/nar/gkm727.

Widlund HR, Fisher DE. Microphthalamia-associated transcription factor: a critical regulator of pigment cell development and survival. *Oncogene.* 2003:3035-3041. doi:10.1038/sj.onc.1206443.

Widmer DS, Cheng PF, Eichhoff OM, et al. Systematic classification of melanoma cells by phenotype-specific gene expression mapping. *Pigment Cell Melanoma Res.* 2012 May;25(3):343-53. doi:10.1111/j.1755-148X.2011.00986.x.

Will CL, Lührmann R. Spliceosome Structure and Function. *Cold Spring Harb Perspect Biol.* 2011 Jul 1;3(7).

Williams R, Lendahl U, Lardelli M. Complementary and combinatorial patterns of Notch gene family expression during early mouse development. *Mechanisms of Development.* 1995;53:357-368.

Wilson DJ, Alessandrini A, Budd RC. MEK1 Activation Rescues Jurkat T Cells from Fas-Induced Apoptosis. *Cellular Immunology.* 1999;77:67-77.

Wilson YM, Richards KL, Ford-perriss ML, Panthier J, Murphy M. Neural crest cell lineage segregation in the mouse neural tube. *Development.* 2004:6153-6162. doi:10.1242/dev.01533.

Woda JM, Pastagia J, Mercola M, Artinger KB. Dlx proteins position the neural plate border and determine adjacent cell fates. *Development.* 2003:331-342. doi:10.1242/dev.00212.

Wolchok JD, Neyns B, Linette G, et al. Ipilimumab monotherapy in patients with pretreated advanced melanoma: a randomised, double-blind, multicentre, phase 2, dose-ranging study. Lancet Oncol. 2010 Feb;11(2):155-164. doi:10.1016/S1470-2045(09)70334-1.

Wong CE, Paratore C, Dours-zimmermann MT, et al. Neural crest–derived cells with stem cell features can be traced back to multiple lineages in the adult skin. *The Journal of Cell Biology.* 2006;175(6):1005-1015. doi:10.1083/jcb.200606062.

Worlitzer MMA, Schwamborn JC. The notch co-repressor protein nkap is highly expressed in adult mouse subventricular zone neural progenitor. *Neuroscience*. 2014;266:138-149.

doi:10.1016/j.neuroscience.2014.02.019.

Wu H, Goel V, Haluska FG. PTEN signaling pathways in melanoma. *Oncogene.* 2003:3113-3122. doi:10.1038/sj.onc.1206451.

Wurdak H, Ittner LM, Lang KS, et al. Inactivation of TGF-β signaling in neural crest stem cells leads to multiple defects reminiscent of DiGeorge syndrome. *Genes & Development.* 2005:530-535. doi:10.1101/gad.317405.530.

Xie WF, Zhang X, Sakano S, Lefebvre, Sandell LJ. Trans-activation of the mouse cartilage-derived rerinoic acid-sensitive protein gene by Sox9. *J Bone Miner Res*. 1999 May;14(5):757-63.

Yan C, Grimm WA, Garner WL, et al. Epithelial to Mesenchymal Transition in Human Skin Wound Healing Is Induced by Tumor Necrosis Factor-α through Bone Morphogenic Protein-2. *Am J Pathol.* 2010;176(5):2247-2258. doi:10.2353/ajpath.2010.090048.

Yao D, Dai C, Peng S. Mechanism of the Mesenchymal–Epithelial Transition and Its Relationship with Metastatic Tumor Formation. *Mol Cancer Res*. 2011;9(December):1608-1620. doi:10.1158/1541-7786.MCR-10-0568.

Yasumoto K, Takeda K, Saito H, Watanabe K. Microphthalmia-associated transcription factor interacts with LEF-1 , a mediator of Wnt signaling. *EMBO J.* 2002;21(11):2703-2714.

Yokoyama S, Woods S, Boyle G, Aoude L, et al. A novel recurrent mutation in MITF predisposes to familial and sporadic melanoma. *Nature.* 480(7375):99-103.

Young HM, Bergner AJ, Simpson MJ, et al. Colonizing while migrating : how do individual enteric neural crest cells behave ? *BMC Biology.* 2014:1-18.

Zhang K, Wong P, Zhang L, Jacobs B, et al. A Notch1-neuregulin1 autocrine signaling loop contributes to melanoma growth. *Oncogene*. 2012 October 25; 31(43):4609-4618.

Zingg D, Debbache J, Schaefer SM, et al. The epigenetic modifier EZH2 controls melanoma growth and metastasis through silencing of distinct tumour suppressors. *Nat Commun*. 2015;2(May 2014):1-17. doi:10.1038/ncomms7051.

Zipser MC, Eichhoff OM, Widmer DS, et al. A proliferative melanoma cell phenotype is responsive to RAF/MEK inhibition independent of BRAF mutation status. *Pigment Cell Melanoma Res.* 2011 Apr;24(2):326-33. doi:10.1111/j.1755-148X.2010.00823.x.

10. Curriculum vitae

CURRICULUM VITAE

Mario-Emanuel Bonalli

Dr. med. vet.
Ackersteinstrasse 180
CH-8049 Zürich
+41 76 518 55 11
mario.bonalli@gmx.ch
17. Mai 1983

CURRICULUM VITAE

Mario Bonalli • Ackersteinstrasse 180 • CH-8049 Zürich

Experience

Since 02/2012 — MD-PhD Student
Institute of Anatomy, University of Zurich
- CRISPR/Cas9-based generation of knockout melanoma cell cultures
- Presentation of research data
- Write and publish scientific articles

Since 02/2012 — Tutor
Histology for medicine students, University of Zurich
- Supervision of students
- Technical assistance
- Co-examiner

Since 04/2011 — Food safety inspector in the Swiss army
Food safety detachement
Rank: First lieutenant

04/2011 - 06/2011 — Project collaborator
Idexx Diavet, Bäch/SZ
- Determination of standard values for laboratory equipment

05/2004 - 07/2004
05/2003 - 08/2003 — Fundraising staff
i.m.i.s. gmbh, Walchwil/ZG
- Team leader
- Introduction of new employees
- Members acquisition

Education

Since 02/2012 — MD-PhD
Institute of Anatomy, University of Zurich
The neural crest: an embryonic model to discover novel key players in melanoma.
Under the direction of Prof. Lukas Sommer

06/2011 - 02/2012 — Master of Science in Medical Biology
Institute of Veterinary Biochemistry and Molecular Biology, University of Zurich
Investigations on molecular mechanisms in mono- and poly-ADP-ribosylation.
Admission to the MD-PhD program prior to completion of the master's degree. Under the direction of Prof. Michael Hottiger

CURRICULUM VITAE

Mario Bonalli • Ackersteinstrasse 180 • CH-8049 Zürich

Education

05/2010 - 10/2010	Scientific internship *Institute for food hygiene and safety, University of Zurich* Epidemiological study on antibiotic resistance in *Salmonella* strains. Under the direction of PD Dr. Herbert Mächler and Prof. Roger Stephan
10/2009	Promotion to Dr. med. vet. *Vetsuisse Faculty, University of Zurich* Dissertation: *„Investigations on phosphospecific interactions in the DNA damage response“.* Under the direction of PD Dr. Manuel Stucki and Prof. Ulrich Hübscher
10/2004 - 10/2009	Study of veterinary medicine (final grade: 5.375) *Vetsuisse Faculty, University of Zurich* Major in biomedical research
08/1998 - 09/2002	High school *State College of Higher Education Limmattal, Urdorf/ZH* Mathematics and natural sciences profile Major in biology and chemistry

Research fellowships

09/2013 - 02/2016	Research fellowship of the Swiss National Science Foundation in the frame of the MD-PhD program
11/2015	Travel Grant (CHF 1000) of the Molecular Life Sciences program

Qualification

11/2014	Course on Ethics in Science
03/2014	Comprehensive Course in Flow Cytometry
01/2014	Practical Course in Advanced Microscopy
12/2012	Advanced Mouse Transgenic Techniques Course
01/2008	LTK Modul 1

CURRICULUM VITAE

Mario Bonalli • Ackersteinstrasse 180 • CH-8049 Zürich

Further activities

07/2013 - 07/2014	European MD-PhD congress, Brunnen/SZ Vice president of the organizing committee
07/2013 - 07/2014	Falling Walls Lab, Brunnen/SZ Organizer

Military career

01/2011 - 04/2011	Practical service as food safety inspector Food safety detachement of the Swiss army, Ittigen/BE
01/2010 - 05/2010	Veterinary officer school in the Swiss army Casern Sand, Schönbühl/BE
01/2003 - 05/2003	Basic training as veterinary soldier in the Swiss army Casern Sand, Schönbühl/BE

Stay abroad

10/2010 - 12/2010	Stay abroad in South America
10/2009 - 12/2009	Stay abroad in Central America
07/2004 - 09/2004	Stay abroad in Australia
08/2003 - 11/2003	Language learning stay in Canada
09/2002 - 12/2002	Stay abroad in Western Africa

Interests

Squash
Badminton (J&S Coach 1)
Snowboard (J&S Coach 1)
Nature photography
Creative design

ICT skills

Microsoft Word / Excel / Powerpoint
Adobe Photoshop / InDesign / Illustrator
Graphpat Prism
Cell Profiler
Flow Jo

Language skills

German (mother tongue)
English (excellent command)
French (good command)

References

On request

CURRICULUM VITAE

Mario Bonalli • Ackersteinstrasse 180 • CH-8049 Zürich

Publications

- Baggiolini, A., Varum, S., Mateos, J.M., Bettosini, D., John, N., **Bonalli, M.**, Ziegler, U., Dimou, L., Clevers, H., Furrer, R., Sommer, L., *Premigratory and Migratory Neural Crest Cells Are Multipotent In Vivo.* Cell Stem Cell 2015 Mar 5;16(3):314-322

- Zingg, D., Debbache, J., Schäfer, S.M., Tuncer, E., Frommel, S.C., Cheng, P., Arenas-Ramirez, N., Haeusel, J., Zhang, Y., **Bonalli, M.**, McCabe, M.T., Creasy, C.L., Levesque, M.P., Boyman, O., Santoro, R., Shakhova, O., Dummer, R., Sommer, L., *The epigenetic modifier EZH2 controls melanoma growth and metastasis through silencing of distinct tumour suppressors.* Nat Commun. 2015 Jan 22;6:6051

- Rosenthal, F., Feijs, K.L.H., Frugier, E., **Bonalli, M.**, Forst, A.H., Imhof, R., Winkler, H.C., Fischer, D., Caflisch, A., Hassa, P.O., Lüscher, B., Hottiger, M., *Macrodomain-containing proteins are new mono-ADP-ribosylhydrolases.* Nat Struct Mol Biol. 2013 Apr:20(4):502-7

- Jungmichel, S., Clapperton, J.A., Lloyd, J., Hari, F.J., Spycher, C., Pavic, L., Li, J., Haire, L.F., **Bonalli, M.**, Larsen, D.H., Lukas, C., Lukas, J., MacMillan, D., Nielsen, M.L., Stucki, M., Smerdon, S.J., *The molecular basis of ATM-dependent dimerization of the Mdc1 DNA damage checkpoint mediator.* Nucl. Acids Res. (2012) 40(9): 3912-3928

- **Bonalli, M.**, Stephan, R., Käppeli, U., Cernela, N., Adank, L., Hächler, H., *Salmonella enterica serotype Kentucky associated with human infections in Switzerland: Genotype and resistance trends 2004-2009.* Food Research International 45 (2012) 953-957

- **Bonalli, M.**, Stephan, R., Käppeli, U., Cernela, N., Adank, L., Hächler, H., *Salmonalla enterica serotype Virchow associated with human infections in Switzerland: 2004-2009.* BMC Infectious Diseases 2011, 11:49

11. Acknowledgements

I would like to express my deepest gratitude and appreciation to the following persons:

Prof. Dr. Lukas Sommer,

for giving me, as a non-biologist, the chance to work and conduct my doctoral thesis in your group. You have always created a motivating and inspiring research environment. You accepted new and innovative ideas and allowed independent working, which left room for personal, scientific development and fulfillment.

Prof. Dr. Konrad Basler, Prof. Dr. Michael Detmar and Prof. Dr. Reinhard Dummer,

for being members of my PhD committee, giving me valuable scientific advice in the course of my studies and for co-reviewing my PhD thesis.

All the members of the Sommer group,

for an excellent scientific and non-scientific atmosphere in the lab, for your contributions to my studies and for interesting and entertaining discussions.

Nicole Bachelin and Monika Jenny

for being a great team in the back office and for your supportive engagement in all sorts of administrative concerns.

PD Dr. Raffaella Santoro and Sergio Leone,

for helping out with ChIP and co-immunoprecipitation experiments.

Prof. Dr. Mitch Levesque and Phil Cheng,

for providing human melanoma cell cultures and for valuable statistical as well as computational support.

Acknowledgements

Dr. Pawel Pelczar and Dr. Mario Hermann,

for providing the CRISPR-CAS9 constructs and giving useful inputs regarding the generation of knockout cells.

Prof. Dr. Ian Frew, Dr. Joachim Albers, Dr. Holger Lehmann, and Martina Calio,

for providing the MuLE Gateway® constructs and additional information regarding molecular cloning.

Kim Ferrari,

for creating the CellProfiler pipelines and for other precious inputs regarding the CellProfiler software.

My family,

for supporting me in all this years and for having created a wonderful and carefree environment to grow up. You have always been perfect role models that made me understand what it means to have a family.

Sévi,

for being a wonderful human being, for accepting me the way I am and for standing by me in an unconditional manner. I am looking forward to all the new challenges that may come towards us!